AD-A256 538

(2)

NAVAL POSTGRADUATE SCHOOL
Monterey, California

THESIS

Design, Development and Testing of a Prototype Optical System for a Next Generation Multiplexed Imager

by

Blake D. Huguenin

June 1992

Thesis Advisor: D. S. Davis

Approved for public release; distribution is unlimited.

Unclassified

SECURITY CLASSIFICATION OF THIS PAGE

REPORT DOCUMENTATION PAGE

Form Approved OMB No 0704 0188

1a REPORT SECURITY CLASSIFICATION Unclassified	1b RESTRICTIVE MARKINGS
2a SECURITY CLASSIFICATION AUTHORITY	3 DISTRIBUTION/AVAILABILITY OF REPORT Approved for public release; Distribution is unlimited
2b DECLASSIFICATION/DOWNGRADING SCHEDULE	
4 PERFORMING ORGANIZATION REPORT NUMBER(S)	5 MONITORING ORGANIZATION REPORT NUMBER(S)
6a NAME OF PERFORMING ORGANIZATION Naval Postgraduate School 6b OFFICE SYMBOL (If applicable) PH/Dv	7a NAME OF MONITORING ORGANIZATION Naval Postgraduate School
6c ADDRESS (City, State, and ZIP Code) Monterey, CA 93943-5000	7b ADDRESS (City, State, and ZIP Code) Monterey, CA 93943-5000
8a NAME OF FUNDING/SPONSORING ORGANIZATION 8b OFFICE SYMBOL (If applicable)	9 PROCUREMENT INSTRUMENT IDENTIFICATION NUMBER
8c ADDRESS (City, State, and ZIP Code)	10 SOURCE OF FUNDING NUMBERS PROGRAM ELEMENT NO / PROJECT NO / TASK NO / WORK UNIT ACCESSION NO

11 TITLE (Include Security Classification)

"Design, Development, and Testing of a Prototype Optical System for a Next Generation Multiplexed Imager"

12 PERSONAL AUTHOR(S)

Blake DelVic Huguenin

13a TYPE OF REPORT	13b TIME COVERED	14 DATE OF REPORT (Year, Month, Day)	15 PAGE COUNT
Master's Thesis	FROM ______ TO ______	June 1992	105

16 SUPPLEMENTARY NOTATION The views expressed in this thesis are those of the author and do not reflect the offical policy or postion of the U.S. Government

17 COSATI CODES			18 SUBJECT TERMS (Continue on reverse if necessary and identify by block number)
FIELD	GROUP	SUB-GROUP	Multiplexed Imaging; Optical Design

19 ABSTRACT (Continue on reverse if necessary and identify by block number)

A proof-of-concept experimental validation of a proposed idea for a prototype optical system was conducted. This system will be incorporated into a new type of infrared, optically multiplexed imaging and multispectral imaging system. This system will use two-sided, transmitting-reflecting encoding Walsh masks to form a two-dimensional optical Kronecker product. First, a ray tracing design was made to model the optical system. Then the optical system was prototyped and ronchigrams were photographed to document the aberrations present in the optical system. It was shown that spherical mirrors could be used to accurately reimage an object onto the encoding masks without significantly affecting the optical accuracy of the image. The geometric aberrations resulting from this design did not significantly effect the overall ability to produce the Kronecker product.

20 DISTRIBUTION/AVAILABILITY OF ABSTRACT [X] UNCLASSIFIED/UNLIMITED ☐ SAME AS RPT ☐ DTIC USERS	21 ABSTRACT SECURITY CLASSIFICATION Unclassified
22a NAME OF RESPONSIBLE INDIVIDUAL D.S. Davis	22b TELEPHONE (Include Area Code) (408) 646-2877 22c OFFICE SYMBOL PH/Dv

DD Form 1473, JUN 86 Previous editions are obsolete SECURITY CLASSIFICATION OF THIS PAGE

S/N 0102-LF-014-6603 Unclassified

Approved for public release; distribution is unlimited.

Design, Development and Testing of a Prototype Optical System for a Next Generation Multiplexed Imager

by

Blake D. Huguenin
Lieutenant, United States Navy
B.S., United States Naval Academy, 1986

Submitted in partial fulfillment
of the requirements for the degree of

MASTER OF SCIENCE IN ENGINEERING SCIENCE

from the

NAVAL POSTGRADUATE SCHOOL
June 1992

Author: ______________________________
Blake D. Huguenin

Approved by: ______________________________
D. S. Davis, Thesis Advisor

____
D. D. Cleary, Second Reader

____
K. E. Woehler, Chairman
Department of Physics

ABSTRACT

A proof-of-concept experimental validation of a proposed idea for a prototype optical system was conducted. This system will be incorporated into a new type of infrared, optically multiplexed imaging and multispectral imaging system. This system will use two-sided, transmitting-reflecting encoding Walsh masks to form a two-dimensional optical Kronecker product. First, a ray tracing design was made to model the optical system. Then the optical system was prototyped and ronchigrams were photographed to document the aberrations present in the optical system. It was shown that spherical mirrors could be used to accurately reimage an object onto the encoding masks without significantly affecting the optical accuracy of the image. The geometric aberrations resulting from this design did not significantly effect the overall ability to produce the Kronecker product.

TABLE OF CONTENTS

I. INTRODUCTION

A. MOTIVATION

This thesis project is one part of a larger research and development program to design and to build a new type of infrared, optically multiplexed imaging and multispectral imaging device. This device was conceived by the author's advisor, D. S. Davis. This unique state-of-the-art imaging system will use spatially orthogonal Walsh functions to encode the entire image at once, rather than use the traditional pixel-by-pixel raster scan method. This new approach will allow both spatial imaging and spectral mapping to be accomplished with a single device. Thus, Davis' system will be highly efficient and versatile enough to provide imaging and target discrimination tasks in infrared remote sensing, astronomy, and surveillance [Ref. 1]. The validity of this technique was demonstrated by R.H. McKenzie, Capt., USMC, in an earlier thesis [Ref. 2], and subsequent thesis research was conducted by B. J. Musselman, LT, USCG, [Ref. 3]; J. P. Sargent, LT, USN, [Ref. 4]; and G. R. Parriott, LT, USN, [Ref. 5].

B. THESIS GOAL

Davis' technique for multiplexed imaging attempts to improve the efficiency of previous imaging systems. As described in Reference 1, the new device will encode images using spatially orthogonal masks and simple discrete infrared detectors.

The approach to image multiplexing using orthogonal masks is certainly not new [Ref 6, 7]. However, previous image multiplexing devices have two characteristics in common: they have employed transmitting-opaque spatial masks, and they have required that these masks be manipulated precisely in two spatial dimensions. These features represent inefficient, cumbersome liabilities in the traditional approaches to multiplexed imaging. The transmitting-opaque mask idea necessarily wastes light that strikes the opaque regions of the masks, with typical losses approximately equal to 50%. The two-dimensional mask manipulation problem has dictated that, to encode n image pixels, $2n^2$ masks must be precisely positioned by an elaborate 2-D opto-mechanical servo system.

Davis' new approach, as depicted in Figure 1, circumvents both difficulties. First, it employs transmitting-reflecting masks and two optical detectors. One detector senses reflected radiation, while the other intercepts the transmitted portion. Second, it was realized by Davis that it is not necessary to manufacture and manipulate a large basis set of masks to multiplex an image [Ref. 1]. A mathematically complete two-dimensional encoding basis set can be generated by manipulating small basis sets of one-dimensional masks, in transmitting-reflecting pairs, and then multiplexing various combinations of the encoded signals.

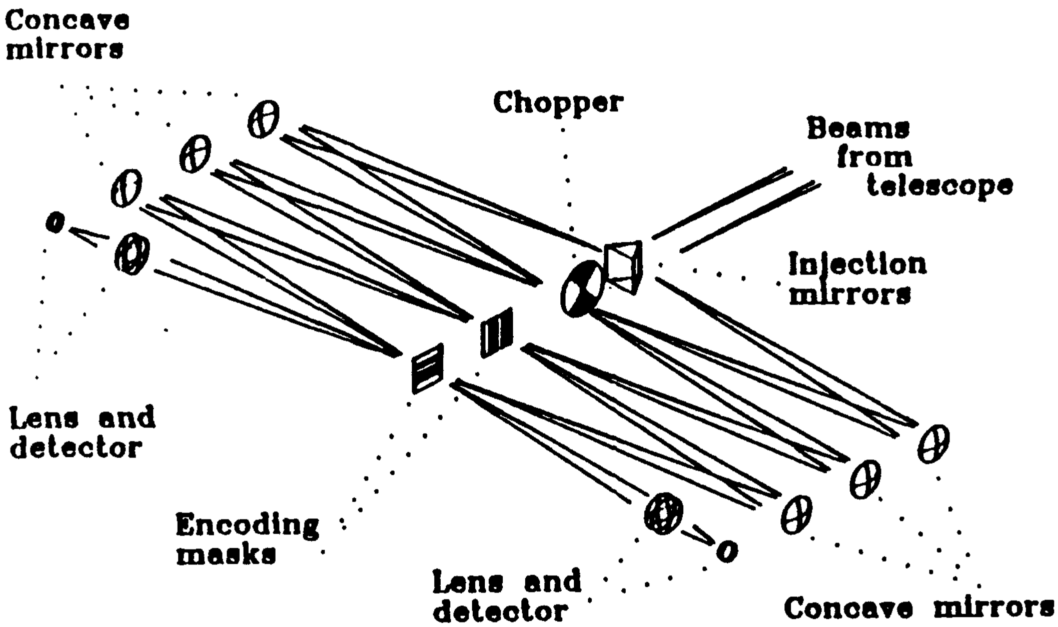

Figure 1 Schematic of New Instrument Configuration

The actual mathematical operation that synthesizes a complete two-dimensional mask encoding basis from one-dimensional components is a Kronecker product [Ref. 6, 8]. The key to understanding the new multiplexing technique is to realize that such a Kronecker product may be performed by purely optical means, as shown in Figure 1 and described in Reference 1. All that is required is a precise reimaging of one transmitting-reflecting one-dimensional mask onto another, from both sides, as shown. When an image field of interest is focused on the first mask, the optical scheme does the rest, as each 2-D encoding function is generated by cycling through various combinations of 1-D masks. There are two potential technical engineering problems that could prevent this scheme from working. The first obstacle is the development of a precise one-dimensional mask positioning servo system. This problem was solved in the aforementioned thesis research of LT Sargent [Ref. 4]. The second potential problem deals with the inherent optical accuracy with which the two-sided masks reimaging can be achieved. This second problem will be addressed by this thesis.

In an earlier thesis, LT Musselman [Ref. 3] demonstrated that physical optics effects (i.e. diffraction) should not have a significant effect on beam quality when images are encoded using the new technique. Therefore, it follows that successful realization of a working optical Kronecker product instrument will depend upon the geometrical optics accuracy with which the two-sided reimaging can be done. Therefore, this thesis research has been concerned with the following questions: (1) Can precise reimaging (and therefore an accurate optical Kronecker product) be accomplished using relatively inexpensive, all-reflecting spherical and planar mirrors? (2) How severe are the geometric aberrations that result from such a design? (3) How will these aberrations affect the overall ability to generate optical products?

II. Ray Tracing Theory

The thesis research of B.J. Musselman [Ref. 3] indicated that physical optics effects, such as diffraction, will have a negligible effect on the design of a prototype multiplexing imaging instrument. Therefore, this thesis project has been conducted entirely within the domain of geometric optics. Within this realm, light is assumed to follow simple mechanical trajectories, called rays, with its propagation governed solely by the basic laws of reflection and refraction.

The advent of the digital computer has lead to the development of efficient numerical procedures for calculating the trajectories of rays through complex optical systems. The interested reader is referred to other sources for specific details on this general theory [Ref. 9, 10]. The commercially available ray tracing software used in this thesis is described more fully in Chapter III. However, because the optical design of the multiplexed imaging system makes use only of simple plane and concave spherical mirrors, it is not necessary to delve into the complete theory of ray tracing. Rather, we have developed a much simpler approach, which is described below.

The reader is directed to Figure 2. For the case of a spherical, concave mirror, an arbitrary ray originates at the object position (X_o, Y_o, Z_o). We wish

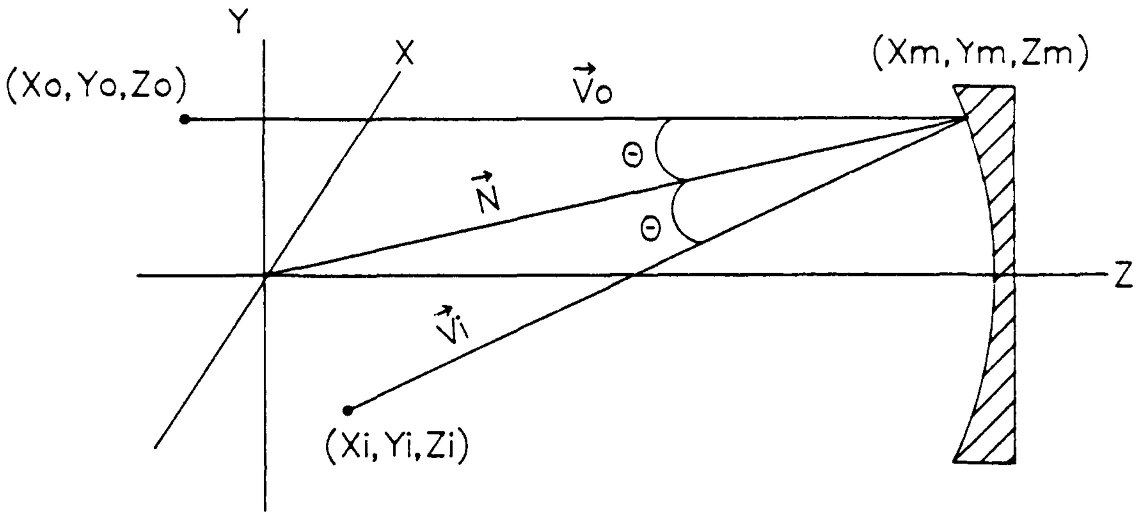

Figure 2 Reflection From a Spherical, Concave Mirror

to calculate the path that the ray will follow when it reflects off the mirror at point (X_m, Y_m, Z_m) and then intersects a surface (X_i, Y_i, Z_i), as shown in Figure 2. To simplify matters, the axis of symmetry of the mirror lies on the z-axis and the center of curvature for the mirror is at the origin. R is the radius of curvature of the spherical surface. All points on the mirror must satisfy the condition $R^2 = X_m^2 + Y_m^2 + Z_m^2$.

The law of reflection governs the ray reflected from the mirror. It is expressed in vector notation as,

$$\frac{\vec{V}_o}{|\vec{V}_o|} \times \frac{\vec{N}}{|\vec{N}|} = \frac{\vec{V}_i}{|\vec{V}_i|} \times \frac{\vec{N}}{|\vec{N}|} \tag{1}$$

or, alternatively,

$$\left(\frac{\vec{V}_o}{|\vec{V}_o|} - \frac{\vec{V}_i}{|\vec{V}_i|} \right) \times \frac{\vec{N}}{|\vec{N}|} = 0 \ , \tag{2}$$

where $\vec{V}_o$ is the vector from (X_o, Y_o, Z_o) to (X_m, Y_m, Z_m), $\vec{V}_i$ is the corresponding vector from (X_m, Y_m, Z_m) to (X_i, Y_i, Z_i), and $\vec{N}$ is the normal or radial vector from the origin to (X_m, Y_m, Z_m).

The physical consequences of this law imply two important ideas:

1. The incident angle is equal to the reflected angle ($\theta_i = \theta_r$).
2. The normal, incident, and reflected rays are all coplanar.

Thus, for the cross product in Equation 2 to equal zero, either $\theta = 0°$ or one of the two terms equals zero. The first case is trivial and not very interesting. However, the second case says that,

$$\frac{\vec{V}_o}{|\vec{V}_o|} - \frac{\vec{V}_i}{|\vec{V}_i|} \parallel \vec{N} \ . \tag{3}$$

The incident, reflected and normal vectors are expressed in component form as follows:

$$\vec{V}_o = (X_m - X_o)\ \hat{i} + (Y_m - Y_o)\ \hat{j} + (Z_m - Z_o)\ \hat{k} \tag{4}$$

$$\vec{V}_i = (X_i - X_m)\ \hat{i} + (Y_i - Y_m)\ \hat{j} + (Z_i - Z_m)\ \hat{k} \tag{5}$$

$$\vec{N} = X_m\ \hat{i} + Y_m\ \hat{j} + Z_m\ \hat{K} \tag{6}$$

If the variables A_o and A_i are defined by,

$$A_o = \sqrt{(X_m - X_o)^2 + (Y_m - Y_o)^2 + (Z_m - Z_o)^2} \tag{7}$$

$$A_i = \sqrt{(X_m - X_i)^2 + (Y_m - Y_i)^2 + (Z_m - Z_i)^2} \tag{8}$$

this leads to,

$$\frac{\vec{V}_o}{|\vec{V}_o|} - \frac{\vec{V}_i}{|\vec{V}_i|} = \left[\frac{X_m - X_o}{A_o} - \frac{X_i - X_m}{A_i}\right]\hat{i} + \left[\frac{Y_m - Y_o}{A_o} - \frac{Y_i - Y_m}{A_i}\right]\hat{j} + \left[\frac{Z_m - Z_o}{A_o} - \frac{Z_i - Z_m}{A_i}\right]\hat{k} \tag{9}$$

$$= \left[\frac{X_m - X_o}{A_o} + \frac{X_m - X_i}{A_i}\right]\hat{i} + \left[\frac{Y_m - Y_o}{A_o} + \frac{Y_m - Y_i}{A_i}\right]\hat{j} + \left[\frac{Z_m - Z_o}{A_o} + \frac{Z_m - Z_i}{A_i}\right]\hat{k}\ . \tag{10}$$

From Equation 3, the $\vec{N}$ is parallel to the left hand side of Equation 9. Therefore, each component of $\vec{N}$ is proportional to the corresponding component of Equation 9,

$$\frac{X_m - X_o}{A_o} + \frac{X_m - X_i}{A_i} = BX_m \tag{11}$$

$$\frac{Y_m - Y_o}{A_o} + \frac{Y_m - Y_i}{A_i} = BY_m \tag{12}$$

$$\frac{Z_m - Z_o}{A_o} + \frac{Z_m - Z_i}{A_i} = BZ_m\ , \tag{13}$$

where B is a positive, and as-yet-to-be-determined, constant.

Numerical ray tracing is based on Equations 11, 12 and 13. The usual approach fixes the position of the object and then allows various rays emanating from the object to reflect off the mirror and to terminate on a designated plane. The designer formulates the optical system on paper, then inputs the parameters into a ray tracing computer program. The program allows several of the parameters to be varied in order to reduce the image error, or aberration.

There are two types of aberrations: chromatic aberrations, which occur from the fact that the refractive index (n) is a function of frequency and monochromatic aberrations, which arise from imperfections of the mirror and from objects off the optical axis (the line connecting the radius of curvature and the center of the mirror). The latter of these is the one of concern for this project, because there are no refractive surfaces in the design. The monochromatic aberrations, to a first approximation, may be further subdivided into spherical aberration, coma, astigmatism, field curvature, and distortion [Ref. 11].

To illustrate the basic principles of ray tracing, two cases will be considered.

1. Assume that a point object is located at the mirror's center of curvature, which is at the origin, $X_o = Y_o = Z_o = 0$. Combining this with Equations 11, 12, and 13 yields,

$$\frac{X_m-0}{\sqrt{(X_m-0)^2+(Y_m-0)^2+(Z_m-0)^2}} + \frac{X_m-X_i}{\sqrt{(X_m-X_i)^2+(Y_m-Y_i)^2+(Z_m-Z_i)^2}} = BX_m \,, \quad \textbf{(14)}$$

and similarly for the Y and Z components. This can be reduced to,

$$\frac{X_m}{R} + \frac{X_m - X_i}{\sqrt{(X_m-X_i)^2+(Y_m-Y_i)^2+(Z_m-Z_i)^2}} = BX_m \text{ , etc. .} \tag{15}$$

Now let a ray pass through the origin and strike anywhere on the surface of the mirror. Obviously, this ray will travel along the normal to the mirror. By the law of reflection, it will then pass through the origin again. We are free, therefore, to define an image plane that contains the origin, $X_i = Y_i = Z_i = 0$. Therefore Equations 15 become,

$$\frac{2X_m}{R} = BX_m \text{ ,} \tag{16}$$

or

$$B = \frac{2}{R} \text{ ,} \tag{17}$$

which specifies the constant B for the system.

2. As a second example, assume the point object is somewhere on the Z-axis, $X_o = Y_o = 0$. Equations 11, 12, and 13 then become,

$$\frac{X_m}{\sqrt{X_m^2+Y_m^2+(Z_m-Z_o)^2}} + \frac{X_m - X_i}{\sqrt{(X_m-X_i)^2+(Y_m-Y_i)^2+(Z_m-Z_i)^2}} = \frac{2}{R}X_m \text{ ,} \tag{18}$$

and similarly for the Y and Z components. From symmetry, the image is expected to lie on the Z axis, ($X_i = Y_i = 0$). Equations 18 then become,

$$\frac{X_m}{\sqrt{X_m^2+Y_m^2+(Z_m-Z_o)^2}} + \frac{X_m}{\sqrt{X_m^2+Y_m^2+(Z_m-Z_i)^2}} = \frac{2}{R}X_m \text{ , etc.} \tag{19}$$

The point at which the mirror surface intersects the Z-axis is called the vertex. The vertex-object distance is $S_o = Z_m - Z_o$, and the vertex-image distance is $S_i = Z_m - Z_i$. Then Equations 19 reduce to,

$$\frac{1}{\sqrt{X_m^2+Y_m^2+S_o^2}} + \frac{1}{\sqrt{X_m^2+Y_m^2+S_i^2}} = \frac{2}{R}. \tag{20}$$

In the paraxial approximation, where $X_m^2 + Y_m^2 << S_o^2$ and $X_m^2 + Y_m^2 << S_i^2$,

$$\frac{1}{\sqrt{S_o^2}} + \frac{1}{\sqrt{S_i^2}} \approx \frac{2}{R}, \tag{21}$$

or,

$$\frac{1}{S_o} + \frac{1}{S_i} = \frac{2}{R}, \tag{22}$$

which is the Gaussian mirror equation [Ref 11].

When the paraxial approximation does not apply, different circular areas at the mirror, corresponding to $X_m^2 + Y_m^2 = \text{constant} = r_m^2$, cause objects to be focused at differing values of S_i:

$$\frac{1}{S_o\sqrt{1+\frac{X_m^2 Y_m^2}{S_o^2}}} + \frac{1}{S_i\sqrt{1+\frac{X_m^2+Y_m^2}{S_i^2}}} = \frac{2}{R} \,. \tag{23}$$

Expanding this equation using the binomial series,

$$\frac{1}{S_o}\left(1-\frac{X_m^2+Y_m^2}{2S_o^2}+\cdots\right) + \frac{1}{S_i^2}\left(1-\frac{X_m^2+Y_m^2}{2S_i^2}+\cdots\right) = \frac{2}{R} \,. \tag{24}$$

For an object at ∞,

$$\frac{1}{S_i}\left(1-\frac{X_m^2+Y_m^2}{2S_i^2}\right) = \frac{2}{R} \,, \tag{25}$$

or,

$$\frac{1}{S_i} - \frac{X_m^2+Y_m^2}{2S_i^3} = \frac{2}{R} \,, \tag{26}$$

which is the third-order spherical aberration [Ref. 11]. The additional lowest-order aberrations may be derived by similar methods.

Historically, it was necessary to perform such calculations for each aberration by hand, and then to recombine them ray-by-ray in order to discern their effects on the overall system performance. Modern ray tracing has removed this chore. We now simply program the computer to predict performance, with all aberrations folded into the calculations at each step. This is the procedure followed throughout this thesis.

III. OPTICAL DESIGN PROCEDURES

A. INTRODUCTION

In the previous chapter, the basic geometric calculations needed to predict ray propagation were discussed. The present chapter discusses how these basic procedures are combined to generate an optimized optical imaging system. The optimization carried out as part of this thesis research are by no means the best possible characterizations of a reimaging system; rather they represent the best design for a system using readily available, off-the-shelf spherical mirrors. It is virtually certain that better performance could be expected from a system employing customized aspheric optics, but such a system would be much more costly then present financial constraints would allow.

The design optimization procedure is straight forward. A geometric object is specified, in general terms, and numerical ray tracing is performed by a computer. Each object point emits rays that pass through various parts of the system. An image plane is specified at the system's output, and the program yields the Cartesian coordinates at which each exiting ray intersects this image plane. Ideally, a perfect imaging system would reimage all rays originating from a given object point into an infinitesimal image plane. However, real optical systems, and the computer models that represent them, exhibit aberrations which cause the exiting rays to intersect the image plane in the neighborhood of the ideal point image, rather than at the point itself. When the intersections of many such rays are plotted, the density of intersection points specifies a point spread function in the image plane. The smaller the point spread function , the better the system approximates the ideal. Referring to Figure 1, the reader will note that the multiplexed imaging system design requires two basic reimaging operations. First, an initial input object (the "chopper" in Figure 1) must be imaged onto the first encoding mask. That mask is then reimaged onto a second encoding mask, to form a Kronecker product [Ref. 6,8]. The optimization of this design requires that the basic characteristics be specified, such as radius of curvature and aperture, for the spherical mirrors used. Hypothetical object points are then placed in the input plane, and numerical ray tracing generates the point spread functions in the designated output plane. The program varies the location(s) and orientation(s) of the mirror(s) in order to minimize the overall point spread function. It then gives the user some numerical parameter, such as RMS ray scatter about a mean image location, that characterizes the point spread function and, hence, predicts image quality.

The commercially available ray tracing software used in this thesis has been the BEAM FOUR system, distributed by Stellar Software of Berkeley, California. The following sections detail the use of BEAM FOUR in the optimization of the multiplexed imaging instrument's optical design.

B. BEAM FOUR

The first phase of this thesis research consisted of designing the optical system to image an object through the two sets of transmitting-reflecting masks, as outlined in the previous section. BEAM FOUR is an IBM PC compatible program that performs ray tracing in Cartesian space. It requires both an optics table and a ray table to generate a ray trace with twelve significant figures of precision. Optics tables specify the optical elements to be used and ray tables indicate how the optical system is to be illuminated. BEAM FOUR has an AUTOADJUST command that will optimize the focus of the system by altering designated parameters. Furthermore, the program is interactive. The optical system, and rays, can be viewed with the LAYOUT command. The (X,Y,Z) coordinates at which rays intersect optical surfaces can be listed with the VERTEX command. There is also a the PLOT command, which is useful in creating spot diagrams to help analyze the optical system's performance by giving a visual representation of the point spread function.

Optics tables are a list of the optical elements to be analyzed by BEAM FOUR. Each optical element is listed in the sequence that it will be encountered by the light. All the characteristics (position, orientation, radius of curvature, etc.) of each optical element is specified in the table under the appropriate header. All optics disc files table are identified with file name extensions of ".OPT". The file preamble lists the number of optical surfaces and the table title on the first line; each column's content on the second line. The following is a list of column headers used:

Index:	index of refraction of the medium in which rays approach a surface
Diameter:	outer diameter or aperture of the optical component
X,Y,Z:	the vertex coordinates of surface
Tilt:	degrees of rotation of the optical element around the X axis
Pitch:	degrees of rotation of the optical element around the Y axis
Roll:	degrees of rotation of the optical element around the Z axis
Curvature:	Value = 1/(radius of curvature); positive means curved towards the +Z axis, negative means curved towards the -Z axis, zero means a flat surface
Figure:	round or square geometrical form
Mirror:	surface identity (mirror, lens, iris)

If one of the optical element's characteristics is not designated, it will use a built-in default value. The default value for the index of refraction is 1.00 and for all other numbers is 0.00. The Z axis is the optical axis.

Ray tables are set up similarly. Each ray's position of origin, initial direction, goal position and final position are designated under the appropriate header. Ray table disc files are identified with file name extensions of ".RAY". The preamble lists the number of rays and the title on the first line; each column's content on the second line. The following is a list of column headers used:

X0,Y0,Z0:	coordinates of ray starting point
U0,V0,W0:	direction cosines at which ray vectors leave X_o, Y_o, Z_o
Xg,Yg,Zg:	X,Y,Z goal coordinates at the final surface
Xf,Yf,Zf:	X,Y,Z actual coordinates at which the ray intersects the final surface
@wave:	changes color of the ray
Note:	indicates the surface at which the ray terminated

Coordinate default values are 0.0, and initial ray directions that are not specified propagate parallel to the Z-axis in the positive Z direction.

The AUTOADJUST optimization feature uses a Gauss-Newton nonlinear iterative least-squares routine to automatically adjust tagged parameters for the least-mean-square discrepancy between the final ray state and user-specified goal. This process works iteratively, and exits when successive reductions in error are smaller than e^{-8}. Up to ten independent parameters may be optimized, the most common being surface location, pitch and radius of curvature. The root-mean-square (RMS) error in the fit is displayed for each iteration so that the operation's progress can be monitored.

A quick and easy way to verify that the trace has done the intended job is to examine it pictorially. The LAYOUT command creates a three-dimensional on-screen diagram of the optical system, complete with rays. The diagram can be rotated about any axis, and there is a zoom feature that allows details to be viewed.

A ray vertex is the point where a ray segment joins the following ray segment by being reflected or refracted at an optical interface. The LAYOUT command gives a quick view of the approximate ray positions, but for a more accurate position the VERTEX LIST command is used. It lists the (X,Y,Z) coordinates of each ray at each optical surface.

The PLOT command displays the spatial relationship of the rays at the final surface on a two-dimensional plot. This helps reveal first-order errors in focusing. Once the system has been refined, a spot diagram can be created using the sub-command RANDOM which uses a Monte Carlo random ray generator to fill the plot.

C. CONSTRAINTS

In designing the optical system, the following constraints were used in the design process:

1. The final multiplexed imaging device will produce images using radiation with radiation up to 20 μm in wavelength. Taking diffraction effects into account, the RMS point spread deviation for the system should not be more than approximately 2 - 3 times the longest wavelength (i.e. about 50 μm, corresponding to BEAM FOUR parameter RMS dev = 0.0050).

2. Since the device will be used in remote sensing applications to view objects at long distances, assume that the maximum angle off the optical axis at which rays will be propagated is ±0.5 arcminutes.

3. When completed, the imaging device will have applications for shipboard, aircraft, or satellite use. Therefore, its physical dimensions should be restricted to about 1 cubic meter.

4. Due to budget considerations, the cost of the optical elements should be minimized. Spherical mirrors are readily available through commercial sources. Therefore, their use is preferred over other shapes in order to be cost effective.

5. All calculations in BEAM FOUR will be done assuming centimeters as units.

D. INITIAL DESIGN

Figure 1 shows the symmetry about the plane containing the chopper and the two masks. Taking advantage of the system's symmetry, only one side of the system needs to be designed then the other side will be the mirror image. The initial design configuration is shown in Figure 3. The line drawn between the center of two optical elements, usually following the optical axis, is the principle ray. Figure 3 has six optical elements. The principle rays connecting these elements will be designated the principle axis. Nine rays of light (one on the optical axis, four spread vertically and four spread horizontally) parallel to the optical axis were used to simulate a point source at infinity. A simple biconvex lens with index of refraction, n = 1.5 is use to focus the light onto the injector mirror. The light is then focused onto the first mask with a spherical mirror. The optimized solution for this configuration is listed in Tables 1 and 2 (HUGA.OPT and HUGA.RAY), and has an RMS point spread deviation = 0.0010 cm. All subsequent BEAM FOUR design configuration tables are contained in Appendices A, and will be referred to by their preamble title. When the second spherical mirror is added to reimage the point source optimally onto the second mask, the system has an RMS point spread deviation

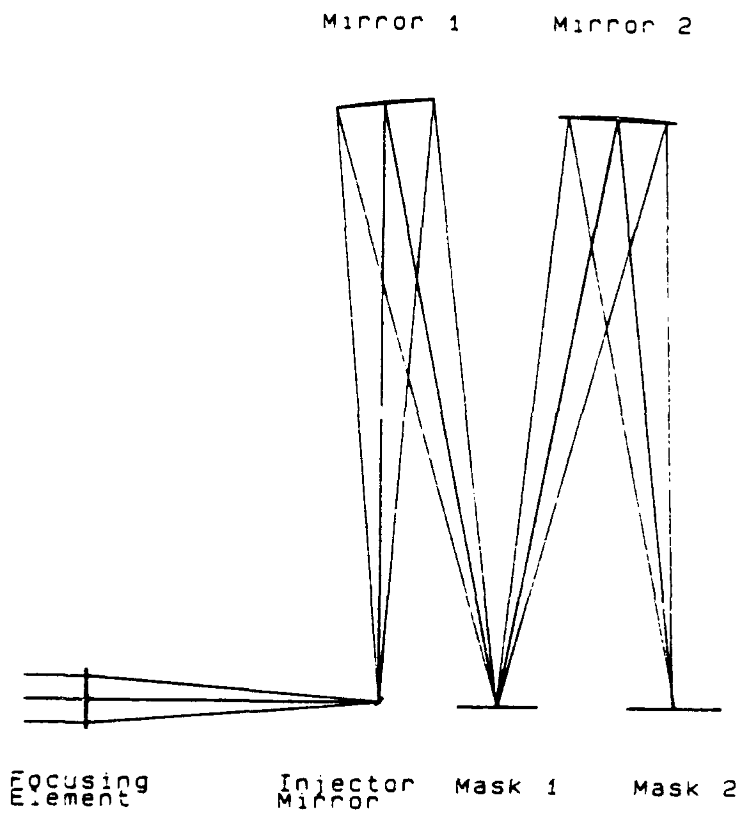

Figure 3 Initial Design Configuration

of 0.0033 cm. This system's parameters are listed in HUGB.OPT and HUGB.RAY.

The next design step was to look at an object located off the optical axis. For the system concerned, locating an object ten meters from the focusing element will approximate an image at infinity. Using the assumption that the object is a maximum of 0.5 arcminutes off the optical axis translates to a lateral displacement of 0.1454 cm at 10 m. Thus, using the previous optical layout in HUGB.OPT and offsetting the point source 0.1454 cm above the optical axis

TABLE 1

OPTICS TABLE FOR THE INITIAL DESIGN

5 surfaces HUGA.OPT

Index	Diameter	X	Z	Pitch	Curvature	Figure	Mirror
	3.0		9.85		0.0074074	Circle	lens
1.5	3.0		9.95		-0.0074074	Circle	lens
	0.5		145.0	-45.0		Square	mirror
	5.0	36.6091	145.0	94.6314	-0.0270400	Circle	mirror
	5.0	-0.17678	151.00	90.0		Square	mirror

TABLE 2

RAY TABLE FOR THE INITIAL DESIGN

9 rays HUGA.RAY

X0	Y0	Xfinal	Yfinal	Zfinal	Xgoal	Ygoal	Zgoal	Note
1.2		-0.1768	0.0000	151.0015	-0.17678		151.0	ok 5
0.6		-0.1768	0.0000	151.0004	-0.17678		151.0	ok 5
0.0		-0.1768	0.0000	150.9994	-0.17678		151.0	ok 5
-0.6		-0.1768	0.0000	150.9984	-0.17678		151.0	ok 5
-1.2		-0.1768	0.0000	150.9972	-0.17678		151.0	ok 5
	1.2	-0.1768	-0.0022	150.9994	-0.17678		151.0	ok 5
	0.6	-0.1768	-0.0011	150.9994	-0.17678		151.0	ok 5
	-0.6	-0.1768	0.0011	150.9994	-0.17678		151.0	ok 5
	-1.2	-0.1768	0.0022	150.9994	-0.17678		151.0	ok 5

yielded an RMS point spread deviation = 0.5813 cm (HUGC.OPT and HUGC.RAY). This was unsatisfactory, being over hundred times the allowable error specified above.

E. ALTERNATE TECHNIQUES

Next, one or both of the spherical mirrors was replaced with aspherical mirrors having more exotic shapes using the SHAPE command in BEAM FOUR. Their positions were also allowed to vary. This yielded only minor improvements in reducing the overall point spread error. For object points on the optical axis, the error was reduced by only 1 - 3 μm. When the source was off the optical axis, the RMS point spread deviation was typically 0.0560 cm. This corresponds to a reduction in error by a factor of ten from the initial trials, but it is still too large.

Davis speculated that the major source of error was in the external biconvex lens focusing element used to simulate a telescope. He suggested using a Petzval lens system to reduce the error when focusing the light. Using the Petzval lens system [Ref. 12:p. 429] to replace the biconvex lens yielded improvements of the same order of magnitude as those achieved when using aspherical mirror surfaces. This degree of image point spread was still too large.

F. FINAL SOLUTION

The persistently large RMS beam spread error present when imaging a point off the optical axis further suggested that this error was caused by the inclusion of the external telescope focusing element. Therefore, in order to test this hypothesis, the external element was eliminated from the design. This is practical since Davis' imaging system itself does not included the external telescope. In eliminating the telescope, the assumption that the radiation propagates through the system in such a way that the object is imaged perfectly at the chopper was made.

Figure 4 shows a diagram of the plane containing the chopper and the two disks with the Walsh encoding masks. Mirror 2 images the first mask onto the second mask, and this mirror's optical axis must bisect the angle formed by the two masks and mirror 2. This requirement arises from the fact that the masks are transmitting and reflecting, in order to generate an optical Kronecker product. Therefore, all the radiation must be reimaged on the second mask. Hence, the first step is to find the optimum position of mirror 2 that gives an acceptable beam spread error at the second mask. By fixing the position of the object (point source) and the image at the centers of mask 1 and 2 respectively, and letting the position of the mirror 2 and its radius of curvature vary, the results in Table 3 were calculated. The radii of curvature (R) listed correspond to standard mirror values that are readily available commercially.

Using the mirror with R = 50 cm, if the point source is moved to the edge of the mask (assume the mask is 5 mm^2), the RMS point spread deviation becomes 0.0025 cm (HUGD.OPT and HUGD1.RAY), which is within the desired limit. This confirmed that the original error was caused by the external telescope focusing elements. Hence, those elements were permanently excluded from the design.

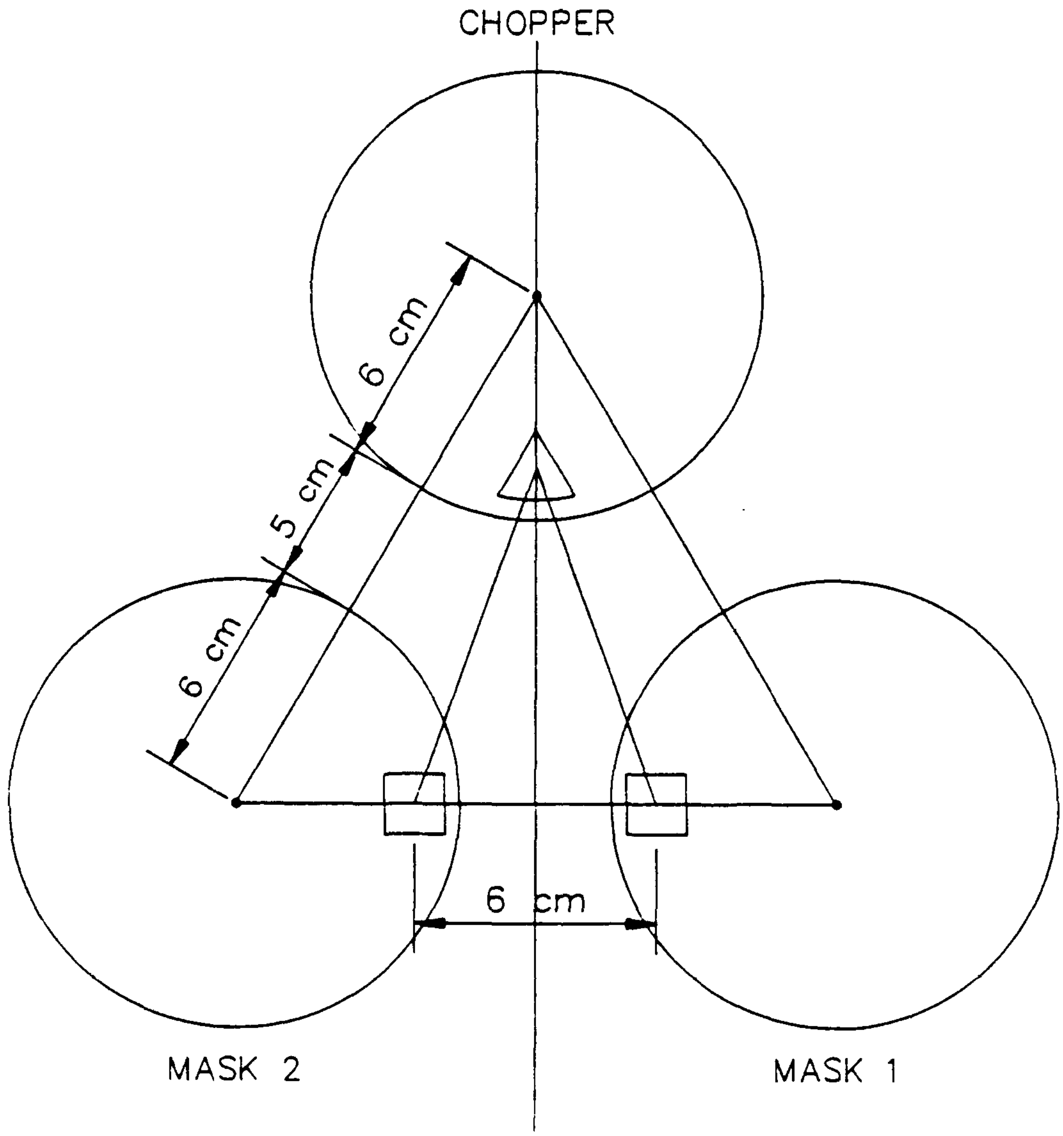

Figure 4 Plane Containing the Chopper and Two Encoding Masks

TABLE 3

RMS POINT SPREAD DEVIATION FOR SEVERAL MIRRORS

Radius of Curvature	RMS Deviation
20 cm	0.0054 cm
30 cm	0.0035 cm
40 cm	0.0026 cm
50 cm	0.0021 cm
60 cm	0.0017 cm

Next, the position and radius of the mirror 1 must be determined. To avoid havirg mirror 1 and 2 physically too close, which might cause mechanical problems when the system is assembled, mirror 1's radius of curvature was chosen to be 60 cm. Analysis of the geometry of the system indicates that this mirror must lie on the extended principle line between mirror 2 and mask 1. This principle line was made the optical axis (Z axis) in the BEAM FOUR by rotating the plane containing the chopper and two encoding masks 2.8° from vertical. The coordinates of the centers of the chopper input, mask 1 and 2 are known from Figure 4. When all this information was input to BEAM FOUR an optimized position of mirror 1 was calculated (HUGE.OPT and HUGE.RAY). An RMS point spread deviation of 0.0041 cm was achieved at mask 1. When this is combined with the position calculated for mirror 2, an overall system RMS point spread deviation = 0.0023 cm (HUGF.OPT and HUGF.RAY) for the image at mask 2 was calculated. When the object was moved to the edge of the mask, the total system RMS point spread deviation was 0.0042 cm (HUGF.OPT and HUGF1.RAY). Thus, this system meets the requirements for the maximum allowable point spread error cited previously in section C of this chapter.

IV. PROTOTYPE OF THE OPTICAL SYSTEM

A. RONCHI TEST PROCEDURES

Experimental evaluation of the actual prototype design required that some objective procedures be adopted for judging image quality. Ideally, a precision interferometric and/or Fourier optics analysis of system performance would have been employed. However, the elaborate apparatus needed to do such analysis was not readily available. Therefore, a conventional Ronchi ruling test was chosen.

Until recently, there were historically two general ways of thinking about image quality in optical systems. The first of these was a purely geometrical optics approach, and was based upon analysis of ray shadow patterns, such as Focault test, Ronchi test, and their relatives [Ref. 13]. The second approach was purely in the domain of physical optics, and involved interferometric analysis of wavefronts exiting from the optical system under test [Ref. 11]. The recent advent of Fourier optics [Ref. 14] has lead to an elegant melding of the two historical approaches. The approach used for this project employed a simple form of the Fourier optics point of view in our system analysis.

To understand this approach, consider first the properties of an ideal imaging system, as it images a point source (a spatial Dirac delta function). If diffraction were not present, the ideal image would be another spatial Dirac delta function. However, because of finite apertures and optical wavelengths, what actually appears in the image plane is a blurred distribution of irradiance, E(x,y). This distribution is called the point spread function, because it describes the image spreading characteristics produced by an isolated point source.

Basic diffraction theory [Ref. 11] shows that the actual distribution of irradiance within the ideal system's point spread function is related to the two-dimensional spatial Fourier transform of the limiting aperture stop, or pupil, of the system. Hence, a system with narrow apertures will exhibit a wider point spread function than will a system with a wide apertures. For systems with a rotational axis of symmetry, it is a common practice to simplify the analysis to a one-dimensional cross-section of the point spread function along a diameter, and to threat this as a corresponding one-dimensional radial Fourier-Bessel transform of the limiting aperture. This cross-section is called the line spread function.

When an extended object, consisting of a continuum of continuous points, the situation becomes slightly more complicated. If the point spread function is invariant across the field of view containing the image, then each image point will be broadened by the same point spread function. The observed image irradiance distribution will be the weighted sum of all these point-by-point contributions. It can be shown [Ref. 11] that this irradiance distribution is the convolution of the point spread function with the ideal distribution that would result in a diffraction-free (geometrical optics limiting) case. The same conclusion holds for the one-dimensional line spread function concept. It is, therefore, apparent that a convenient way to quantify the quality of an image produced by a system is to measure the point spread and/or line spread functions of that system. Since the point spread and line spread functions always manifest themselves as components in a spatial convolution, it is also common practice to express them in Fourier transform form, so that the convolutions may be considered using the Fourier convolution theorem. The Fourier transforms are called optical transfer functions, and their modulii are the modulation transfer functions. To analyze the prototype system, the direct point/line spread functions, rather than the transfer functions were used. A reasonable measure of image quality is the RMS distribution, or standard deviation, of irradiances about the point or line spread function's mean coordinates.

When optical aberrations are present in the system, the point and line spread function ideas may be extended to include those effects. Aberrations will, in general, introduce asymmetries and distortions into the spread functions. They may also destroy the translational invariance of the functions, but this problem may be minimized by considering only narrow fields of view, as was the case in this thesis research. In this event, the line and point spread functions are still spatial Fourier transforms, but they are transforms of virtual apertures, with complex spatial characteristics. In any event, the resulting spread functions are still useful measures of image quality.

For this thesis research, we have chosen to quantify system performance using the RMS width of the line spread function. This proved to be convenient, because the line spread function can be obtained relatively easily from a conventional Ronchi test.

Figure 5 shows a t" ical arrangement used to perform a Ronchi test. The centers of the light, the mirror and the reticle must all be in the same plane. The slit is placed in the plane containing the reticle, with the slit parallel to the reticle. When the slit is illuminated, a concave mirror will reflect the light and form an image of the slit on the reticle. If the slit width is substantially narrower than the spacing of the reticle rulings and the mirror is placed at a distance equal to its radius of curvature from both the reticle and the slit, the resulting image magnification is minus one. Thus, when the image is centered on either a dark or clear reticle line, the system's exit pupil (the mirror) seen when looking through the reticle will be uniformly dark or light, if the line spread function is substantially narrower than one half a reticle ruling spacing. When the mirror is at a position other than the radius of curvature, the magnitude of magnification for the image formed will not be one. The resulting image's line spread can be greater than the width of the reticle rulings, and the exit pupil will appear to be crossed by light and dark contours, or fringes. Thus, the Ronchi test is a sensitive procedure for focusing the system (by minimizing the line spread function) and for establishing an experimental upper limit of the line spread function. [Ref 11]

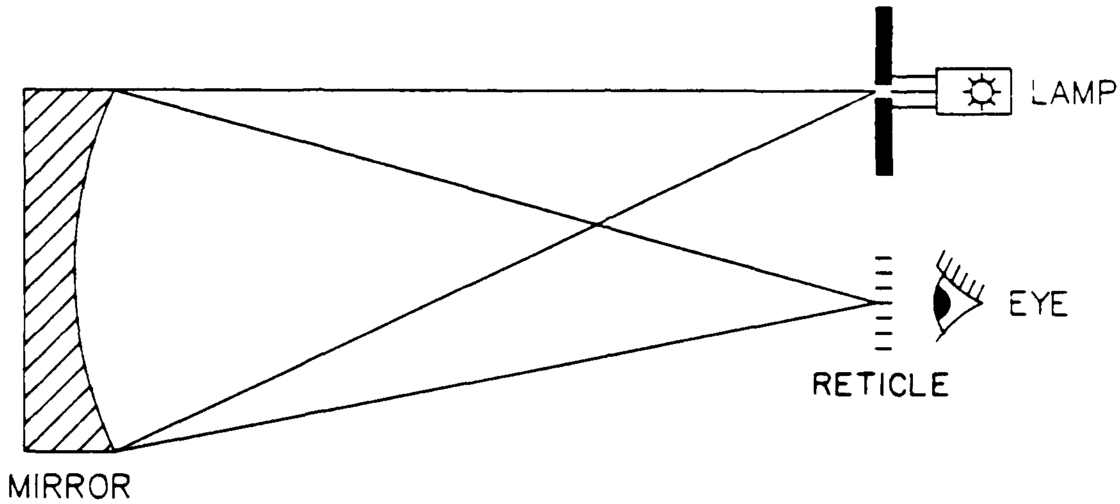

Figure 5 Setup for the Ronchi Test

B. PROCUREMENT

Based on the final solution for the basic optical design problem as described in Chapter III. F., the prototype for the optical system will use two spherical mirrors with radii of curvature R_1 = 60 cm and R_2 = 50 cm and diameters D_1 = 5.04 cm and D_2 = 2.54 cm. However, when an attempt to procure the mirrors was made, it was discovered that none of the major companies had these mirrors in stock. Therefore, due to the limited time the author had to complete this project, two spherical mirrors with R_1 = 152 cm (60 inch) and R_2 = 127 cm (50 inch) were obtained from Edmund Scientific Co. By using these mirrors, the same design can be used, but all physical dimensions have to be multiplied by 2.54 to convert from centimeters to inches. Another adjustment had to made to compensate for these mirrors. Originally, the mirrors in the design were to have diameters, D_1 = 5.08 cm and D_2 = 2.54 cm, corresponding to f-ratios of f/5.9 and f/9.8, respectively. The mirrors available had D_1 = 8.89 cm (f/8.6) and D_2 = 6.35 cm (f/10). Mirror holders had been purchased ahead of time to fit the mirrors in the original design. Therefore, adapters were made in the physics fabrication shop that support the mirrors using the original mirror holders. A drawing of one of the adapters is shown in Figure 6. The discrepancies between the actual mirror's f-ratios and those of the original design also required modification of the detailed design calculations to predict system performance.

Use of alternate mirrors caused yet another problem. In anticipation that the system would incorporate mirrors with radii of curvature approximately 50 cm, Davis had purchased commercially manufactured Ronchi rulings with density as high as could be accommodated by such a system. However, when the mechanical dimensions were scaled up to accommodate the alternate mirrors, those Ronchi rulings were too dense. Therefore, two sets of Ronchi rulings were generated at densities of one and two line cycles per millimeter. The process was a two step operation. First, AutoCAD software was used to produce precise tracings on a high definition Hewlett-Packard 7550A plotter. Second, the resulting plots were transferred to transparencies, using a conventional office copy machine.

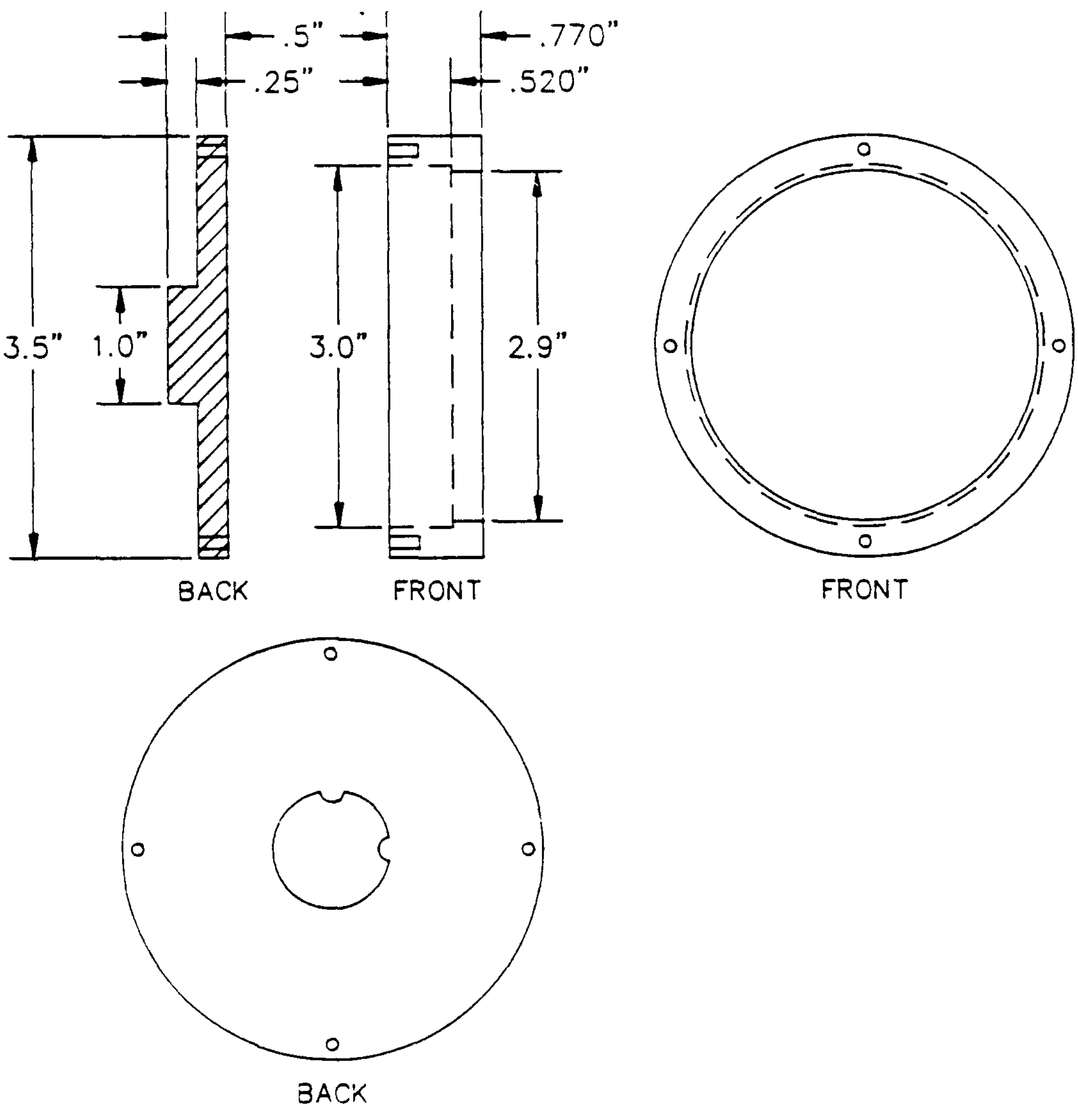

Figure 6 Mirror Adapter

C. DETERMINING THE RADII OF CURVATURE

As stated in the previous section, the prototype optical system had to incorporate off-the-shelf mirrors whose characteristics were quite different from the those specified by the original design. Before assembling and testing the optical system, the actual radii of curvature for each mirror had to be measured and verified because the manufacturer, Edmund Scientific, guaranteed the radii of curvature tolerances to only ± 2%. The version of the Ronchi test described above was used to make these measurements.

A one line per millimeter Ronchi reticle was placed at a distance approximately equal to the radius of curvature from the mirror. A light source with a variable intensity was placed behind the slit to illuminate the mirror through the slit. With the slit open several millimeters and high light intensity, the mirror was tilted and translated to form an image on the center of the reticle. While looking through the reticle at the exit pupil (mirror surface), the intensity of the light was reduced and the slit was stopped down (width was reduced) until an image with several dark and light lines appeared across the exit pupil. This is called a ronchigram. Then, the mirror was mounted on a micropositioner so that it could be translated both perpendicularly to the reticle's rulings and, independently , parallel to the reticle normal. Using the micropositioner, the mirror was moved until all the fringes disappeared and a uniform field of illumination was seen. This was the position where the mirror was focused, because the line spread function was sufficiently narrow. The focused position of the mirror was found to be uncertain to ±0.5 mm (given estimated uncertainties in the relative positions of the slit and Ronchi reticle). This corresponds to a radius of curvature uncertainty of ±0.1 cm.

Using the one line per millimeter reticle, the ronchigram showed no curvature of the fringe pattern in the out-of-focus configuration. With the two lines per millimeter reticle, the fringes began to show a small amount of curvature, indicating various aberrations in the mirror.

To summarize, the radii of curvature for both mirrors were measured and found to be:

$$R_1 = 128.7 \pm 0.1 \text{ cm}$$

$$R_2 = 152.3 \pm 0.1 \text{ cm.}$$

D. OPTICAL SYSTEM ALIGNMENT

Given the actual mirror radii of curvature, it was then necessary to update the basic optical system design to more accurately model the laboratory setup. Entering the actual radii of curvature for mirror 1 and mirror 2 into BEAM FOUR, the optimum coordinates of all the system's optical element's centers were determined. These are detailed in files HUGG.OPT and HUGG.RAY and are summarized in Table 4. Using these values, a working prototype optical system was assembled on a conventional flat optical table. The center of mask 1 is at the origin of the system and is located 11.7 cm above the optical table.

The X axis is parallel to the shorter axis of the optical table, the Y axis is vertical, and the Z axis is parallel to the longer axis of the optical table.

Table 4

COORDINATES FOR THE OPTICAL SYSTEM

	X (cm)	Y (cm)	Z (cm)
Light Source	7.6	23.4	- 0.5
Mirror 1	0.0	0.0	151.0
Mask 1	0.0	0.0	0.0
Mirror 2	15.2	0.0	128.0
Mask 2	15.2	0.0	- 0.9

The optical procedures are as follows:

First, position and align the light source, mirror 1 and mask 1 using simple mechanical measuring methods (i.e. a meter stick). Replace mask 1 with the Ronchi ruling reticle and perform the Ronchi test to achieve optimum focus (see Figure D-1). Because the angle separating the light source and the reticle somewhat exceeds the regime where the paraxial ray approximation holds, the image quality is poorer than that achieved earlier during the radii of curvature measurements. Note that the tilt of the fringes off vertical is approximately parallel to a line drawn from the centers of the light source and the reticle. This is evidence for astigmatism and coma in the image. Approximately three fringes are visible at the position of best focus.

Next, replace the Ronchi reticle with a flat mirror and position mirror 2 and the reticle in place of mask 2. Again perform the Ronchi test and adjust the position of mirror 2 until the optimum focus is achieved (see Figure E-1). Again, approximately three fringes are visible, implying about the same amount of off-axis image aberration as was present in the previous step.

V. ANALYSIS OF THE RESULTS

A. RONCHIGRAM RECORDS OF EXPERIMENTAL RESULTS

To aid in the analysis of the results, the ronchigrams seen at mask 1 and mask 2 were photographed. Davis suggested that the Ronchi ruling reticle and slit be rotated in the vertical plane at 30° increments to show how any system optical aberrations might vary with angle. These images appear in Appendices D and E. Pictures were also taken of the images formed when determining the radius of curvature for mirrors 1 and 2, and are contained in Appendices B and C. Several pictures were also taken when mirrors 1 and 2 were moved away from optimum focus to show how this affected the number of ronchigram fringes seen. These pictures were taken with black and white TMAX 400 KODAK film, with an aperture setting of 5.6, and shutter speed of 1/4 second. The camera used was a Nikon F3 with a 80 - 200 zoom lens.

B. THEORETICAL APPROXIMATIONS OF SYSTEM LINE SPREAD FUNCTIONS

As stated before (see section III. A.), ray spot diagrams can be very useful in analyzing optical systems. An example of a typical spot diagram, produced using a spherical mirror with a point source and the image plane located slightly beyond its center of curvature, is shown in Figure 7. Using BEAM FOUR, spot

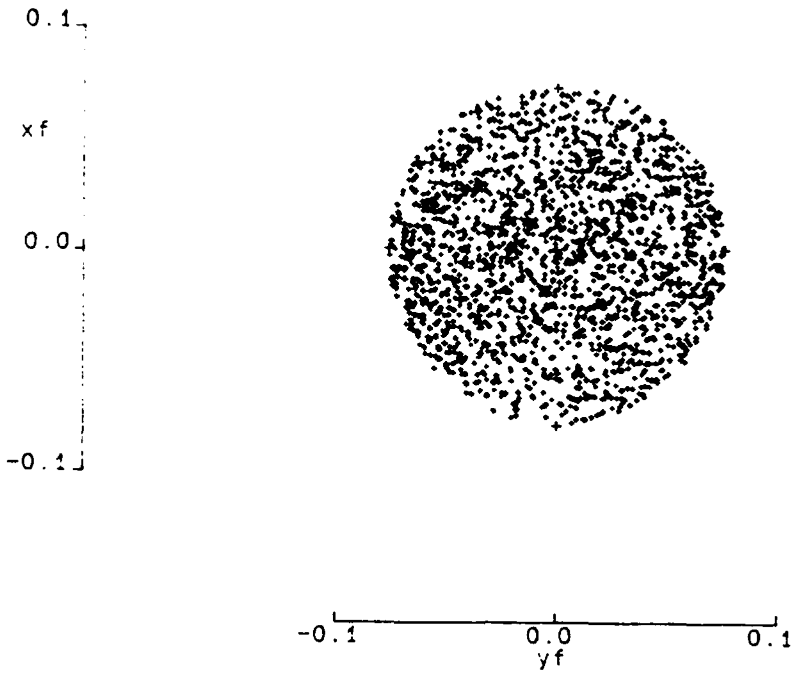

Figure 7 Spot Diagram

diagrams were calculated. When many numerically generated rays, uniformly distributed in space and angle variables, is allowed to "illuminate" a numerical model of an optical system, the local density of spots on a spot diagram should be a reasonable predictor of expected radiative flux in that vicinity. By using such an approach, the theoretical predictions for the width of the line spread functions were calculated that should characterize the actual optical system, including all first and higher-order geometrical aberrations. When a large number of rays were used, the RMS scatter of spots about the beam centroid was chosen as a reasonable measure of predicted line spread. The two lines per millimeter Ronchi ruling reticle used for the experiments will produce observable fringes whenever the line spread width exceeds 0.025 cm. If the RMS line spread deviation for the spot diagrams is assumed to represent the line width produced at the designated surface, and proper geometric scaling is taken into account, then the number of fringes that should be seen in each experimental ronchigram can be predicted, at least approximately, on theoretical grounds.

To get the most accurate prediction, several hundred rays should be used to fill the modeled mirror with light. BEAM FOUR is limited to 99 rays per calculation, which makes the statistical analysis of the spot diagrams somewhat dubious. Therefore, three sets of independent rays were used to search for trends and to check that the predicted number of fringes approached the actual number of fringes seen in the ronchigrams.

C. SUMMARY AND COMPARISON OF THEORY AND EXPERIMENT

As stated in the previous section, three set of rays were generated to attempt to develop a trend in the predicted number of fringes seen in the ronchigrams. The first sets of rays (P45) consisted of five point sources in a line, with nine rays of light (one ray striking the center of the mirror, four rays fanned vertically, and four rays fanned horizontally) emanating from each point source. The second sets of rays (P25i) used the initial set of rays without the four rays from each point source closest to the edge of the mirror. The third set of rays (P25o) copied the original set of rays without the four fanned rays from each point source closest to the center. Table 5 contains the results from these three simulations. Appendix F contains the BEAM FOUR optical tables and ray tables used to produce these line spread predictions. Appendix G contains the plots of the line spread scatter diagrams obtained for the ray tables in P45.

TABLE 5

PREDICTED AND ACTUAL NUMBER OF HALF FRINGES

	P25o	P25i	P45	Actual #
R_1 Mirror 1	0.3	0.2	0.2	< 1
R_2 Mirror 2	0.3	0.1	0.2	< 1
Mask 1 Vertical Slit	8.3	7.0	7.8	3
Mask 1 Horizontal Slit	8.2	6.8	7.7	2
Mask 2 Vertical Slit	10.9	10.3	8.3	3
Mask 2 Horizontal Slit	4.1	2.1	3.4	2

Although the ray tables used for P25o and P25i both have the same number of rays, the predicted numbers of half fringes for these calculations are different. This occurs because the rays striking the mirror closest to its center most closely adhere to the paraxial approximation, which minimized aberration-induced line spreading. If a ray table with several thousand rays was used to calculate the predicted number of half fringes, the predictions should converge to the observed number of half fringes.

D. SOURCES OF ERROR

Throughout the prototyping phase of this project there were several potential sources of error that had to be considered before the final analysis of the system could be completed. The two major sources were the ability to position the optical elements accurately, and the optical quality of the reticle used in the Ronchi test/procedure.

1. Positions of Optical Elements

Although BEAM FOUR was able to calculate the optimum position of each optical element to twelve significant figures, in practice, the optical elements' position could only be measured to within one millimeter when they were positioned on the optical table. This uncertainty affected the measurements taken when the radii of curvature were determined for mirror 1 and mirror 2. The problem was further compounded when the optical elements were positioned, based on the radii of curvature that were determined. To achieve the best results, a three-dimensional (X,Y,Z) micro-positioner that can also adjust the tilt and pitch of the mirrors should be used. Also, a more accurate means of determining the optical elements' locations relative to the designated origin should be used. Only coarse measurements, using a meter stick with millimeter rulings, were made for this project.

2. Ronchi Reticles

When the alternate mirrors were substituted for the mirrors that were originally specified, the reticles that were originally purchased were no longer useful because of their high ruling density. Therefore, "home-made" reticles were generated to use in the Ronchi test and positioning of the spherical mirrors in the optical system. Due to both the manner in which the ink was absorbed onto the paper to create the rulings and to the ability of the photocopying process to reproduce the lines on a transparency sheet, the home-made reticles were far from perfect. The rulings were not uniform in width, and their edges were extremely jagged. These imperfections affected the ronchigrams photographed in Appendices B - E. Thus, the widths of observed Ronchi fringes must be considered to be less accurate than would be the case had high quality reticles been available.

E. INTERPRETING THE ABERRATIONS

The ronchigrams produced for this project show several different characteristics. A rough, bumpy (see Figure C-1) texture occurs when the entrance slit for the light source is very narrow and the camera is focused extremely well. This mottled texture can be produced by two sources: (1) mirror surface imperfections, and (2) blemishes in the Ronchi reticles. Both effects appear here. The half moon effect (see Figure C-2) is produced by astigmatism and coma. The Yin-Yang effect (see Figure D-6) arises because the system uses a three-dimensional off-axis optical configuration in which the spherical mirrors "twist" the light about the principle rays. It is strongest near the center of the mirrors. [Ref. 13]

1. R_1 Mirror 1

The uniform dark field seen in Figure B-1 indicates that: (1) the mirror is at a distance equal to its radius of curvature from the reticle, (2) that the line spread function is substantially narrower than one Ronchi ruling cycle, and (3) that the image is centered on a dark reticle ruling. Figure G-1 shows the simulation of the line spread for this situation. The nearly uniform spacing of the dots indicate that there should be no major aberrations. Figures B-2 through Figure B-4 show that moving the mirror ± 5.0 mm from optimum focus will increase the number of observed Ronchi fringes by one. No significant, unexpected aberrations are evident in this mirror; it appears to be a perfect sphere to within the tolerances that this test can measure.

2. R_2 Mirror 2

The essentially uniform field in Figure C-1 indicates that the mirror is approximately at a distance equal to its radius of curvature from the reticle, as was the situation in the previous case. Figure G-2 shows the simulation of the line spread for this situation. The nearly uniform spacing of the dots implies that there should be no major aberrations affecting the image. However, the rounded fringes in Figure C-2 and Figure C-3 indicate that a slight astigmatism exists in this configuration. It may be that this astigmatism is more apparent in mirror 2 than in mirror 1 because of the larger off-axis angle between the light source and the reticle (1.5° and 1.2° respectively) for mirror 2.

3. Partial System Containing Mirror 1 and Mask 1

Figures D-1 through D-6 show how the aberrations of the optical system affect the light propagating through the system with the entrance slit and reticle at various orientations about the principle ray.

a. Figure D-1

The entrance slit and the reticle were both vertical to produce this ronchigram. Approximately 1.5 fringes are visible. The aforementioned Yin-Yang pattern is visible near the center of the mirror. Figure G-3 shows the line spread simulation of this configuration. The wavy, horizontal shear suggests that some aberration will be introduced by this setup. Comparison of ronchigram in Figure D-1 and the simulation in Figure G-3 requires some care. As was discussed previously in section V. B., only a very limited number of rays could be used to simulate the line spread function. This limitation precludes using spot scatter diagrams with high density, which would permit reliable line spread statistics to be determined. Consequently, it is noted that almost all <u>calculated</u> line spread widths are intrinsically wider than their corresponding observed line spread widths. This trend is repeated for all succeeding ronchigrams.

b. Figure D-2

The entrance slit and the reticle were both rotated 30 ° from vertical to produce this ronchigram. The picture was overexposed, but approximately 1.5 fringes are visible. This indicates that the 30° rotation did not induce any appreciable increase in the overall system aberration.

c. Figure D-3

The entrance slit and the reticle were both rotated 60 ° from vertical to produce this ronchigram. Approximately 1.5 fringes are visible here also. The Yin-Yang effect is slightly visible near the center of the mirror. The conclusion , therefore, is that the 60° rotation does not cause a significant deterioration in image quality either.

d. Figure D-4

The entrance slit and the reticle were both rotated 90° from vertical (horizontal) to produce this ronchigram. Approximately one fringe is visible. The Yin-Yang effect is visible near the center of the mirror. Figure G-4 shows the line spread simulation of this configuration. The wavy, vertical shear suggests that some additional aberration will be introduced by this configuration. However, note from the scale in Figure G-4 that this shear is less than 10% of the overall line spread width. This effect should be unmeasurable with the Ronchi test used here. Indeed, no obvious evidence of it is seen.

e. Figure D-5

The entrance slit and the reticle were both rotated 120 ° from vertical to produce this ronchigram. Approximately one fringe is visible. This appears to be the best orientation for a line object because it produces the fewest Ronchi fringes and the least amount of aberration overall, for a single mirror.

f. Figure D-6

The entrance slit and the reticle were both rotated 150 ° from vertical to produce this ronchigram. Approximately one fringe is visible. The Yin-Yang effect is visible near the center of the mirror, so this configuration is not quite as aberration free as the previous case.

4. Complete System Containing 2 Mirrors and 2 Masks

Figures E-1 through E-6 show how the aberrations of the optical system affect the light propagating through the system with the slit and reticle at various orientations about the principle ray. The ronchigrams were photographed at the position of Mask 2.

a. Figure E-1

The entrance slit and the reticle were both vertical to produce this ronchigram. Approximately 1.5 fringes are visible. Figure G-5 shows the line spread simulation of this configuration. The wavy, horizontal shear suggests that some additional aberration will be introduced by this setup, but again it is too small to detect directly with this Ronchi test. There is some evidence also for coma, as shown by the variable width of the spot diagram.

b. Figure E-2

The entrance slit and the reticle were both rotated 30 ° from vertical to produce this ronchigram. Approximately 1.5 fringes are visible. The half-moon effect is visible in this photograph. As described earlier (see section V.E. and Reference 13), this Ronchi pattern is indicative of both astigmatism and coma.

c. Figure E-3

The entrance slit and the reticle were both rotated 60 ° from vertical to produce this ronchigram. Approximately 1.5 fringes are visible. The half-moon effect is visible in this photograph. Note that the curvature of the fringes is more pronounced than in Figure E-2, indicating that even more astigmatism and coma are present at this orientation.

d. Figure E-4

The entrance slit and the reticle were both rotated 90 ° from vertical (horizontal) to produce this ronchigram. Approximately 1.5 fringes are visible. The most distorted half-moon pattern is visible in this photograph, implying the most severe coma and astigmatism are seen at this orientation.

Figure G-6 shows the line spread simulation of this configuration. The wavy, vertical shear suggests that some aberration will be introduced by this setup. More obviously, the left margin of the calculated line spread function is substantially wider than is the right margin. This is characteristic of substantial coma, and is entirely consistent with the experimental observations. Figure G-7 shows the line spread simulation in Figure G-6 using 1100 uniformly distributed rays to illuminate the mirror. The other line spread functions in Appendix G also have a similar shape when they are illuminated in this manner.

e. Figure E-5

The entrance slit and the reticle were both rotated 120 ° from vertical to produce this ronchigram. Approximately 1.5 fringes are visible. The half-moon effect is not as extreme in this photograph as in the previous ones. Similar to the ronchigram in Figure D-5 (produced at the same orientation), this ronchigram shows the least aberration and the best focus of the ronchigrams.

f. Figure E-6

The entrance slit and the reticle were both rotated 150 ° from vertical to produce this ronchigram. Approximately 1.5 fringes are visible. The half-moon effect is visible in this photograph, at about the same level as in Figure E-5.

F. FINAL ANALYSIS

It is therefore concluded that the system aberrations, as predicted by the calculations and measured by the Ronchi test, are within the acceptable tolerances. The basic optical design of the multiplexing imager can successfully incorporate simple spherical mirrors, without introducing a noticeable degradation in system performance.

VI. CONCLUSIONS AND RECOMMENDATIONS

As stated in the introduction, the primary goal of this thesis was to address the following questions: (1) Can a small object be reimaged accurately onto two-sided encoding Walsh masks using inexpensive, concave, spherical mirrors? (2) If so, what is the optimum configuration to achieve this? These questions have been answered successfully. The prototype optical system used two mirrors with radii of curvature R_1 = 128.70 cm and R_2 = 152.30 cm and their locations specified in Table 4. When the system dimensions are scaled, the prototype was sightly larger than the original goal for the imaging system of one square meter. Once the actual disks with the transmitting-reflecting encoding Walsh masks, the chopper and the positioning system are developed, the spacing between the optical elements can be measured and used to refine the optical system. This may well reduce the radii of curvature needed for the mirrors used in reimaging, thus reducing the overall dimensions of the imaging system.

The initial design specification to keep the RMS point spread function less than 50 μm was met. This kept the aberrations in the optical system to a minimum. In a previous thesis by LT Musselman [Ref. 3], it was shown that diffraction should not seriously effect the multiplexed imaging instrument at the middle-infrared wavelength. This thesis research complemented that work, showing that geometric aberrations will not preclude the development of such an instrument. Although small amount of astigmatism and coma were evident in the ronchigrams photographed at the positions of mask 1 and mask 2 (see Appendices D and E), it may be possible to reduce these aberrations if aspherical mirrors are used. However, it does not appear that the aberrations will significantly degrade the instrumental performance.

It is recommended that further thesis research be conducted to continue the full development of an infrared imaging system.

APPENDIX A

5 surfaces HUGA.OPT

Index	Diameter	X	Z	Pitch	Curvature	Figure	Mirror
	3.0		9.85		0.0074074	Circle	lens
1.5	3.0		9.95		-0.0074074	Circle	lens
	0.5		145.0	-45.0		Square	mirror
	5.0	36.6091	145.0	94.6314	-0.0270400	Circle	mirror
	5.0	-0.17678	151.00	90.0		Square	mirror

9 rays HUGA.RAY

X0	Y0	Xfinal	Yfinal	Zfinal	Xgoal	Ygoal	Zgoal	Note
1.2		-0.1768	0.0000	151.0015	-0.17678		151.0	ok 5
0.6		-0.1768	0.0000	151.0004	-0.17678		151.0	ok 5
0.0		-0.1768	0.0000	150.9994	-0.17678		151.0	ok 5
-0.6		-0.1768	0.0000	150.9984	-0.17678		151.0	ok 5
-1.2		-0.1768	0.0000	150.9972	-0.17678		151.0	ok 5
	1.2	-0.1768	-0.0022	150.9994	-0.17678		151.0	ok 5
	0.6	-0.1768	-0.0011	150.9994	-0.17678		151.0	ok 5
	-0.6	-0.1768	0.0011	150.9994	-0.17678		151.0	ok 5
	-1.2	-0.1768	0.0022	150.9994	-0.17678		151.0	ok 5

7 surfaces HUGB.OPT

Index	Diameter	X	Z	Pitch	Curve	Figure	Mirror
	3.0		9.85		0.0074074	Circle	lens
1.5	3.0		9.95		-0.0074074	Circle	lens
	0.5		145.0	-45.0		Square	mirror
	5.0	36.6091	145.0	94.6314	-0.0270400	Circle	mirror
	5.0	-0.17678	151.0	90.0		Square	mirror
	5.0	35.9147	158.0	86.0846	-0.0274200	Circle	mirror
	5.0	-0.17678	160.0	90.0		Square	lens

9 rays HUGB.RAY

X0	Y0	Xfinal	Yfinal	Zfinal	Xgoal	Ygoal	Zgoal	Note
1.2		-0.1768	0.0000	159.9930	-0.17678		160.0	ok 7
0.6		-0.1768	0.0000	159.9965	-0.17678		160.0	ok 7
0.0		-0.1768	0.0000	159.9998	-0.17678		160.0	ok 7
-0.6		-0.1768	0.0000	160.0032	-0.17678		160.0	ok 7
-1.2		-0.1768	0.0000	160.0067	-0.17678		160.0	ok 7
	1.2	-0.1768	0.0072	159.9998	-0.17678		160.0	ok 7
	0.6	-0.1768	0.0037	159.9998	-0.17678		160.0	ok 7
	-0.6	-0.1768	-0.0037	159.9998	-0.17678		160.0	ok 7
	-1.2	-0.1768	-0.0072	159.9998	-0.17678		160.0	ok 7

7 surfaces HUGC.OPT

Index	Diameter	X	Z	Pitch	Curvature	Figure	Mirror
	3.0		1000.85		0.0074074	Circle	lens
1.50	3.0		1000.95		-0.0074074	Circle	lens
	0.7		1136.00	-45		Square	mirror
	5.0	36.6091	1136.00	94.6313	-0.0270400	Circle	mirror
	4.0	-0.17678	1142.00	90		Square	mirror
	6.0	35.9147	1149.00	86.0846	-0.0274200	Circle	mirror
	4.0	-0.17678	1151.00	90		Square	iris

9 rays HUGC.RAY

XO	UO	VO	Xfinal	Yfina l	Zfinal	Xgoal	Yg	Zgoal	note	
0.14544	-1.45 e-4		-0.177	0.000	1150.9791	-0.1768		1151.9804	ok	7
0.14544	0.35 e-3		-0.177	0.000	1151.0476	-0.1768		1151.9804	ok	7
0.14544	1.10 e-3		-0.177	0.000	1151.1515	-0.1768		1151.9804	ok	7
0.14544	-6.50 e-4		-0.177	0.000	1150.9094	-0.1768		1151.9804	ok	7
0.14544	-1.40 e-3		-0.177	0.000	1150.8063	-0.1768		1151.9804	ok	7
0.14544	-1.45 e-4	0.80 e-3	-0.177	0.107	1150.9792	-0.1768		1151.9804	ok	
0.14544	-1.45 e-4	4.25 e-4	-0.177	0.057	1150.9791	-0.1768		1151.9804	ok	
0.14544	-1.45 e-4	-4.25 e-4	-0.177	-0.057	1150.9791	-0.1768		1151.9804	ok	
0.14544	-1.45 e-4	-0.80 e-3	-0.177	-0.107	1150.9792	-0.1768		1151.9804	ok	

2 Surfaces HUGD.OPT

Diam	X	Z	Pit	Curv	Figure	Mirror
2.54	-3.0	49.9294	0.0001	-0.0200	Circle	mirror
5.0	-6.0				Square	iris

9 rays HUGD.RAY

XO	UO	VO	Yfinal	Xfinal	Ygoal	Xgoal	note	
	-6.10 e-2		0.0000	-5.9999		-6.0	ok	7
	-5.10 e-2		0.0000	-6.0022		-6.0	ok	7
	-4.10 e-2		0.0000	-6.0044		-6.0	ok	7
	-7.10 e-2		0.0000	-5.9977		-6.0	ok	7
	-8.10 e-2		0.0000	-5.9956		-6.0	ok	7
	-6.10 e-2	1.25 e-2	0.0018	-5.9999		-6.0	ok	
	-6.10 e-2	-1.25 e-2	-0.0018	-5.9999		-6.0	ok	
	-6.10 e-2	2.50 e-2	0.0035	-5.9999		-6.0	ok	
	-6.10 e-2	-2.50 e-2	-0.0035	-5.9999		-6.0	ok	

9 rays HUGD1.RAY

XO	UO	VO	Yfinal	Xfinal	Ygoal	Xgoal	note	
0.25	-6.50 e-2		0.0000	-6.2502		-6.25	ok	7
0.25	-4.50 e-2		0.0000	-6.2558		-6.25	ok	7
0.25	-5.50 e-2		0.0000	-6.2530		-6.25	ok	7
0.25	-7.50 e-2		0.0000	-6.2473		-6.25	ok	7
0.25	-8.50 e-2		0.0000	-6.2445		-6.25	ok	7
0.25	-6.50 e-2	2.50 e-2	0.0035	-6.2502		-6.25	ok	
0.25	-6.50 e-2	-2.50 e-2	-0.0035	-6.2502		-6.25	ok	
0.25	-6.50 e-2	1.25 e-2	0.0018	-6.2502		-6.25	ok	
0.25	-6.50 e-2	-1.25 e-2	-0.0018	-6.2502		-6.25	ok	

2 Surfaces HUGE.OPT

X	Z	Tilt	Pitch	Curve	Figure	Mirror	Diam
0.0	60.5016	-4.3225	-1.4033	-0.0164	Circ	Mirror	5.08
0.0	0.0		3.4447		Square	Iris	2.0

9 rays HUGE.RAY

XO	YO	ZO	@wave	UO	VO	Yfinal	Xfinal	Yg	Xg	note	
2.9976	-9.2224	-0.1202	g	-4.86 e-2	14.98 e-2	0.000	-0.000			ok	2
2.9976	-9.2224	-0.1202	m	-4.86 e-2	15.98 e-2	-0.002	0.002			ok	2
2.9976	-9.2224	-0.1202	c	-4.86 e-2	13.98 e-2	0.003	-0.002			ok	2
2.9976	-9.2224	-0.1202	r	-3.86 e-2	14.98 e-2	0.002	0.004			ok	2
2.9976	-9.2224	-0.1202	b	-5.86 e-2	14.98 e-2	-0.002	-0.004			ok	2
2.9976	-9.2224	-0.1202		-4.86 e-2	12.98 e-2	0.005	-0.005			ok	2
2.9976	-9.2224	-0.1202		-4.86 e-2	16.98 e-2	-0.005	0.004			ok	2
2.9976	-9.2224	-0.1202		-2.86 e-2	14.98 e-2	0.005	0.007			ok	2
2.9976	-9.2224	-0.1202		-6.86 e-2	14.98 e-2	-0.004	-0.008			ok	2

4 Surfaces HUGF.OPT

X	Z	Tilt	Pitch	Curve	Figure	Mirror	Diam
0.0	60.5016	-4.3183	-1.4033	-0.0164	Circ	Mirror	5.08
0.0	0.0		3.4447		Square	Iris	2.0
0.0000	-50.0194		3.4418	0.0200	Circ	Mirror	2.54
5.9892	-0.3605		3.4447		Square	Iris	2.0

9 rays HUGF.RAY

X0	Y0	Z0	@wave	U0	V0	Yfinal	Xfinal	Yg	Xgoal	note
2.9946	-9.2224	-0.1803	g	-4.86 e-2	14.98 e-2	0.000	5.989		5.9892	ok 4
2.9946	-9.2224	-0.1803	m	-4.86 e-2	15.98 e-2	0.002	5.987		5.9892	ok 4
2.9946	-9.2224	-0.1803	c	-4.86 e-2	13.98 e-2	-0.002	5.991		5.9892	ok 4
2.9946	-9.2224	-0.1803	r	-3.86 e-2	14.98 e-2	-0.002	5.988		5.9892	ok 4
2.9946	-9.2224	-0.1803	b	-5.86 e-2	14.98 e-2	0.002	5.990		5.9892	ok 4
2.9946	-9.2224	-0.1803		-4.86 e-2	12.98 e-2	-0.003	5.994		5.9892	ok 4
2.9946	-9.2224	-0.1803		-4.86 e-2	16.98 e-2	0.003	5.985		5.9892	ok 4
2.9946	-9.2224	-0.1803		-2.86 e-2	14.98 e-2	-0.004	5.987		5.9892	ok 4
2.9946	-9.2224	-0.1803		-6.86 e-2	14.98 e-2	0.005	5.991		5.9892	ok 4

9 rays HUGF1.RAY

X0	Y0	Z0	@wave	U0	V0	Yfinal	Xfinal	Yg	Xgoal	note
2.9946	-9.4224	-0.1803	g	-4.86 e-2	14.98 e-2	-0.194	5.989	-0.2	5.9892	ok 4
2.9946	-9.4224	-0.1803	m	-4.86 e-2	15.98 e-2	-0.192	5.987	-0.2	5.9892	ok 4
2.9946	-9.4224	-0.1803	c	-4.86 e-2	13.98 e-2	-0.197	5.992	-0.2	5.9892	ok 4
2.9946	-9.4224	-0.1803	r	-3.86 e-2	14.98 e-2	-0.197	5.989	-0.2	5.9892	ok 4
2.9946	-9.4224	-0.1803	b	-5.86 e-2	14.98 e-2	-0.192	5.990	-0.2	5.9892	ok 4
2.9946	-9.4224	-0.1803		-4.86 e-2	13.88 e-2	-0.197	5.992	-0.2	5.9892	ok 4
2.9946	-9.4224	-0.1803		-4.86 e-2	16.98 e-2	-0.190	5.984	-0.2	5.9892	ok 4
2.9946	-9.4224	-0.1803		-2.86 e-2	14.98 e-2	-0.199	5.988	-0.2	5.9892	ok 4
2.9946	-9.4224	-0.1803		-6.86 e-2	14.98 e-2	-0.189	5.991	-0.2	5.9892	ok 4

4 Surfaces HUGG.OPT

X	Z	Tilt	Pitch	Curve	Figure	Mirror	Diam
0.0	59.4284	-4.3996	-1.4283	-0.0167	Circle	Mirror	5.08
0.0	0.0		3.4447		Square	Mirror	4.0
6.0	50.3747	-0.0054	3.3989	-0.0197	Circle	Mirror	2.90
5.9892	-0.3605		3.4447		Square	Iris	4.0

9 rays HUGG.RAY

X0	Y0	Z0	@wave	U0	V0	Yfinal	Xfinal	Yg	Xgoal	note
2.9946	-9.2224	-0.1803	g	-4.86 e-2	14.98 e-2	-0.000	5.989		5.9892	ok 4
2.9946	-9.2224	-0.1803	m	-4.86 e-2	15.98 e-2	0.001	5.987		5.9892	ok 4
2.9946	-9.2224	-0.1803	c	-4.86 e-2	13.98 e-2	-0.001	5.992		5.9892	ok 4
2.9946	-9.2224	-0.1803	r	-3.86 e-2	14.98 e-2	-0.002	5.988		5.9892	ok 4
2.9946	-9.2224	-0.1803	b	-5.86 e-2	14.98 e-2	0.002	5.991		5.9892	ok 4
2.9946	-9.2224	-0.1803		-4.86 e-2	12.98 e-2	-0.003	5.994		5.9892	ok 4
2.9946	-9.2224	-0.1803		-4.86 e-2	16.98 e-2	0.002	5.985		5.9892	ok 4
2.9946	-9.2224	-0.1803		-2.86 e-2	14.98 e-2	-0.005	5.986		5.9892	ok 4
2.9946	-9.2224	-0.1803		-6.86 e-2	14.98 e-2	0.004	5.992		5.9892	ok 4

APPENDIX B

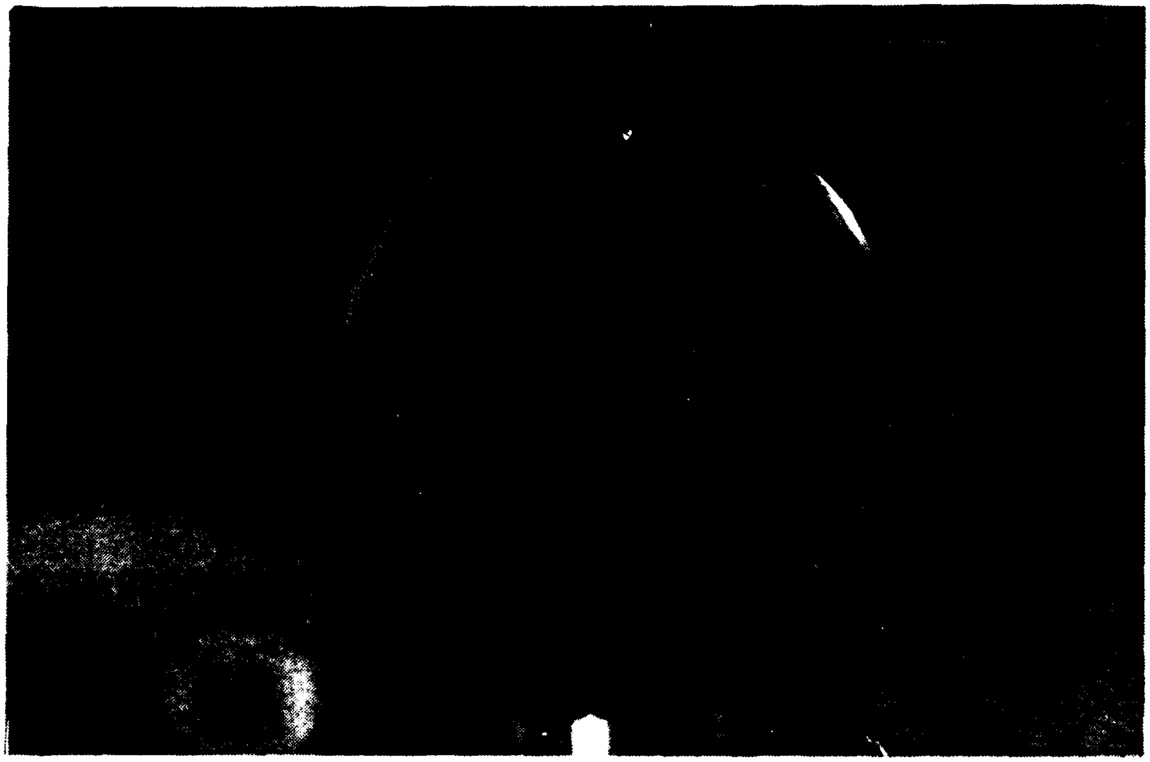

Figure B-1 Ronchigram of Mirror 1 at a Distance Equal to its Radius of Curvature (R_1) from the Reticle and the Entrance Slit

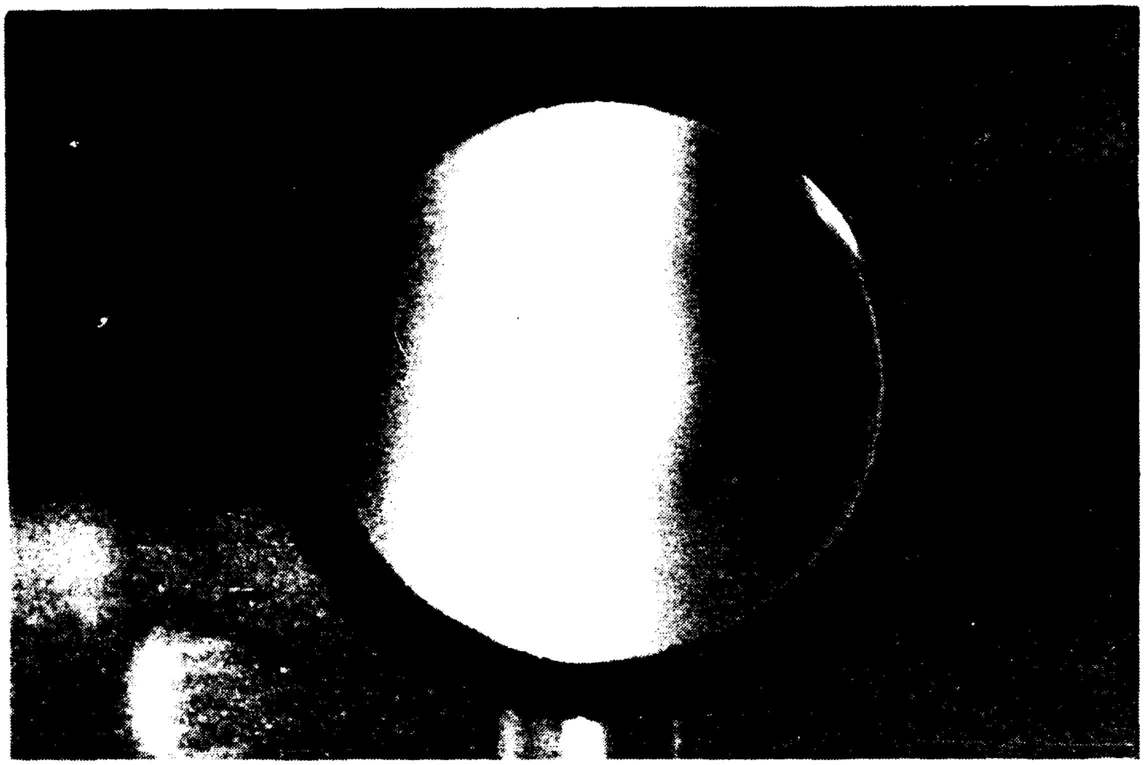

Figure B-2 Ronchigram of Mirror 1 at a Distance Equal to its Radius of Curvature (R_1) + 5 mm from the Reticle and the Entrance Slit

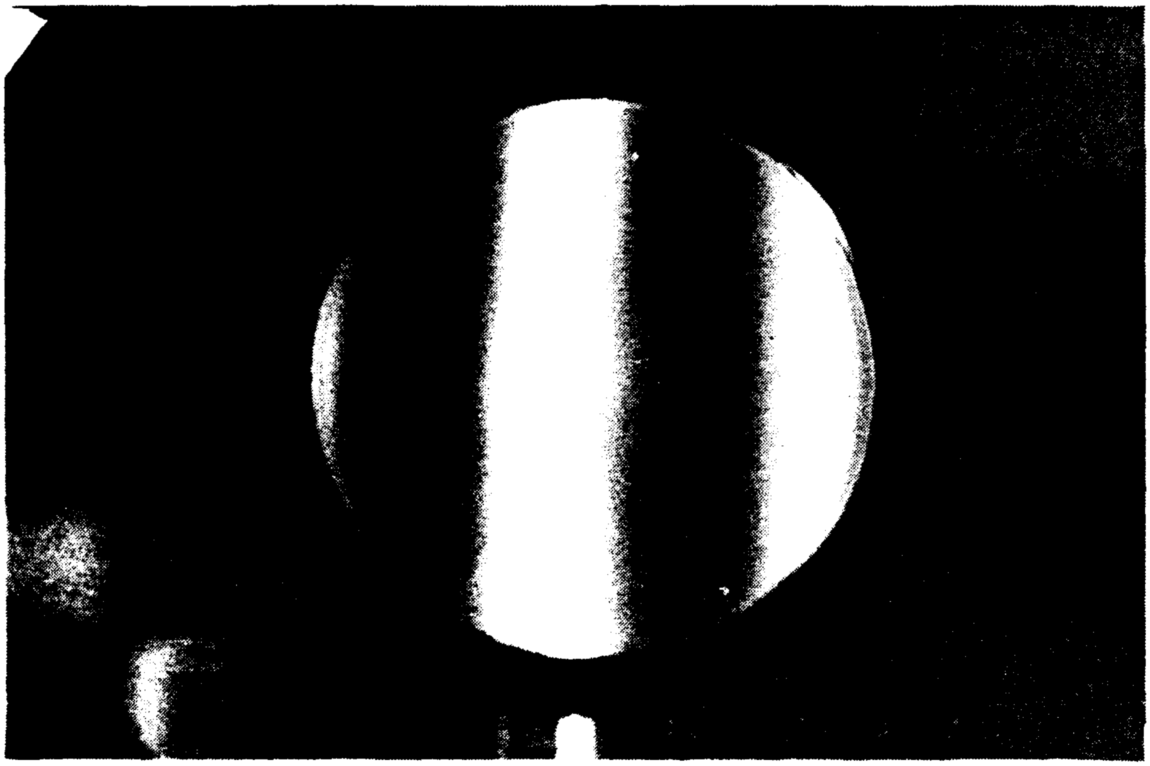

Figure B-3 Ronchigram of Mirror 1 at a Distance Equal to its Radius of Curvature (R_1) + 10 mm form the Reticle and the Entrance Slit

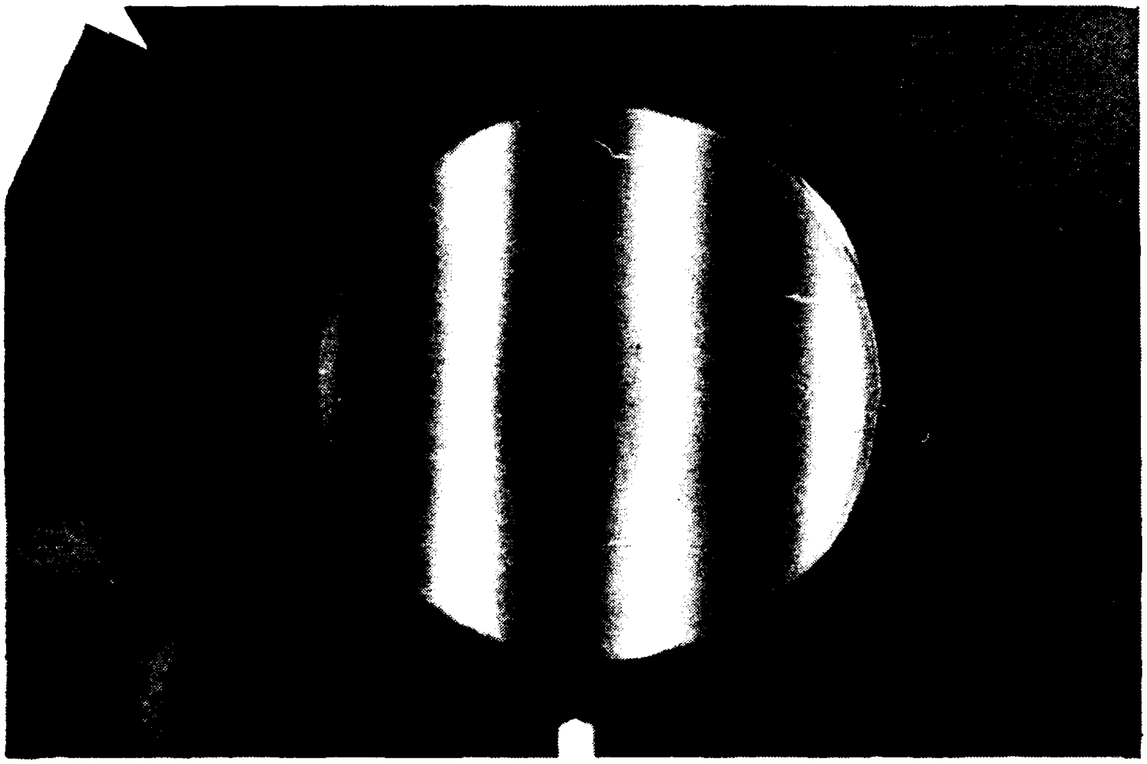

Figure B-4 Ronchigram of Mirror 1 at a Distance Equal to its Radius of Curvature (R_1) + 15 mm from the Reticle and the Entrance Slit

APPENDIX C

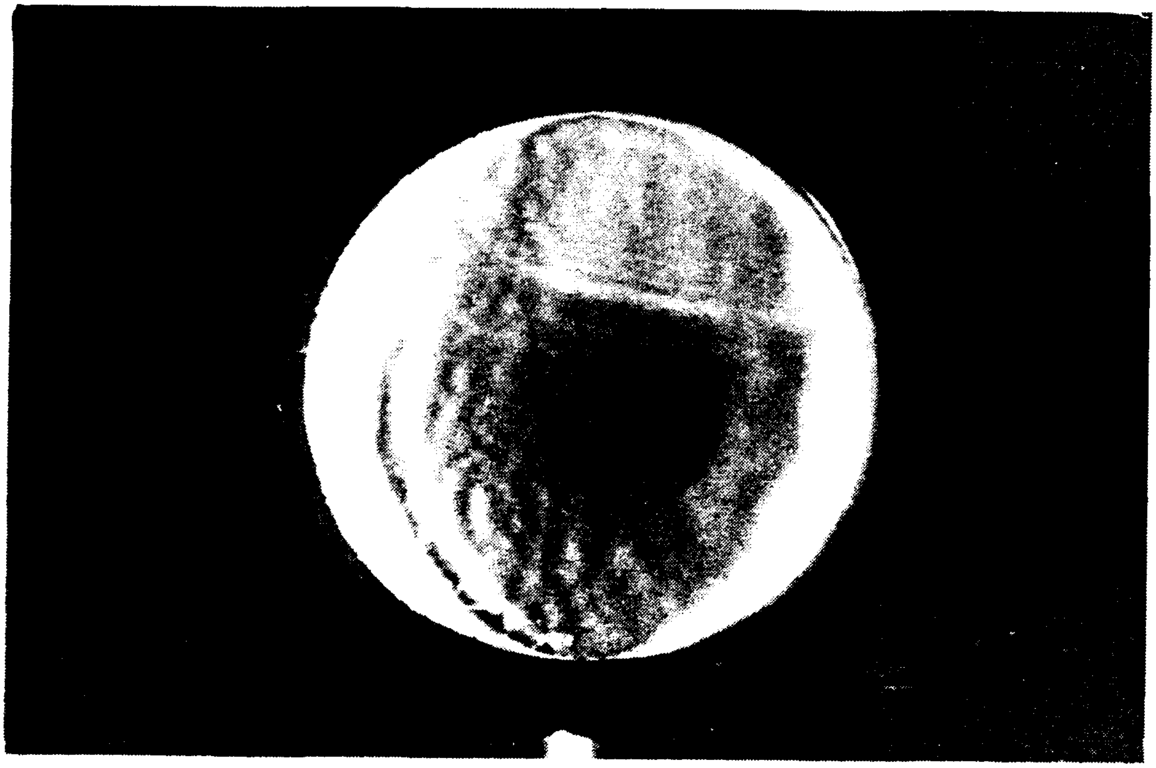

Figure C-1 Ronchigrams of Mirror 2 at a Distance Equal to its Radius of Curvature (R_2) from the Reticle and the Entrance Slit

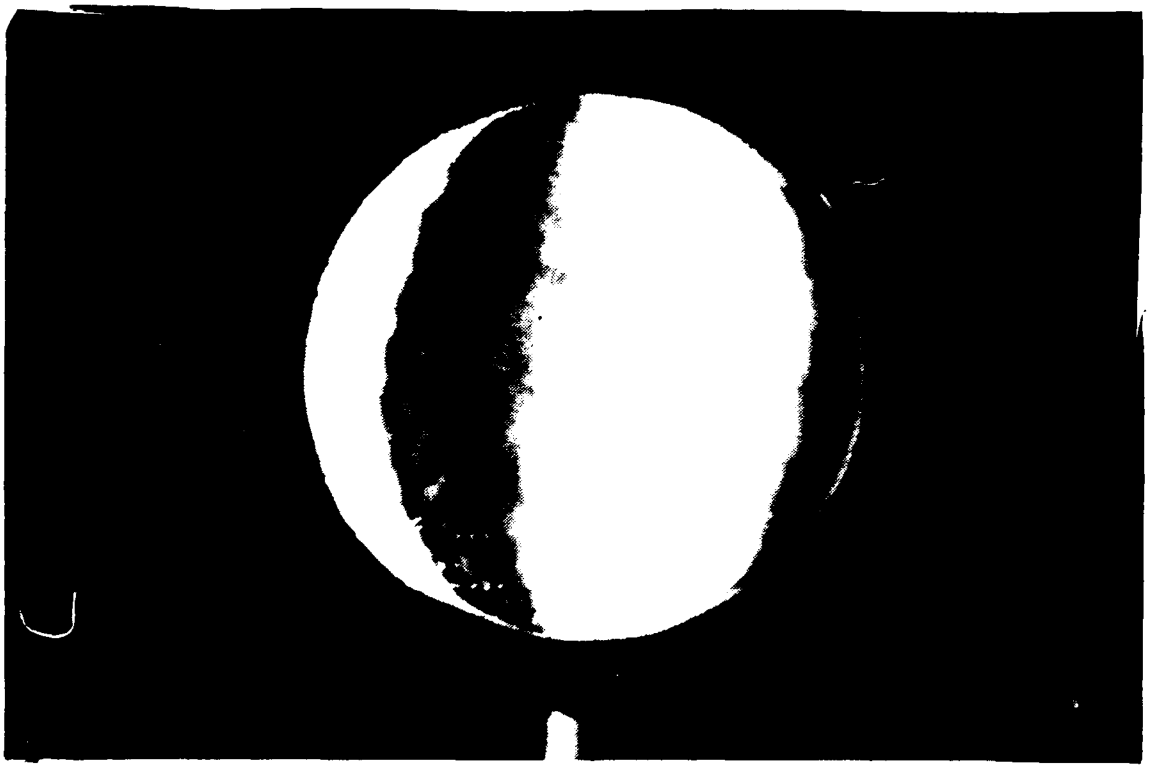

Figure C-1 Ronchigram of Mirror 2 at a Distance Equal to its Radius of Curvature (R_2) + 5 mm from the Reticle and the Entrance Slit

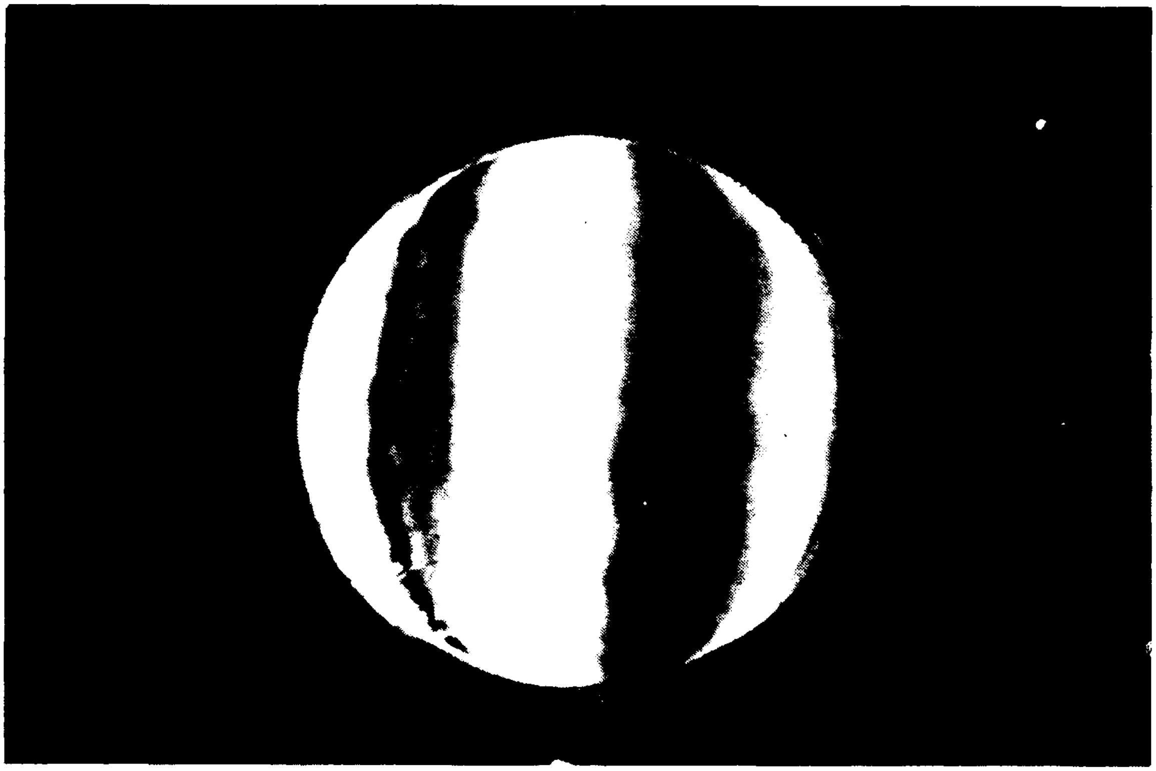

Figure C-3 Ronchigram of Mirror 2 at a Distance Equal to its Radius of Curvature (R_2)+ 10 mm from the Reticle and Entrance Slit

APPENDIX D

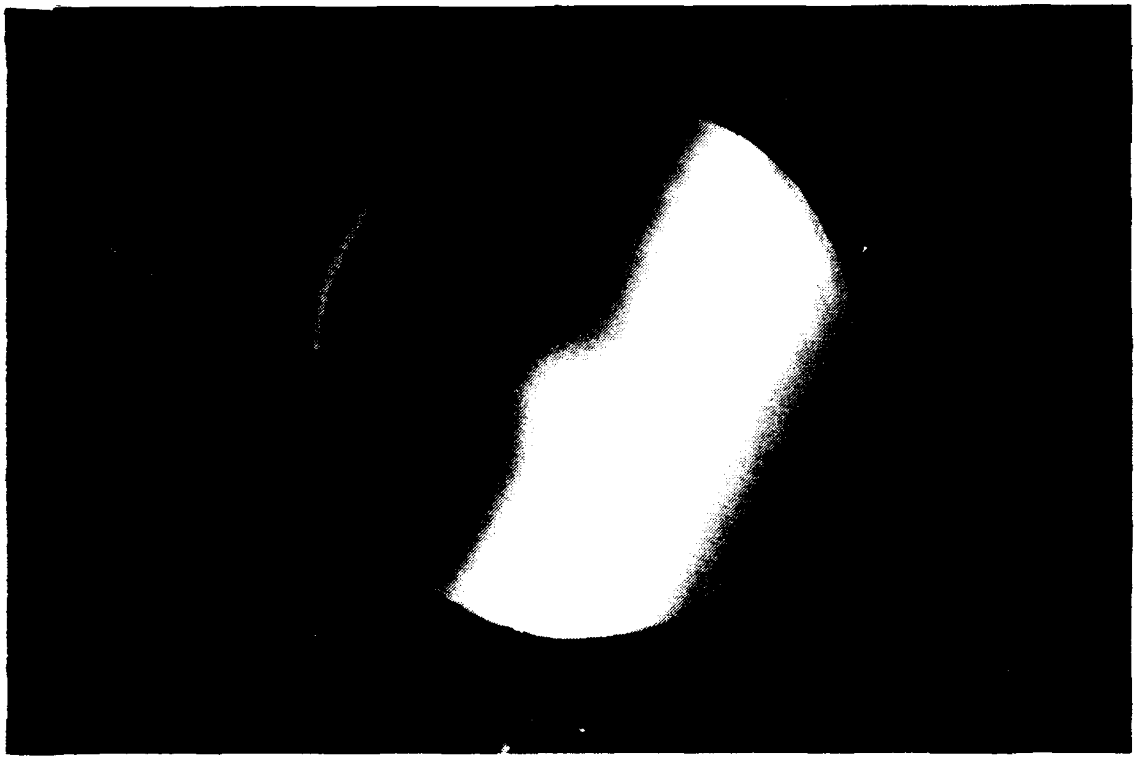

Figure D-1 Ronchigram at Mask 1, Vertical Reticle and Entrance Slit

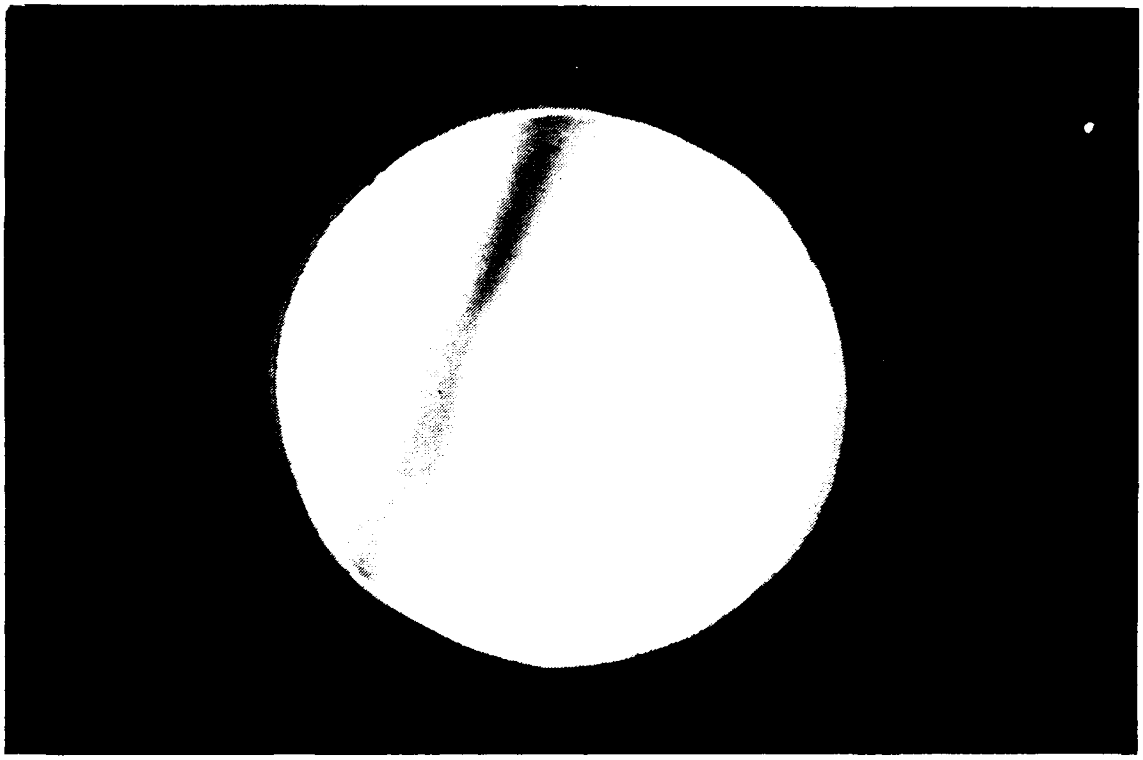

Figure D-2 Ronchigram at Mask 2,

Reticle and Entrance Slit Rotated 30° from Vertical

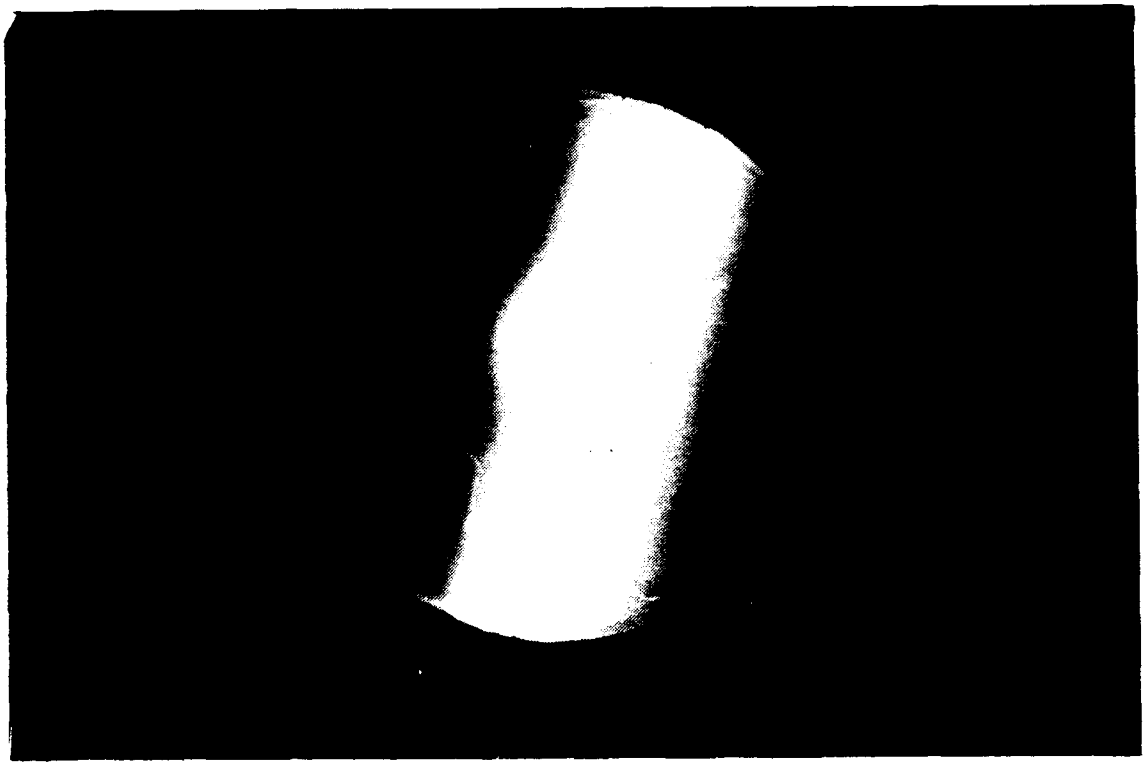

Figure D-3 Ronchigram at Mask 1,

Reticle and Entrance Slit Rotated 60° from Vertical

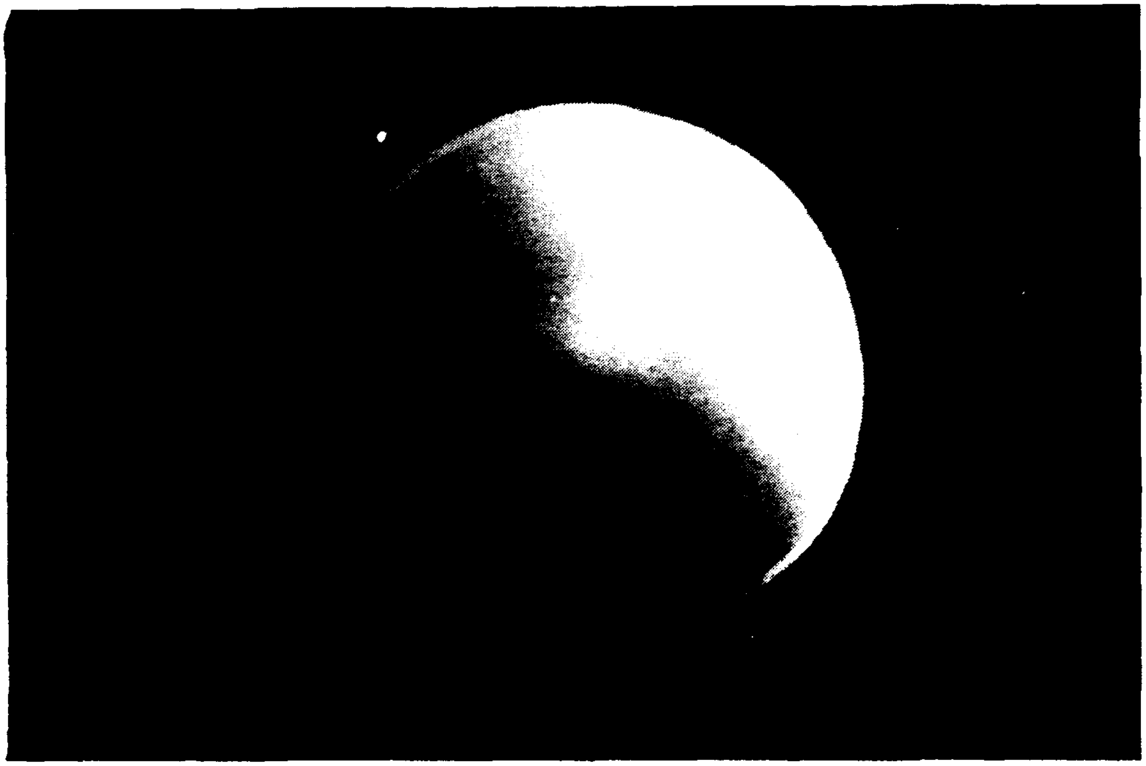

Figure D-3 Ronchigram at Mask 1,

Reticle and Entrance Slit Rotated 90° from Vertical

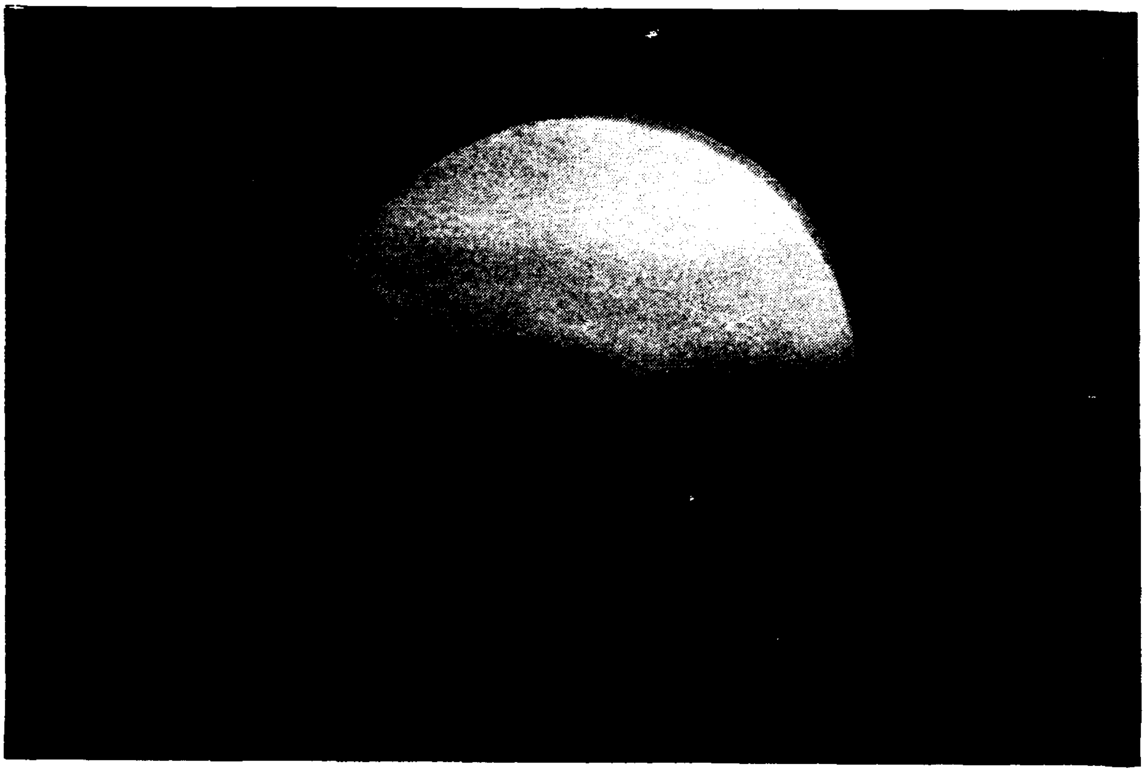

Figure D-5 Ronchigram at Mask 1

Reticle and Entrance Slit Rotated 120° from Vertical

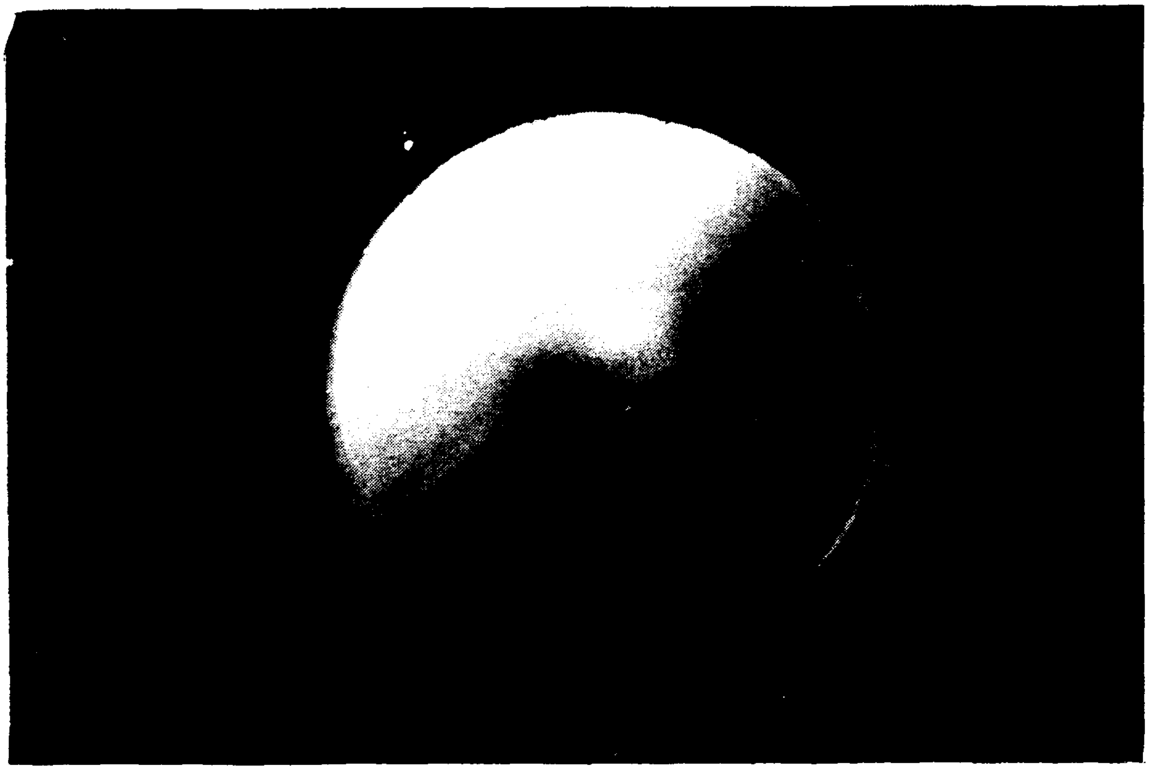

Figure D-6 Ronchigram at Mask 1,

Reticle and Entrance Slit Rotated 150° from Vertical

APPENDIX E

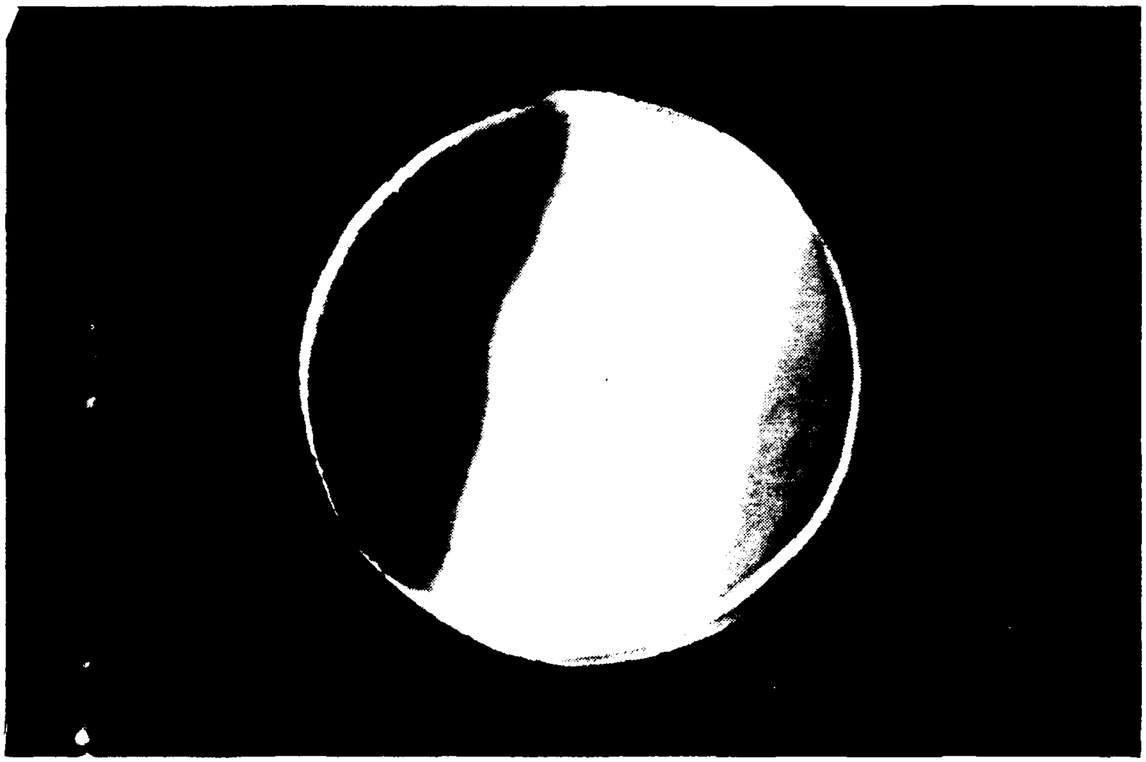

Figure E-1 Ronchigram at Mask 2, Vertical Reticle and Entrance Slit

Figure E-2 Ronchigram at Mask 2,

Reticle and Entrance Slit Rotated 30° from Vertical

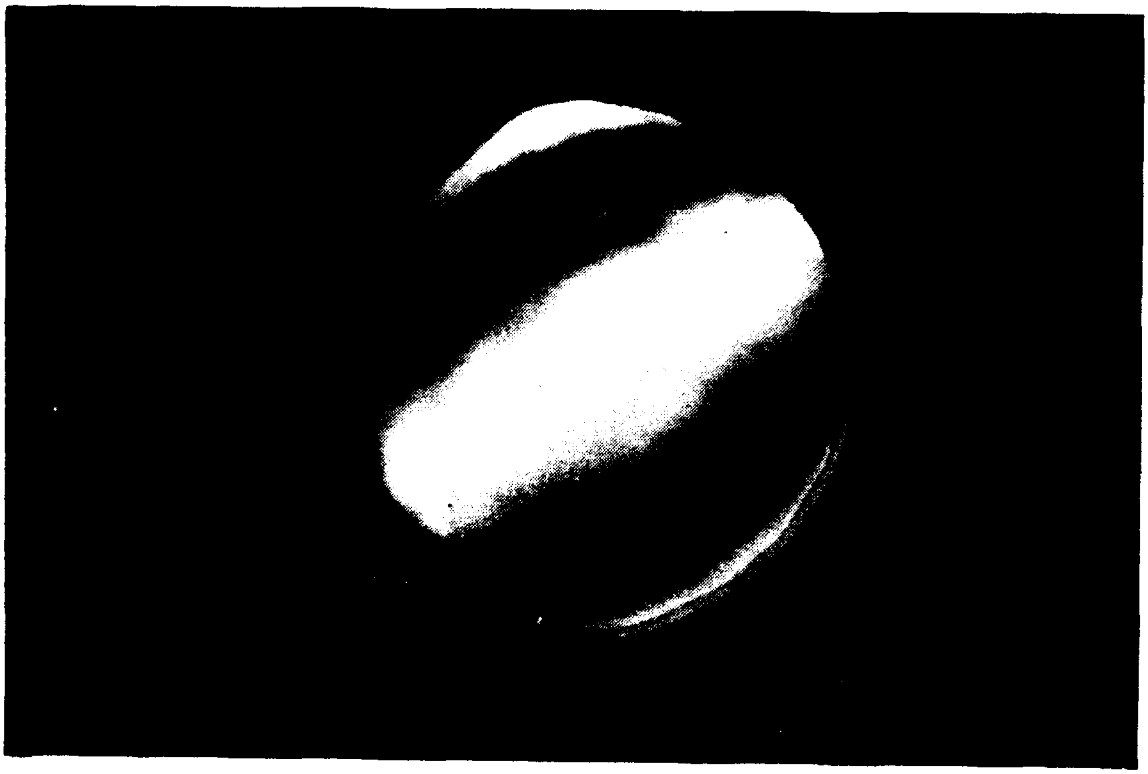

Figure E-3 Ronchigram at Mask 2,

Reticle and Entrance Slit Rotated 60° from Vertical

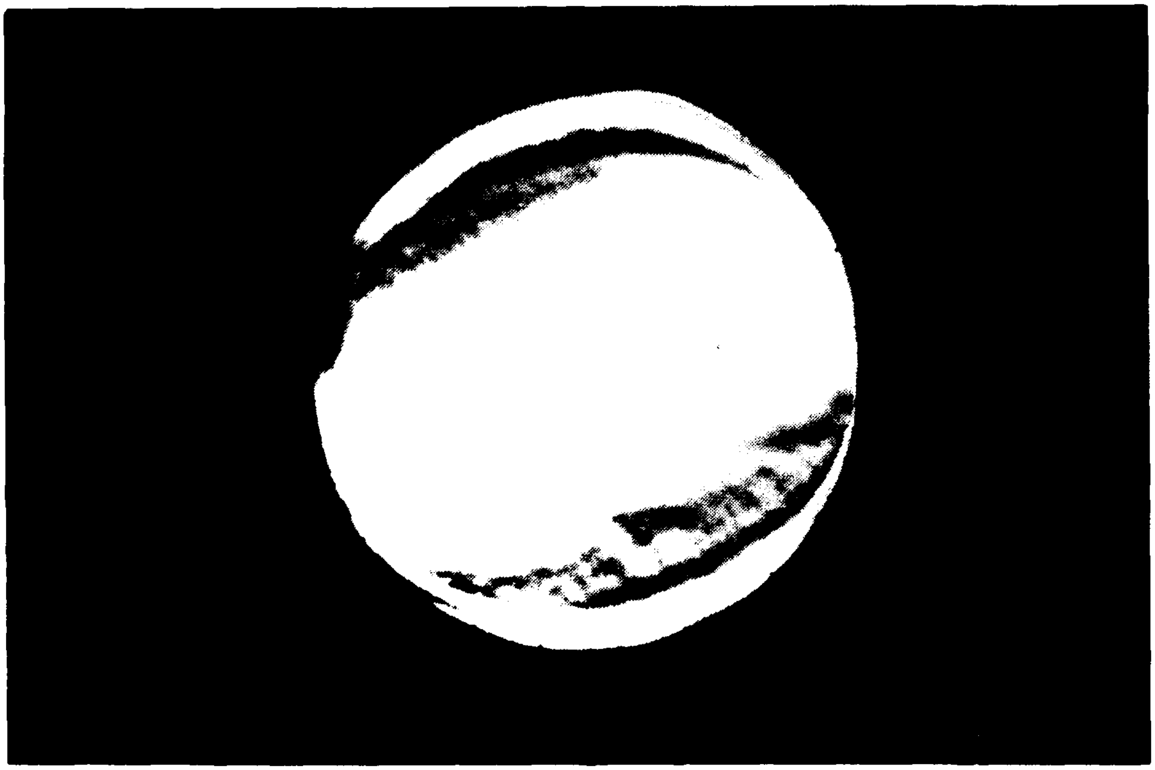

Figure E-4 Ronchigram at Mask 2,

Reticle and Entrance Slit Rotated 90° from Vertical

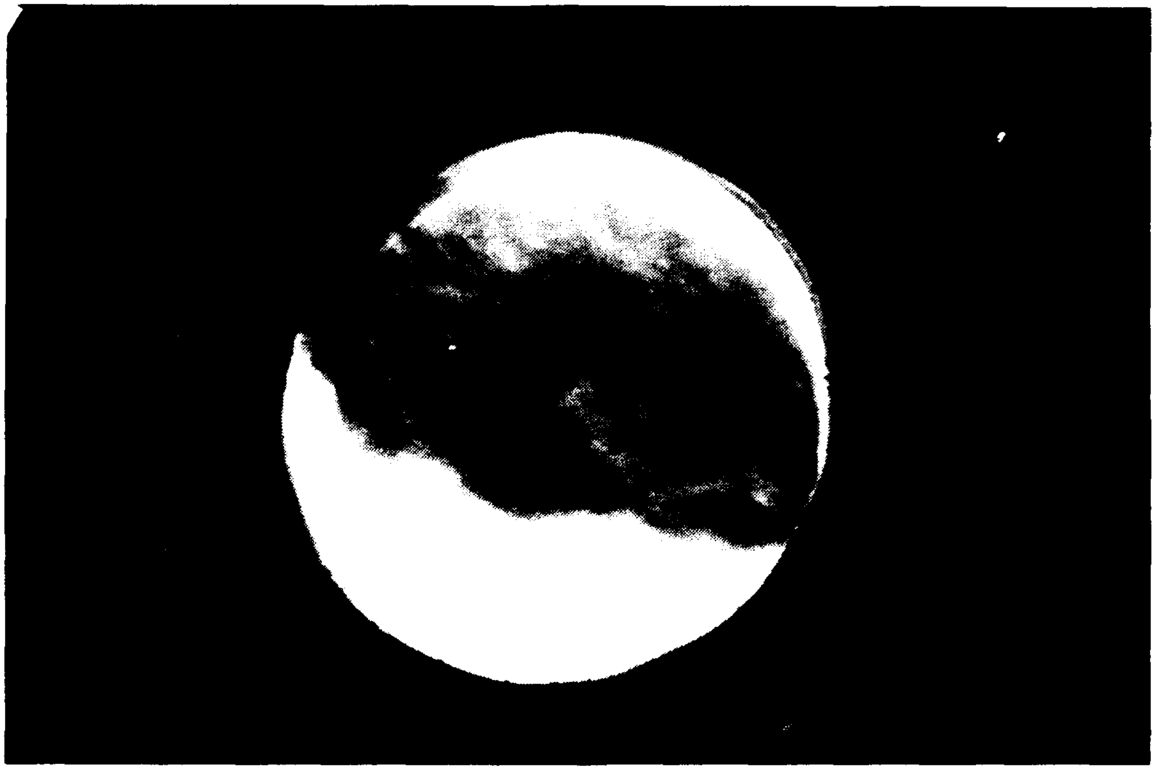

Figure E-5 Ronchigram at Mask 2,

Reticle and Entrance Slit Rotated 120° from Vertical

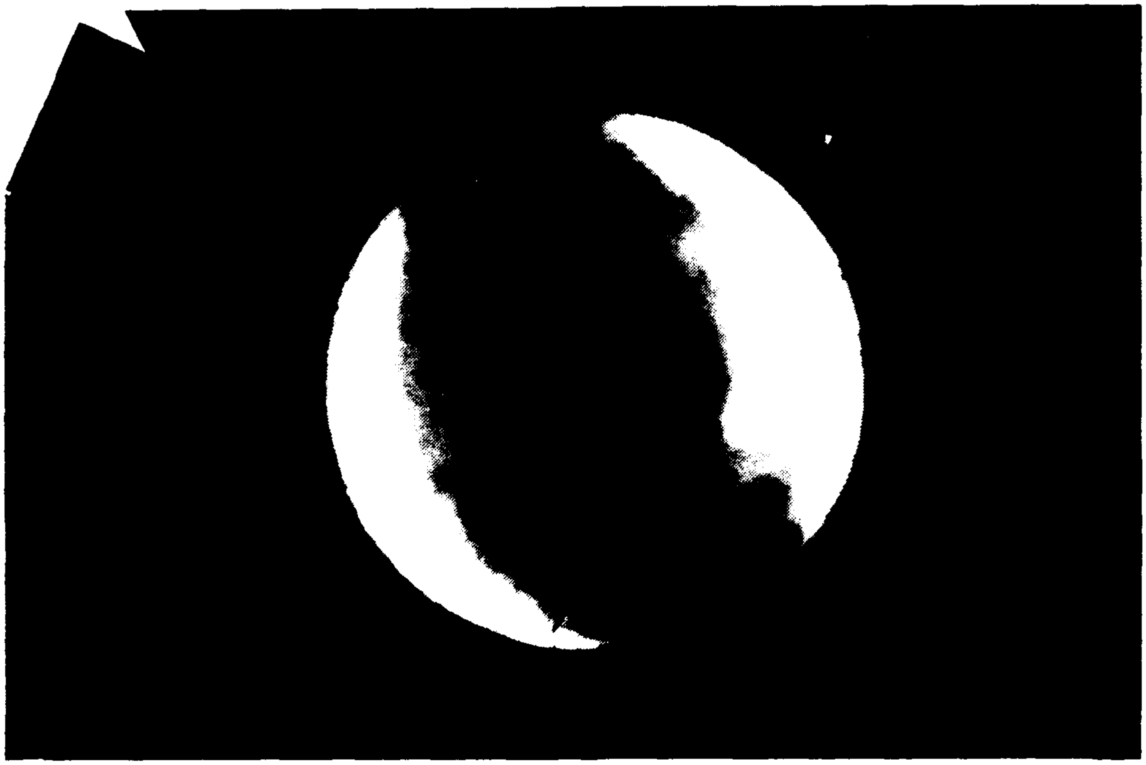

Figure E-6 Ronchigram at Mask 2,

Reticle and Entrance Slit Rotated 150° from Vertical

APPENDIX F

KEY FOR APPENDIX F

SPOT1.XXX tables were used to produce line spread functions to determine the radius of curvature for Mirror 1 (R = 60"). SPOT2.XXX tables were used to produce line spread functions to determine the radius of curvature for Mirror 2 (R = 50"). The SPOTS.OPT table was used with SPOTS.RAY (horizontal line) and SPOTZ.RAY (vertical line) tables to produce a line spread function at Mask 2. SPOTS1.RAY (horizontal line) and SPOTZ1.RAY (vertical line) tables were used to produce line spread functions at Mask 1. Ray tables with an "a" (XXXXXa.RAY) were used for P45, ray tables with a "b" (XXXXXb.RAY) were used for P25i, and ray tables without an "a" or "b" were used for P25o.

2 surfaces SPOT1.OPT

Z	pitch	curve	figure	mirror	Diameter		
59.96	-0.6162	-0.016678	circle	mirror	3.0		
			square	iris			

25 rays SPOT1.RAY

X0	Y0	@WAVE	U0	V0	Xf	Yf	Xg	Yg
1.39			r -2.318 e-2		-0.1000	0.0000	-0.1	
1.39			r -2.318 e-2	2.40 e-2	-0.1000	-0.0002	-0.1	
1.39			r -2.318 e-2	-2.40 e-2	-0.1000	0.0002	-0.1	
1.39			r -4.70 e-2		-0.0994	0.0000	-0.1	
1.39			r 0.42 e-3		-0.1007	0.0000	-0.1	
1.34			g -2.21 e-2		-0.0501	0.0000	-0.05	
1.34			g -2.234 e-2	2.48 e-2	-0.0501	-0.0002	-0.05	
1.34			g -2.234 e-2	-2.48 e-2	-0.0501	0.0002	-0.05	
1.34			g -4.64 e-2		-0.0495	0.0000	-0.05	
1.34			g 1.26 e-3		-0.0507	0.0000	-0.05	
1.29			c -2.15 e-2		-0.0001	0.0000		
1.29			c -2.15 e-2	-2.5 e-2	-0.0001	0.0002		
1.29			c -2.15 e-2	2.5 e-2	-0.0001	-0.0002		
1.29			c -4.54 e-2		0.0004	0.0000		
1.29			c 0.3 e-2		-0.0006	0.0000		
1.24			b -2.068 e-2		0.0499	0.0000	0.05	
1.24			b -2.068 e-2	-2.48 e-2	0.0499	0.0002	0.05	
1.24			b -2.068 e-2	2.48 e-2	0.0499	-0.0002	0.05	
1.24			b 0.32 e-2		0.0494	0.0000	0.05	
1.24			b -4.46 e-2		0.0504	0.0000	0.05	
1.19			m -1.984 e-2		0.0999	0.0000	0.1	
1.19			m -1.984 e-2	-2.41 e-2	0.0999	0.0002	0.1	
1.19			m -1.984 e-2	2.41 e-2	0.0999	-0.0002	0.1	
1.19			m -4.34 e-2		0.1003	0.0000	0.1	
1.19			m 0.38 e-2		0.0994	0.0000	0.1	

2 surfaces SPOT2.OPT

Z	pitch	curve	figure	mirror	Diameter		
50.67	-0.7292	-0.019735	circle	mirror	2.5		
			square	iris			

25 rays SPOT2.RAY

X0	Y0	@WAVE	U0	V0	Xf	Yf	Xg	Yg	Note
1.39		r	-2.742 e-2		-0.0999	0.0000	-0.1		ok 2
1.39		r	-2.742 e-2	2.34 e-2	-0.0999	-0.0001	-0.1		ok 2
1.39		r	-2.742 e-2	-2.34 e-2	-0.0999	0.0001	-0.1		ok 2
1.39		r	-5.07 e-2		-0.0993	0.0000	-0.1		ok 2
1.39		r	-0.39 e-2		-0.1005	0.0000	-0.1		ok 2
1.34		g	-2.644 e-2		-0.0499	0.0000	-0.05		ok 2
1.34		g	-2.644 e-2	2.23 e-2	-0.0499	-0.0001	-0.05		ok 2
1.34		g	-2.644 e-2	-2.44 e-2	-0.0499	0.0001	-0.05		ok 2
1.34		g	-4.92 e-2		-0.0494	0.0000	-0.05		ok 2
1.34		g	-0.29 e-2		-0.0505	0.0000	-0.05		ok 2
1.29		c	-2.545 e-2		0.0000	0.0000			ok 2
1.29		c	-2.545 e-2	-2.35 e-2	0.0000	0.0001			ok 2
1.29		c	-2.545 e-2	2.35 e-2	0.0000	-0.0001			ok 2
1.29		c	-4.87 e-2		0.0005	0.0000			ok 2
1.29		c	-0.2 e-2		-0.0005	0.0000			ok 2
1.24		b	-2.446 e-2		0.0500	0.0000	0.05		ok 2
1.24		b	-2.446 e-2	-2.30 e-2	0.0500	0.0001	0.05		ok 2
1.24		b	-2.446 e-2	2.30 e-2	0.0500	-0.0001	0.05		ok 2
1.24		b	-0.14 e-2		0.0495	0.0000	0.05		ok 2
1.24		b	-4.77 e-2		0.0504	0.0000	0.05		ok 2
1.19		m	-2.347 e-2		0.1000	0.0000	0.1		ok 2
1.19		m	-2.347 e-2	-2.35 e-2	0.1000	0.0001	0.1		ok 2
1.19		m	-2.347 e-2	2.35 e-2	0.1000	-0.0001	0.1		ok 2
1.19		m	-4.70 e-2		0.1004	0.0000	0.1		ok 2
1.19		m			0.0996	0.0000	0.1		ok 2

4 Surfaces SPOTS.OPT

X	Z	Tilt	Pitch	Curve	Figure	Mirror	Diam
0.0	59.4284	-4.3996	-1.4283	-0.0167	Circ	Mirror	2.9
0.0	0.0		3.4447		Square	Mirror	4.0
6.0000	50.3747	-0.0054	3.3989;	-0.0197	Circ	Mirror	3.00
5.9892	-0.3605		3.4447		Square	Iris	4.0

25 rays SPOTS.RAY

X0	Y0	Z0	U 0	V0	Xfinal	Yfinal	Xgoal	Ygoal	note
2.9946	-9.3224	-0.1803	-4.96 e-2	15.43 e-2	5.988	-0.096	5.9892	-0.1	ok 4
2.9946	-9.3224	-0.1803	-4.95 e-2	17.75 e-2	5.983	-0.092	5.9892	-0.1	ok 4
2.9946	-9.3224	-0.1803	-4.96 e-2	13.10 e-2	5.994	-0.100	5.9892	-0.1	ok 4
2.9946	-9.3224	-0.1803	-2.56 e-2	15.43 e-2	5.985	-0.102	5.9892	-0.1	ok 4
2.9946	-9.3224	-0.1803	-7.31 e-2	15.43 e-2	5.992	-0.090	5.9892	-0.1	ok 4
2.9946	-9.2724	-0.1803	-4.955 e-2	15.35 e-2	5.989	-0.048	5.9892	-0.05	ok 4
2.9946	-9.2724	-0.1803	-4.955 e-2	17.71 e-2	5.983	-0.044	5.9892	-0.05	ok 4
2.9946	-9.2724	-0.1803	-4.955 e-2	13.05 e-2	5.994	-0.051	5.9892	-0.05	ok 4
2.9946	-9.2724	-0.1803	-2.56 e-2	15.35 e-2	5.985	-0.053	5.9892	-0.05	ok 4
2.9946	-9.2724	-0.1803	-7.31 e-2	15.35 e-2	5.992	-0.042	5.9892	-0.05	ok 4
2.9946	-9.2224	-0.1803	-4.96 e-2	15.27 e-2	5.989	0.001	5.9892		ok 4
2.9946	-9.2224	-0.1803	-4.95 e-2	17.61 e-2	5.983	0.003	5.9892		ok 4
2.9946	-9.2224	-0.1803	-4.96 e-2	12.95 e-2	5.994	-0.003	5.9892		ok 4
2.9946	-9.2224	-0.1803	-2.56 e-2	15.28 e-2	5.985	-0.005	5.9892		ok 4
2.9946	-9.2224	-0.1803	-7.31 e-2	15.26 e-2	5.992	0.006	5.9892		ok 4
2.9946	-9.1724	-0.1803	-4.96 e-2	15.19 e-2	5.989	0.049	5.9892	0.05	ok 4
2.9946	-9.1724	-0.1803	-4.95 e-2	17.5 e-2	5.984	0.051	5.9892	0.05	ok 4
2.9946	-9.1724	-0.1803	-4.97 e-2	12.85 e-2	5.994	0.046	5.9892	0.05	ok 4
2.9946	-9.1724	-0.1803	-2.56 e-2	15.20 e-2	5.986	0.044	5.9892	0.05	ok 4
2.9946	-9.1724	-0.1803	-7.31 e-2	15.18 e-2	5.992	0.054	5.9892	0.05	ok 4
2.9946	-9.1224	-0.1803	-4.96 e-2	15.11 e-2	5.989	0.097	5.9892	0.1	ok 4
2.9946	-9.1224	-0.1803	-4.95 e-2	17.4 e-2	5.984	0.099	5.9892	0.1	ok 4
2.9946	-9.1224	-0.1803	-4.97 e-2	12.75 e-2	5.994	0.095	5.9892	0.1	ok 4
2.9946	-9.1224	-0.1803	-2.56 e-2	15.12 e-2	5.986	0.092	5.9892	0.1	ok 4
2.9946	-9.1224	-0.1803	-7.31 e-2	15.10 e-2	5.992	0.102	5.9892	0.1	ok 4

25 rays SPOTS1.RAY

X0	Y0	Z0	U 0	V0	Xfinal	Yfinal	Xgoal	Ygoal	note
2.9946	-9.3224	-0.1803	-4.96 e-2	15.43 e-2	0.007	0.087		-0.1	ok 2
2.9946	-9.3224	-0.1803	-4.95 e-2	17.75 e-2	0.012	0.078		-0.1	ok 2
2.9946	-9.3224	-0.1803	-4.96 e-2	13.10 e-2	0.001	0.097		-0.1	ok 2
2.9946	-9.3224	-0.1803	-2.56 e-2	15.43 e-2	0.013	0.093		-0.1	ok 2
2.9946	-7.3224	-0.1803	-7.31 e-2	15.43 e-2	0.000	0.082		-0.1	ok 2
2.9946	-9.2724	-0.1803	-4.955 e-2	15.35 e-2	0.006	0.038		-0.05	ok 2
2.9946	-9.2724	-0.1803	-4.955 e-2	17.71 e-2	0.012	0.029		-0.05	ok 2
2.9946	-9.2724	-0.1803	-4.955 e-2	13.05 e-2	0.001	0.047		-0.05	ok 2
2.9946	-9.2724	-0.1803	-2.56 e-2	15.35 e-2	0.013	0.044		-0.05	ok 2
2.9946	-9.2724	-0.1803	-7.31 e-2	15.35 e-2	0.000	0.033		-0.05	ok 2
2.9946	-9.2224	-0.1803	-4.96 e-2	15.27 e-2	0.006	-0.010			ok 2
2.9946	-9.2224	-0.1803	-4.95 e-2	17.61 e-2	0.012	-0.019			ok 2
2.9946	-9.2224	-0.1803	-4.96 e-2	12.95 e-2	0.001	-0.001			ok 2
2.9946	-9.2224	-0.1803	-2.56 e-2	15.28 e-2	0.012	-0.005			ok 2
2.9946	-9.2224	-0.1803	-7.31 e-2	15.26 e-2	0.000	-0.016			ok 2
2.9946	-9.1724	-0.1803	-4.96 e-2	15.19 e-2	0.006	-0.059		0.05	ok 2
2.9946	-9.1724	-0.1803	-4.95 e-2	17.5 e-2	0.011	-0.067		0.05	ok 2
2.9946	-9.1724	-0.1803	-4.97 e-2	12.85 e-2	0.001	-0.050		0.05	ok 2
2.9946	-9.1724	-0.1803	-2.56 e-2	15.20 e-2	0.012	-0.053		0.05	ok 2
2.9946	-9.1724	-0.1803	-7.31 e-2	15.18 e-2	-0.000	-0.064		0.05	ok 2
2.9946	-9.1224	-0.1803	-4.96 e-2	15.11 e-2	0.006	-0.107		0.1	ok 2
2.9946	-9.1224	-0.1803	-4.95 e-2	17.4 e-2	0.011	-0.115		0.1	ok 2
2.9946	-9.1224	-0.1803	-4.97 e-2	12.75 e-2	0.000	-0.099		0.1	ok 2
2.9946	-9.1224	-0.1803	-2.56 e-2	15.12 e-2	0.012	-0.102		0.1	ok 2
2.9946	-9.1224	-0.1803	-7.31 e-2	15.10 e-2	-0.000	-0.113		0.1	ok 2

25 rays SPOTZ.RAY

XO	YO	ZO	U O	VO	Xfinal	Yfinal	Xgoal	Ygoal	note
3.0946	-9.2224	-0.1803	-5.12 e-2	15.27 e-2	6.087	0.001	6.0892		ok 4
3.0946	-9.2224	-0.1803	-5.11 e-2	17.61 e-2	6.082	0.004	6.0892		ok 4
3.0946	-9.2224	-0.1803	-5.13 e-2	12.95 e-2	6.093	-0.002	6.0892		ok 4
3.0946	-9.2224	-0.1803	-2.76 e-2	15.28 e-2	6.085	-0.005	6.0892		ok 4
3.0946	-9.2224	-0.1803	-7.47 e-2	15.26 e-2	6.090	0.007	6.0892		ok 4
3.0446	-9.2224	-0.1803	-5.035 e-2	15.27 e-2	6.038	0.001	6.0392		ok 4
3.0446	-9.2224	-0.1803	-5.035 e-2	17.61 e-2	6.033	0.004	6.0392		ok 4
3.0446	-9.2224	-0.1803	-5.055 e-2	12.95 e-2	6.044	-0.002	6.0392		ok 4
3.0446	-9.2224	-0.1803	-2.65 e-2	15.26 e-2	6.035	-0.005	6.0392		ok 4
3.0446	-9.2224	-0.1803	-7.38 e-2	15.27 e-2	6.041	0.006	6.0392		ok 4
2.9946	-9.2224	-0.1803	-4.96 e-2	15.27 e-2	5.989	0.001	5.9392		ok 4
2.9946	-9.2224	-0.1803	-4.95 e-2	17.61 e-2	5.983	0.003	5.9892		ok 4
2.9946	-9.2224	-0.1803	-4.96 e-2	12.95 e-2	5.994	-0.003	5.9892		ok 4
2.9946	-9.2224	-0.1803	-2.56 e-2	15.28 e-2	5.985	-0.005	5.9892		ok 4
2.9946	-9.2224	-0.1803	-7.31 e-2	15.26 e-2	5.992	0.006	5.9892		ok 4
2.9446	-9.2224	-0.1803	-4.88 e-2	15.27 e-2	5.939	0.000	5.9392		ok 4
2.9446	-9.2224	-0.1803	-4.87 e-2	17.57 e-2	5.934	0.003	5.9392		ok 4
2.9446	-9.2224	-0.1803	-4.89 e-2	12.92 e-2	5.945	-0.003	5.9392		ok 4
2.9446	-9.2224	-0.1803	-2.52 e-2	15.28 e-2	5.936	-0.005	5.9392		ok 4
2.9446	-9.2224	-0.1803	-7.26 e-2	15.26 e-2	5.943	0.006	5.9392		ok 4
2.8946	-9.2224	-0.1803	-4.79 e-2	15.28 e-2	5.890	0.000	5.8892		ok 4
2.8946	-9.2224	-0.1803	-4.79 e-2	17.58 e-2	5.885	0.003	5.8892		ok 4
2.8946	-9.2224	-0.1803	-4.80 e-2	12.92 e-2	5.895	-0.003	5.8892		ok 4
2.8946	-9.2224	-0.1803	-2.45 e-2	15.28 e-2	5.886	-0.005	5.8892		ok 4
2.8946	-9.2224	-0.1803	-7.17 e-2	15.27 e-2	5.894	0.005	5.8892		ok 4

25 rays SPOTZ1.RAY

XO	YO	ZO	U O	VO	Xfinal	Yfinal	Xgoal	Ygoal	note
3.0946	-9.2224	-0.1803	-5.12 e-2	15.27 e-2	-0.092	-0.011	-0.1		ok 2
3.0946	-9.2224	-0.1803	-5.11 e-2	17.61 e-2	-0.086	-0.019	-0.1		ok 2
3.0946	-9.2224	-0.1803	-5.13 e-2	12.95 e-2	-0.098	-0.002	-0.1		ok 2
3.0946	-9.2224	-0.1803	-2.76 e-2	15.28 e-2	-0.086	-0.005	-0.1		ok 2
3.0946	-9.2224	-0.1803	-7.47 e-2	15.26 e-2	-0.098	-0.016	-0.1		ok 2
3.0446	-9.2224	-0.1803	-5.035 e-2	15.27 e-2	-0.043	-0.010	-0.05		ok 2
3.0446	-9.2224	-0.1803	-5.035 e-2	17.61 e-2	-0.037	-0.019	-0.05		ok 2
3.0446	-9.2224	-0.1803	-5.055 e-2	12.95 e-2	-0.048	-0.002	-0.05		ok 2
3.0446	-9.2224	-0.1803	-2.65 e-2	15.26 e-2	-0.037	-0.005	-0.05		ok 2
3.0446	-9.2224	-0.1803	-7.38 e-2	15.27 e-2	-0.049	-0.016	-0.05		ok 2
2.9946	-9.2224	-0.1803	-4.96 e-2	15.27 e-2	0.006	-0.010			ok 2
2.9946	-9.2224	-0.1803	-4.95 e-2	17.61 e-2	0.012	-0.019			ok 2
2.9946	-9.2224	-0.1803	-4.96 e-2	12.95 e-2	0.001	-0.001			ok 2
2.9946	-9.2224	-0.1803	-2.56 e-2	15.28 e-2	0.012	-0.005			ok 2
2.9946	-9.2224	-0.1803	-7.31 e-2	15.26 e-2	0.000	-0.016			ok 2
2.9446	-9.2224	-0.1803	-4.88 e-2	15.27 e-2	0.055	-0.010	0.05		ok 2
2.9446	-9.2224	-0.1803	-4.87 e-2	17.57 e-2	0.060	-0.019	0.05		ok 2
2.9446	-9.2224	-0.1803	-4.89 e-2	12.92 e-2	0.050	-0.001	0.05		ok 2
2.9446	-9.2224	-0.1803	-2.52 e-2	15.28 e-2	0.062	-0.005	0.05		ok 2
2.9446	-9.2224	-0.1803	-7.26 e-2	15.26 e-2	0.049	-0.015	0.05		ok 2
2.8946	-9.2224	-0.1803	-4.79 e-2	15.28 e-2	0.105	-0.010	0.1		ok 2
2.8946	-9.2224	-0.1803	-4.79 e-2	17.58 e-2	0.109	-0.018	0.1		ok 2
2.8946	-9.2224	-0.1803	-4.80 e-2	12.92 e-2	0.099	-0.001	0.1		ok 2
2.8946	-9.2224	-0.1803	-2.45 e-2	15.28 e-2	0.111	-0.005	0.1		ok 2
2.8946	-9.2224	-0.1803	-7.17 e-2	15.27 e-2	0.098	-0.015	0.1		ok 2

45 rays SPOT1a.RAY

X0	Y0	@WAVE	U0	V0	Xf	Yf	Xg	Yg	Note
1.39		r	-2.318 e-2		-0.1000	0.0000	-0.1		ok 2
1.39		r	-2.318 e-2	2.40 e-2	-0.1000	-0.0002	-0.1		ok 2
1.39		r	-2.318 e-2	-2.40 e-2	-0.1000	0.0002	-0.1		ok 2
1.39			-2.318 e-2	1.20 e-2	-0.1000	-0.0001	-0.1		ok 2
1.39			-2.318 e-2	-1.20 e-2	-0.1000	0.0001	-0.1		ok 2
1.39		r	-4.70 e-2		-0.0994	0.0000	-0.1		ok 2
1.39		r	0.42 e-3		-0.1007	0.0000	-0.1		ok 2
1.39			-3.51 e-2		-0.0997	0.0000	-0.1		ok 2
1.39			-1.15 e-2		-0.1004	0.0000	-0.1		ok 2
1.34		g	-2.21 e-2		-0.0501	0.0000	-0.05		ok 2
1.34		g	-2.234 e-2	2.48 e-2	-0.0501	-0.0002	-0.05		ok 2
1.34		g	-2.234 e-2	-2.48 e-2	-0.0501	0.0002	-0.05		ok 2
1.34		g	-4.64 e-2		-0.0495	0.0000	-0.05		ok 2
1.34		g	1.26 e-3		-0.0507	0.0000	-0.05		ok 2
1.34			-2.234 e-2	1.24 e-2	-0.0501	-0.0001	-0.05		ok 2
1.34			-2.234 e-2	-1.24 e-2	-0.0501	0.0001	-0.05		ok 2
1.34			-3.48 e-2		-0.0498	0.0000	-0.05		ok 2
1.34			-0.98 e-2		-0.0504	0.0000	-0.05		ok 2
1.29		c	-2.15 e-2		-0.0001	0.0000			ok 2
1.29		c	-2.15 e-2	-2.5 e-2	-0.0001	0.0002			ok 2
1.29		c	-2.15 e-2	2.5 e-2	-0.0001	-0.0002			ok 2
1.29			-2.15 e-2	-1.25 e-2	-0.0001	0.0001			ok 2
1.29			-2.15 e-2	1.25 e-2	-0.0001	-0.0001			ok 2
1.29		c	-4.54 e-2		0.0004	0.0000			ok 2
1.29		c	0.3 e-2		-0.0006	0.0000			ok 2
1.29			-3.42 e-2		0.0002	0.0000			ok 2
1.29			-0.9 e-2		-0.0004	0.0000			ok 2
1.24		b	-2.068 e-2		0.0499	0.0000	0.05		ok 2
1.24		b	-2.068 e-2	-2.48 e-2	0.0499	0.0002	0.05		ok 2
1.24		b	-2.068 e-2	2.48 e-2	0.0499	-0.0002	0.05		ok 2
1.24			-2.068 e-2	-1.24 e-2	0.0499	0.0001	0.05		ok 2
1.24			-2.068 e-2	1.24 e-2	0.0499	-0.0001	0.05		ok 2
1.24		b	0.32 e-2		0.0494	0.0000	0.05		ok 2
1.24		b	-4.46 e-2		0.0504	0.0000	0.05		ok 2
1.24			-3.34 e-2		0.0501	0.0000	0.05		ok 2
1.24			-0.83 e-2		0.0496	0.0000	0.05		ok 2
1.19		m	-1.984 e-2		0.0999	0.0000	0.1		ok 2
1.19		m	-1.984 e-2	-2.41 e-2	0.0999	0.0002	0.1		ok 2
1.19		m	-1.984 e-2	2.41 e-2	0.0999	-0.0002	0.1		ok 2
1.19			-1.984 e-2	-1.2 e-2	0.0999	0.0001	0.1		ok 2
1.19			-1.984 e-2	1.2 e-2	0.0999	-0.0001	0.1		ok 2
1.19		m	-4.34 e-2		0.1003	0.0000	0.1		ok 2
1.19		m	0.38 e-2		0.0994	0.0000	0.1		ok 2
1.19			-3.26 e-2		0.1001	0.0000	0.1		ok 2
1.19			-0.75 e-2		0.0996	0.0000	0.1		ok 2

45 rays SPOT2a.RAY

X0	Y0	@WAVE	U0	V0	Xf	Yf	Xg	Yg	Note
1.39		r	-2.742 e-2		-0.0999	0.0000	-0.1		ok 2
1.39		r	-2.742 e-2	2.34 e-2	-0.0999	-0.0001	-0.1		ok 2
1.39		r	-2.742 e-2	-2.34 e-2	-0.0999	0.0001	-0.1		ok 2
1.39			-2.742 e-2	1.17 e-2	-0.0999	-0.0001	-0.1		ok 2
1.39			-2.742 e-2	-1.17 e-2	-0.0999	0.0001	-0.1		ok 2
1.39		r	-5.07 e-2		-0.0993	0.0000	-0.1		ok 2
1.39		r	-0.39 e-2		-0.1005	0.0000	-0.1		ok 2
1.39			-3.9 e-2		-0.0996	0.0000	-0.1		ok 2
1.39			-1.55 e-2		-0.1002	0.0000	-0.1		ok 2
1.34		g	-2.644 e-2		-0.0499	0.0000	-0.05		ok 2
1.34		g	-2.644 e-2	2.33 e-2	-0.0499	-0.0001	-0.05		ok 2
1.34		g	-2.644 e-2	-2.33 e-2	-0.0499	0.0001	-0.05		ok 2
1.34			-2.644 e-2	1.16 e-2	-0.0499	-0.0001	-0.05		ok 2
1.34			-2.644 e-2	-1.16 e-2	-0.0499	0.0001	-0.05		ok 2
1.34		g	-4.92 e-2		-0.0494	0.0000	-0.05		ok 2
1.34		g	-0.29 e-2		-0.0505	0.0000	-0.05		ok 2
1.34			-3.8 e-2		-0.0497	0.0000	-0.05		ok 2
1.34			-1.48 e-2		-0.0502	0.0000	-0.05		ok 2
1.29		c	-2.545 e-2		0.0000	0.0000			ok 2
1.29		c	-2.545 e-2	-2.35 e-2	0.0000	0.0001			ok 2
1.29		c	-2.545 e-2	2.35 e-2	0.0000	-0.0001			ok 2
1.29			-2.545 e-2	-1.17 e-2	0.0000	0.0001			ok 2
1.29			-2.545 e-2	1.17 e-2	0.0000	-0.0001			ok 2
1.29		c	-4.87 e-2		0.0005	0.0000			ok 2
1.29		c	-0.2 e-2		-0.0005	0.0000			ok 2
1.29			-3.7 e-2		0.0003	0.0000			ok 2
1.29			-1.4 e-2		-0.0002	0.0000			ok 2
1.24		b	-2.446 e-2		0.0500	0.0000	0.05		ok 2
1.24		b	-2.446 e-2	-2.30 e-2	0.0500	0.0001	0.05		ok 2
1.24		b	-2.446 e-2	2.30 e-2	0.0500	-0.0001	0.05		ok 2
1.24			-2.446 e-2	-1.15 e-2	0.0500	0.0001	0.05		ok 2
1.24			-2.446 e-2	1.15 e-2	0.0500	-0.0001	0.05		ok 2
1.24		b	-0.14 e-2		0.0495	0.0000	0.05		ok 2
1.24		b	-4.77 e-2		0.0504	0.0000	0.05		ok 2
1.24			-3.60 e-2		0.0502	0.0000	0.05		ok 2
1.24			-1.3 e-2		0.0498	0.0000	0.05		ok 2
1.19		m	-2.347 e-2		0.1000	0.0000	0.1		ok 2
1.19		m	-2.347 e-2	-2.35 e-2	0.1000	0.0001	0.1		ok 2
1.19		m	-2.347 e-2	2.35 e-2	0.1000	-0.0001	0.1		ok 2
1.19			-2.347 e-2	-1.18 e-2	0.1000	0.0001	0.1		ok 2
1.19			-2.347 e-2	1.18 e-2	0.1000	-0.0001	0.1		ok 2
1.19		m	-4.70 e-2		0.1004	0.0000	0.1		ok 2
1.19		m			0.0996	0.0000	0.1		ok 2
1.19			-3.50 e-2		0.1002	0.0000	0.1		ok 2
1.19			-1.2 e-2		0.0998	0.0000	0.1		ok 2

45 rays SPOTS1a.RAY

X0	Y0	Z0	U 0	V0	Xfinal	Yfinal	Xgoal	Ygoal	note
2.9946	-9.3224	-0.1803	-4.96 e-2	15.43 e-2	0.007	0.087		-0.1	ok 2
2.9946	-9.3224	-0.1803	-4.95 e-2	17.75 e-2	0.012	0.078		-0.1	ok 2
2.9946	-9.3224	-0.1803	-4.96 e-2	13.10 e-2	0.001	0.097		-0.1	ok 2
2.9946	-9.3224	-0.1803	-4.96 e-2	16.58 e-2	0.009	0.082		-0.1	ok 2
2.9946	-9.3224	-0.1803	-4.96 e-2	14.25 e-2	0.004	0.092		-0.1	ok 2
2.9946	-9.3224	-0.1803	-2.56 e-2	15.43 e-2	0.013	0.093		-0.1	ok 2
2.9946	-9.3224	-0.1803	-7.31 e-2	15.43 e-2	0.000	0.082		-0.1	ok 2
2.9946	-9.3224	-0.1803	-3.76 e-2	15.43 e-2	0.010	0.090		-0.1	ok 2
2.9946	-9.3224	-0.1803	-6.1 e-2	15.43 e-2	0.004	0.084		-0.1	ok 2
2.9946	-9.2724	-0.1803	-4.955 e-2	15.35 e-2	0.006	0.038		-0.05	ok 2
2.9946	-9.2724	-0.1803	-4.955 e-2	17.71 e-2	0.012	0.029		-0.05	ok 2
2.9946	-9.2724	-0.1803	-4.955 e-2	13.05 e-2	0.001	0.047		-0.05	ok 2
2.9946	-9.2724	-0.1803	-4.955 e-2	16.55 e-2	0.009	0.034		-0.05	ok 2
2.9946	-9.2724	-0.1803	-4.955 e-2	14.15 e-2	0.004	0.043		-0.05	ok 2
2.9946	-9.2724	-0.1803	-2.56 e-2	15.35 e-2	0.013	0.044		-0.05	ok 2
2.9946	-9.2724	-0.1803	-7.31 e-2	15.35 e-2	0.000	0.033		-0.05	ok 2
2.9946	-9.2724	-0.1803	-3.8 e-2	15.35 e-2	0.009	0.041		-0.05	ok 2
2.9946	-9.2724	-0.1803	-6.15 e-2	15.35 e-2	0.003	0.036		-0.05	ok 2
2.9946	-9.2224	-0.1803	-4.96 e-2	15.27 e-2	0.006	-0.010			ok 2
2.9946	-9.2224	-0.1803	-4.95 e-2	17.61 e-2	0.012	-0.019			ok 2
2.9946	-9.2224	-0.1803	-4.96 e-2	12.95 e-2	0.001	-0.001			ok 2
2.9946	-9.2224	-0.1803	-4.96 e-2	16.4 e-2	0.009	-0.014			ok 2
2.9946	-9.2224	-0.1803	-4.96 e-2	14.1 e-2	0.004	-0.006			ok 2
2.9946	-9.2224	-0.1803	-2.56 e-2	15.27 e-2	0.012	-0.005			ok 2
2.9946	-9.2224	-0.1803	-7.31 e-2	15.27 e-2	0.000	-0.016			ok 2
2.9946	-9.2224	-0.1803	-3.70 e-2	15.27 e-2	0.009	-0.007			ok 2
2.9946	-9.2224	-0.1803	-6.1 e-2	15.27 e-2	0.003	-0.013			ok 2
2.9946	-9.1724	-0.1803	-4.96 e-2	15.19 e-2	0.006	-0.059		0.05	ok 2
2.9946	-9.1724	-0.1803	-4.95 e-2	17.5 e-2	0.011	-0.067		0.05	ok 2
2.9946	-9.1724	-0.1803	-4.97 e-2	12.85 e-2	0.001	-0.050		0.05	ok 2
2.9946	-9.1724	-0.1803	-4.96 e-2	16.35 e-2	0.009	-0.063		0.05	ok 2
2.9946	-9.1724	-0.1803	-4.96 e-2	14.05 e-2	0.003	-0.055		0.05	ok 2
2.9946	-9.1724	-0.1803	-2.56 e-2	15.20 e-2	0.012	-0.053		0.05	ok 2
2.9946	-9.1724	-0.1803	-7.31 e-2	15.18 e-2	-0.000	-0.064		0.05	ok 2
2.9946	-9.1724	-0.1803	-3.85 e-2	15.19 e-2	0.009	-0.056		0.05	ok 2
2.9946	-9.1724	-0.1803	-6.1 e-2	15.19 e-2	0.003	-0.061		0.05	ok 2
2.9946	-9.1224	-0.1803	-4.96 e-2	15.11 e-2	0.006	-0.107		0.1	ok 2
2.9946	-9.1224	-0.1803	-4.95 e-2	17.4 e-2	0.011	-0.115		0.1	ok 2
2.9946	-9.1224	-0.1803	-4.97 e-2	12.75 e-2	0.000	-0.099		0.1	ok 2
2.9946	-9.1224	-0.1803	-4.96 e-2	16.25 e-2	0.008	-0.111		0.1	ok 2
2.9946	-9.1224	-0.1803	-4.96 e-2	13.9 e-2	0.003	-0.103		0.1	ok 2
2.9946	-9.1224	-0.1803	-2.56 e-2	15.12 e-2	0.012	-0.102		0.1	ok 2
2.9946	-9.1224	-0.1803	-7.31 e-2	15.10 e-2	-0.000	-0.113		0.1	ok 2
2.9946	-9.1224	-0.1803	-3.85 e-2	15.1 e-2	0.009	-0.105		0.1	ok 2
2.9946	-9.1224	-0.1803	-6.1 e-2	15.1 e-2	0.003	-0.110		0.1	ok 2

```
45 rays                             SPOTSa.RAY
  XO         YO         ZO           U O         VO         Xfinal  Yfinal Xgoal   Ygoal    note
------:-------:-------:-----------:---------:-------:------:-------:-----:-----
2.9946:-9.3224:-0.1803:-4.96   e-2:15.43 e-2:  5.988:-0.096:5.9892 :-0.1 :ok   4
2.9946:-9.3224:-0.1803:-4.95   e-2:17.75 e-2:  5.983:-0.092:5.9892 :-0.1 :ok   4
2.9946:-9.3224:-0.1803:-4.96   e-2:13.10 e-2:  5.994:-0.100:5.9892 :-0.1 :ok   4
2.9946:-9.3224:-0.1803:-4.96   e-2:16.58 e-2:  5.986:-0.094:5.9892 :-0.1 :ok   4
2.9946:-9.3224:-0.1803:-4.96   e-2:14.25 e-2:  5.991:-0.098:5.9892 :-0.1 :ok   4
2.9946:-9.3224:-0.1803:-2.56   e-2:15.43 e-2:  5.985:-0.102:5.9892 :-0.1 :ok   4
2.9946:-9.3224:-0.1803:-7.31   e-2:15.43 e-2:  5.992:-0.090:5.9892 :-0.1 :ok   4
2.9946:-9.3224:-0.1803:-3.76   e-2:15.43 e-2:  5.987:-0.099:5.9892 :-0.1 :ok   4
2.9946:-9.3224:-0.1803:-6.1    e-2:15.43 e-2:  5.990:-0.093:5.9892 :-0.1 :ok   4
2.9946:-9.2724:-0.1803:-4.955  e-2:15.35 e-2:  5.989:-0.048:5.9892 :-0.05:ok   4
2.9946:-9.2724:-0.1803:-4.955  e-2:17.71 e-2:  5.983:-0.044:5.9892 :-0.05:ok   4
2.9946:-9.2724:-0.1803:-4.955  e-2:13.05 e-2:  5.994:-0.051:5.9892 :-0.05:ok   4
2.9946:-9.2724:-0.1803:-4.955  e-2:16.55 e-2:  5.986:-0.046:5.9892 :-0.05:ok   4
2.9946:-9.2724:-0.1803:-4.955  e-2:14.15 e-2:  5.991:-0.049:5.9892 :-0.05:ok   4
2.9946:-9.2724:-0.1803:-2.56   e-2:15.35 e-2:  5.985:-0.053:5.9892 :-0.05:ok   4
2.9946:-9.2724:-0.1803:-7.31   e-2:15.35 e-2:  5.992:-0.042:5.9892 :-0.05:ok   4
2.9946:-9.2724:-0.1803:-3.8    e-2:15.35 e-2:  5.987:-0.050:5.9892 :-0.05:ok   4
2.9946:-9.2724:-0.1803:-6.15   e-2:15.35 e-2:  5.990:-0.045:5.9892 :-0.05:ok   4
2.9946:-9.2224:-0.1803:-4.96   e-2:15.27 e-2:  5.989: 0.001:5.9892 :     :ok   4
2.9946:-9.2224:-0.1803:-4.95   e-2:17.61 e-2:  5.983: 0.003:5.9892 :     :ok   4
2.9946:-9.2224:-0.1803:-4.96   e-2:12.95 e-2:  5.994:-0.003:5.9892 :     :ok   4
2.9946:-9.2224:-0.1803:-4.96   e-2:16.4  e-2:  5.986: 0.002:5.9892 :     :ok   4
2.9946:-9.2224:-0.1803:-4.96   e-2:14.1  e-2:  5.991:-0.001:5.9892 :     :ok   4
2.9946:-9.2224:-0.1803:-2.56   e-2:15.27 e-2:  5.985:-0.005:5.9892 :     :ok   4
2.9946:-9.2224:-0.1803:-7.31   e-2:15.27 e-2:  5.992: 0.006:5.9892 :     :ok   4
2.9946:-9.2224:-0.1803:-3.70   e-2:15.27 e-2:  5.987:-0.002:5.9892 :     :ok   4
2.9946:-9.2224:-0.1803:-6.1    e-2:15.27 e-2:  5.990: 0.003:5.9892 :     :ok   4
2.9946:-9.1724:-0.1803:-4.96   e-2:15.19 e-2:  5.989: 0.049:5.9892 : 0.05:ok   4
2.9946:-9.1724:-0.1803:-4.95   e-2:17.5  e-2:  5.984: 0.051:5.9892 : 0.05:ok   4
2.9946:-9.1724:-0.1803:-4.97   e-2:12.85 e-2:  5.994: 0.046:5.9892 : 0.05:ok   4
2.9946:-9.1724:-0.1803:-4.96   e-2:16.35 e-2:  5.986: 0.050:5.9892 : 0.05:ok   4
2.9946:-9.1724:-0.1803:-4.96   e-2:14.05 e-2:  5.991: 0.047:5.9892 : 0.05:ok   4
2.9946:-9.1724:-0.1803:-2.56   e-2:15.20 e-2:  5.986: 0.044:5.9892 : 0.05:ok   4
2.9946:-9.1724:-0.1803:-7.31   e-2:15.18 e-2:  5.992: 0.054:5.9892 : 0.05:ok   4
2.9946:-9.1724:-0.1803:-3.85   e-2:15.19 e-2:  5.987: 0.046:5.9892 : 0.05:ok   4
2.9946:-9.1724:-0.1803:-6.1    e-2:15.19 e-2:  5.991: 0.051:5.9892 : 0.05:ok   4
2.9946:-9.1224:-0.1803:-4.96   e-2:15.11 e-2:  5.989: 0.097:5.9892 : 0.1 :ok   4
2.9946:-9.1224:-0.1803:-4.95   e-2:17.4  e-2:  5.984: 0.099:5.9892 : 0.1 :ok   4
2.9946:-9.1224:-0.1803:-4.97   e-2:12.75 e-2:  5.994: 0.095:5.9892 : 0.1 :ok   4
2.9946:-9.1224:-0.1803:-4.96   e-2:16.25 e-2:  5.987: 0.098:5.9892 : 0.1 :ok   4
2.9946:-9.1224:-0.1803:-4.96   e-2:13.9  e-2:  5.992: 0.096:5.9892 : 0.1 :ok   4
2.9946:-9.1224:-0.1803:-2.56   e-2:15.12 e-2:  5.986: 0.092:5.9892 : 0.1 :ok   4
2.9946:-9.1224:-0.1803:-7.31   e-2:15.10 e-2:  5.992: 0.102:5.9892 : 0.1 :ok   4
2.9946:-9.1224:-0.1803:-3.85   e-2:15.1  e-2:  5.988: 0.095:5.9892 : 0.1 :ok   4
2.9946:-9.1224:-0.1803:-6.1    e-2:15.1  e-2:  5.991: 0.099:5.9892 : 0.1 :ok   4
```

45 rays SPOTZ1a.RAY

X0	Y0	Z0	U0	V0	Xfinal	Yfinal	Xgoal	Ygoal	note
3.0946	-9.2224	-0.1803	-5.12 e-2	15.27 e-2	-0.092	-0.011	-0.1		ok 2
3.0946	-9.2224	-0.1803	-5.11 e-2	17.61 e-2	-0.086	-0.019	-0.1		ok 2
3.0946	-9.2224	-0.1803	-5.13 e-2	12.95 e-2	-0.098	-0.002	-0.1		ok 2
3.0946	-9.2224	-0.1803	-5.12 e-2	14.1 e-2	-0.095	-0.006	-0.1		ok 2
3.0946	-9.2224	-0.1803	-5.12 e-2	16.37 e-2	-0.089	-0.015	-0.1		ok 2
3.0946	-9.2224	-0.1803	-2.76 e-2	15.28 e-2	-0.086	-0.005	-0.1		ok 2
3.0946	-9.2224	-0.1803	-7.47 e-2	15.26 e-2	-0.098	-0.016	-0.1		ok 2
3.0946	-9.2224	-0.1803	-3.9 e-2	15.28 e-2	-0.089	-0.008	-0.1		ok 2
3.0946	-9.2224	-0.1803	-6.3 e-2	15.28 e-2	-0.095	-0.013	-0.1		ok 2
3.0446	-9.2224	-0.1803	-5.035 e-2	15.27 e-2	-0.043	-0.010	-0.05		ok 2
3.0446	-9.2224	-0.1803	-5.035 e-2	17.61 e-2	-0.037	-0.019	-0.05		ok 2
3.0446	-9.2224	-0.1803	-5.055 e-2	12.95 e-2	-0.048	-0.002	-0.05		ok 2
3.0446	-9.2224	-0.1803	-5.035 e-2	16.50 e-2	-0.040	-0.015	-0.05		ok 2
3.0446	-9.2224	-0.1803	-5.035 e-2	14.0 e-2	-0.046	-0.006	-0.05		ok 2
3.0446	-9.2224	-0.1803	-2.65 e-2	15.26 e-2	-0.037	-0.005	-0.05		ok 2
3.0446	-9.2224	-0.1803	-7.38 e-2	15.27 e-2	-0.049	-0.016	-0.05		ok 2
3.0446	-9.2224	-0.1803	-3.85 e-2	15.26 e-2	-0.040	-0.007	-0.05		ok 2
3.0446	-9.2224	-0.1803	-6.25 e-2	15.26 e-2	-0.046	-0.013	-0.05		ok 2
2.9946	-9.2224	-0.1803	-4.96 e-2	15.27 e-2	0.006	-0.010			ok 2
2.9946	-9.2224	-0.1803	-4.95 e-2	17.61 e-2	0.012	-0.019			ok 2
2.9946	-9.2224	-0.1803	-4.96 e-2	12.95 e-2	0.001	-0.001			ok 2
2.9946	-9.2224	-0.1803	-4.96 e-2	16.45 e-2	0.009	-0.015			ok 2
2.9946	-9.2224	-0.1803	-4.96 e-2	14.05 e-2	0.003	-0.006			ok 2
2.9946	-9.2224	-0.1803	-2.56 e-2	15.28 e-2	0.012	-0.005			ok 2
2.9946	-9.2224	-0.1803	-7.31 e-2	15.26 e-2	0.000	-0.016			ok 2
2.9946	-9.2224	-0.1803	-3.8 e-2	15.28 e-2	0.009	-0.008			ok 2
2.9946	-9.2224	-0.1803	-6.2 e-2	15.28 e-2	0.003	-0.013			ok 2
2.9446	-9.2224	-0.1803	-4.88 e-2	15.27 e-2	0.055	-0.010	0.05		ok 2
2.9446	-9.2224	-0.1803	-4.87 e-2	17.57 e-2	0.060	-0.019	0.05		ok 2
2.9446	-9.2224	-0.1803	-4.89 e-2	12.92 e-2	0.050	-0.001	0.05		ok 2
2.9446	-9.2224	-0.1803	-4.87 e-2	16.4 e-2	0.058	-0.014	0.05		ok 2
2.9446	-9.2224	-0.1803	-4.87 e-2	14.0 e-2	0.053	-0.005	0.05		ok 2
2.9446	-9.2224	-0.1803	-2.52 e-2	15.28 e-2	0.062	-0.005	0.05		ok 2
2.9446	-9.2224	-0.1803	-7.26 e-2	15.26 e-2	0.049	-0.015	0.05		ok 2
2.9446	-9.2224	-0.1803	-3.65 e-2	15.28 e-2	0.059	-0.007	0.05		ok 2
2.9446	-9.2224	-0.1803	-6.1 e-2	15.28 e-2	0.052	-0.013	0.05		ok 2
2.8946	-9.2224	-0.1803	-4.79 e-2	15.28 e-2	0.105	-0.010	0.1		ok 2
2.8946	-9.2224	-0.1803	-4.79 e-2	17.58 e-2	0.109	-0.018	0.1		ok 2
2.8946	-9.2224	-0.1803	-4.80 e-2	12.92 e-2	0.099	-0.001	0.1		ok 2
2.8946	-9.2224	-0.1803	-4.79 e-2	16.5 e-2	0.107	-0.014	0.1		ok 2
2.8946	-9.2224	-0.1803	-4.79 e-2	14.0 e-2	0.102	-0.005	0.1		ok 2
2.8946	-9.2224	-0.1803	-2.45 e-2	15.28 e-2	0.111	-0.005	0.1		ok 2
2.8946	-9.2224	-0.1803	-7.17 e-2	15.27 e-2	0.098	-0.015	0.1		ok 2
2.8946	-9.2224	-0.1803	-3.55 e-2	15.28 e-2	0.108	-0.007	0.1		ok 2
2.8946	-9.2224	-0.1803	-6.1 e-2	15.28 e-2	0.101	-0.013	0.1		ok 2

45 rays SPOTZa.RAY

X0	Y0	Z0	U0	V0	Xfinal	Yfinal	Xgoal	Ygoal	note
3.0946	-9.2224	-0.1803	-5.12 e-2	15.27 e-2	6.087	0.001	6.0892		ok 4
3.0946	-9.2224	-0.1803	-5.11 e-2	17.61 e-2	6.082	0.004	6.0892		ok 4
3.0946	-9.2224	-0.1803	-5.13 e-2	12.95 e-2	6.093	-0.002	6.0892		ok 4
3.0946	-9.2224	-0.1803	-5.12 e-2	14.1 e-2	6.090	-0.001	6.0892		ok 4
3.0946	-9.2224	-0.1803	-5.12 e-2	16.37 e-2	6.085	0.002	6.0892		ok 4
3.0946	-9.2224	-0.1803	-2.76 e-2	15.28 e-2	6.085	-0.005	6.0892		ok 4
3.0946	-9.2224	-0.1803	-7.47 e-2	15.26 e-2	6.090	0.007	6.0892		ok 4
3.0946	-9.2224	-0.1803	-3.9 e-2	15.28 e-2	6.086	-0.002	6.0892		ok 4
3.0946	-9.2224	-0.1803	-6.3 e-2	15.28 e-2	6.089	0.004	6.0892		ok 4
3.0446	-9.2224	-0.1803	-5.035 e-2	15.27 e-2	6.038	0.001	6.0392		ok 4
3.0446	-9.2224	-0.1803	-5.035 e-2	17.61 e-2	6.033	0.004	6.0392		ok 4
3.0446	-9.2224	-0.1803	-5.055 e-2	12.95 e-2	6.044	-0.002	6.0392		ok 4
3.0446	-9.2224	-0.1803	-5.035 e-2	16.50 e-2	6.035	0.002	6.0392		ok 4
3.0446	-9.2224	-0.1803	-5.035 e-2	14.0 e-2	6.041	-0.001	6.0392		ok 4
3.0446	-9.2224	-0.1803	-2.65 e-2	15.26 e-2	6.035	-0.005	6.0392		ok 4
3.0446	-9.2224	-0.1803	-7.38 e-2	15.27 e-2	6.041	0.006	6.0392		ok 4
3.0446	-9.2224	-0.1803	-3.85 e-2	15.26 e-2	6.037	-0.002	6.0392		ok 4
3.0446	-9.2224	-0.1803	-6.25 e-2	15.26 e-2	6.040	0.004	6.0392		ok 4
2.9946	-9.2224	-0.1803	-4.96 e-2	15.27 e-2	5.989	0.001	5.9392		ok 4
2.9946	-9.2224	-0.1803	-4.95 e-2	17.61 e-2	5.983	0.003	5.9892		ok 4
2.9946	-9.2224	-0.1803	-4.96 e-2	12.95 e-2	5.994	-0.003	5.9892		ok 4
2.9946	-9.2224	-0.1803	-4.96 e-2	16.45 e-2	5.986	0.002	5.9892		ok 4
2.9946	-9.2224	-0.1803	-4.96 e-2	14.05 e-2	5.992	-0.001	5.9892		ok 4
2.9946	-9.2224	-0.1803	-2.56 e-2	15.28 e-2	5.985	-0.005	5.9892		ok 4
2.9946	-9.2224	-0.1803	-7.31 e-2	15.26 e-2	5.992	0.006	5.9892		ok 4
2.9946	-9.2224	-0.1803	-3.8 e-2	15.28 e-2	5.987	-0.002	5.9892		ok 4
2.9946	-9.2224	-0.1803	-6.2 e-2	15.28 e-2	5.990	0.003	5.9892		ok 4
2.9446	-9.2224	-0.1803	-4.88 e-2	15.27 e-2	5.939	0.000	5.9392		ok 4
2.9446	-9.2224	-0.1803	-4.87 e-2	17.57 e-2	5.934	0.003	5.9392		ok 4
2.9446	-9.2224	-0.1803	-4.89 e-2	12.92 e-2	5.945	-0.003	5.9392		ok 4
2.9446	-9.2224	-0.1803	-4.87 e-2	16.4 e-2	5.937	0.002	5.9392		ok 4
2.9446	-9.2224	-0.1803	-4.87 e-2	14.0 e-2	5.942	-0.001	5.9392		ok 4
2.9446	-9.2224	-0.1803	-2.52 e-2	15.28 e-2	5.936	-0.005	5.9392		ok 4
2.9446	-9.2224	-0.1803	-7.26 e-2	15.26 e-2	5.943	0.006	5.9392		ok 4
2.9446	-9.2224	-0.1803	-3.65 e-2	15.28 e-2	5.938	-0.002	5.9392		ok 4
2.9446	-9.2224	-0.1803	-6.1 e-2	15.28 e-2	5.941	0.003	5.9392		ok 4
2.8946	-9.2224	-0.1803	-4.79 e-2	15.28 e-2	5.890	0.000	5.8892		ok 4
2.8946	-9.2224	-0.1803	-4.79 e-2	17.58 e-2	5.885	0.003	5.8892		ok 4
2.8946	-9.2224	-0.1803	-4.80 e-2	12.92 e-2	5.895	-0.003	5.8892		ok 4
2.8946	-9.2224	-0.1803	-4.79 e-2	16.5 e-2	5.887	0.002	5.8892		ok 4
2.8946	-9.2224	-0.1803	-4.79 e-2	14.0 e-2	5.893	-0.002	5.8892		ok 4
2.8946	-9.2224	-0.1803	-2.45 e-2	15.28 e-2	5.886	-0.005	5.8892		ok 4
2.8946	-9.2224	-0.1803	-7.17 e-2	15.27 e-2	5.894	0.005	5.8892		ok 4
2.8946	-9.2224	-0.1803	-3.55 e-2	15.28 e-2	5.888	-0.002	5.8892		ok 4
2.8946	-9.2224	-0.1803	-6.1 e-2	15.28 e-2	5.892	0.003	5.8892		ok 4

25 rays SPOT1b.RAY

X0	Y0	@WAVE	U0	V0	Xf	Yf	Xg	Yg	Note
1.39		r	-2.318 e-2		-0.1000	0.0000	-0.1		ok 2
1.39			-2.318 e-2	1.20 e-2	-0.1000	-0.0001	-0.1		ok 2
1.39			-2.318 e-2	-1.20 e-2	-0.1000	0.0001	-0.1		ok 2
1.39			-3.51 e-2		-0.0997	0.0000	-0.1		ok 2
1.39			-1.15 e-2		-0.1004	0.0000	-0.1		ok 2
1.34		g	-2.21 e-2		-0.0501	0.0000	-0.05		ok 2
1.34			-2.234 e-2	1.24 e-2	-0.0501	-0.0001	-0.05		ok 2
1.34			-2.234 e-2	-1.24 e-2	-0.0501	0.0001	-0.05		ok 2
1.34			-3.48 e-2		-0.0498	0.0000	-0.05		ok 2
1.34			-0.98 e-2		-0.0504	0.0000	-0.05		ok 2
1.29		c	-2.15 e-2		-0.0001	0.0000			ok 2
1.29			-2.15 e-2	-1.25 e-2	-0.0001	0.0001			ok 2
1.29			-2.15 e-2	1.25 e-2	-0.0001	-0.0001			ok 2
1.29			-3.42 e-2		0.0002	0.0000			ok 2
1.29			-0.9 e-2		-0.0004	0.0000			ok 2
1.24		b	-2.068 e-2		0.0499	0.0000	0.05		ok 2
1.24			-2.068 e-2	-1.24 e-2	0.0499	0.0001	0.05		ok 2
1.24			-2.068 e-2	1.24 e-2	0.0499	-0.0001	0.05		ok 2
1.24			-3.34 e-2		0.0501	0.0000	0.05		ok 2
1.24			-0.83 e-2		0.0496	0.0000	0.05		ok 2
1.19		m	-1.984 e-2		0.0999	0.0000	0.1		ok 2
1.19			-1.984 e-2	-1.2 e-2	0.0999	0.0001	0.1		ok 2
1.19			-1.984 e-2	1.2 e-2	0.0999	-0.0001	0.1		ok 2
1.19			-3.26 e-2		0.1001	0.0000	0.1		ok 2
1.19			-0.75 e-2		0.0996	0.0000	0.1		ok 2

25 rays SPOT2b.RAY

X0	Y0	@WAVE	U0	V0	Xf	Yf	Xg	Yg	Note
1.39		r	-2.742 e-2		-0.0999	0.0000	-0.1		ok 2
1.39			-2.742 e-2	1.17 e-2	-0.0999	-0.0001	-0.1		ok 2
1.39			-2.742 e-2	-1.17 e-2	-0.0999	0.0001	-0.1		ok 2
1.39			-3.9 e-2		-0.0996	0.0000	-0.1		ok 2
1.39			-1.55 e-2		-0.1002	0.0000	-0.1		ok 2
1.34		g	-2.644 e-2		-0.0499	0.0000	-0.05		ok 2
1.34			-2.644 e-2	1.16 e-2	-0.0499	-0.0001	-0.05		ok 2
1.34			-2.644 e-2	-1.16 e-2	-0.0499	0.0001	-0.05		ok 2
1.34			-3.8 e-2		-0.0497	0.0000	-0.05		ok 2
1.34			-1.48 e-2		-0.0502	0.0000	-0.05		ok 2
1.29		c	-2.545 e-2		0.0000	0.0000			ok 2
1.29			-2.545 e-2	-1.17 e-2	0.0000	0.0001			ok 2
1.29			-2.545 e-2	1.17 e-2	0.0000	-0.0001			ok 2
1.29			-3.7 e-2		0.0003	0.0000			ok 2
1.29			-1.4 e-2		-0.0002	0.0000			ok 2
1.24		b	-2.446 e-2		0.0500	0.0000	0.05		ok 2
1.24			-2.446 e-2	-1.15 e-2	0.0500	0.0001	0.05		ok 2
1.24			-2.446 e-2	1.15 e-2	0.0500	-0.0001	0.05		ok 2
1.24			-3.60 e-2		0.0502	0.0000	0.05		ok 2
1.24			-1.3 e-2		0.0498	0.0000	0.05		ok 2
1.19		m	-2.347 e-2		0.1000	0.0000	0.1		ok 2
1.19			-2.347 e-2	-1.18 e-2	0.1000	0.0001	0.1		ok 2
1.19			-2.347 e-2	1.18 e-2	0.1000	-0.0001	0.1		ok 2
1.19			-3.50 e-2		0.1002	0.0000	0.1		ok 2
1.19			-1.2 e-2		0.0998	0.0000	0.1		ok 2

```
25 rays                                    SPOTS1b.RAY
  XO        YO        ZO        UO         VO          Xfinal  Yfinal Xgoal Ygoal   note
------:-------:-------:-----------:---------:-------:------:------:-----: -----
2.9946:-9.3224:-0.1803:-4.96  e-2:15.43 e-2:  0.007: 0.087:       :-0.1 :ok  2
2.9946:-9.3224:-0.1803:-4.96  e-2:16.58 e-2:  0.009: 0.082:       :-0.1 :ok  2
2.9946:-9.3224:-0.1803:-4.96  e-2:14.25 e-2:  0.004: 0.092:       :-0.1 :ok  2
2.9946:-9.3224:-0.1803:-3.76  e-2:15.43 e-2:  0.010: 0.090:       :-0.1 :ok  2
2.9946:-9.3224:-0.1803:-6.1   e-2:15.43 e-2:  0.004: 0.084:       :-0.1 :ok  2
2.9946:-9.2724:-0.1803:-4.955 e-2:15.35 e-2:  0.006: 0.038:       :-0.05:ok  2
2.9946:-9.2724:-0.1803:-4.955 e-2:16.55 e-2:  0.009: 0.034:       :-0.05:ok  2
2.9946:-9.2724:-0.1803:-4.955 e-2:14.15 e-2:  0.004: 0.043:       :-0.05:ok  2
2.9946:-9.2724:-0.1803:-3.8   e-2:15.35 e-2:  0.009: 0.041:       :-0.05:ok  2
2.9946:-9.2724:-0.1803:-6.15  e-2:15.35 e-2:  0.003: 0.036:       :-0.05:ok  2
2.9946:-9.2224:-0.1803:-4.96  e-2:15.27 e-2:  0.006:-0.010:       :     :ok  2
2.9946:-9.2224:-0.1803:-4.96  e-2:16.4  e-2:  0.009:-0.014:       :     :ok  2
2.9946:-9.2224:-0.1803:-4.96  e-2:14.1  e-2:  0.004:-0.006:       :     :ok  2
2.9946:-9.2224:-0.1803:-3.70  e-2:15.27 e-2:  0.009:-0.007:       :     :ok  2
2.9946:-9.2224:-0.1803:-6.1   e-2:15.27 e-2:  0.003:-0.013:       :     :ok  2
2.9946:-9.1724:-0.1803:-4.96  e-2:15.19 e-2:  0.006:-0.059:       : 0.05:ok  2
2.9946:-9.1724:-0.1803:-4.96  e-2:16.35 e-2:  0.009:-0.063:       : 0.05:ok  2
2.9946:-9.1724:-0.1803:-4.96  e-2:14.05 e-2:  0.003:-0.055:       : 0.05:ok  2
2.9946:-9.1724:-0.1803:-3.85  e-2:15.19 e-2:  0.009:-0.056:       : 0.05:ok  2
2.9946:-9.1724:-0.1803:-6.1   e-2:15.19 e-2:  0.003:-0.061:       : 0.05:ok  2
2.9946:-9.1224:-0.1803:-4.96  e-2:15.11 e-2:  0.006:-0.107:       : 0.1 :ok  2
2.9946:-9.1224:-0.1803:-4.96  e-2:16.25 e-2:  0.008:-0.111:       : 0.1 :ok  2
2.9946:-9.1224:-0.1803:-4.96  e-2:13.9  e-2:  0.003:-0.103:       : 0.1 :ok  2
2.9946:-9.1224:-0.1803:-3.85  e-2:15.1  e-2:  0.009:-0.105:       : 0.1 :ok  2
2.9946:-9.1224:-0.1803:-6.1   e-2:15.1  e-2:  0.003:-0.110:       : 0.1 :ok  2
```

```
25 rays                                    SPOTSb.RAY
  XO        YO        ZO        UO         VO          Xfinal  Yfinal Xgoal  Ygoal    note
------:-------:-------:-----------:---------:-------:------:-------:-----:------
2.9946:-9.3224:-0.1803:-4.96  e-2:15.43 e-2:  5.988:-0.096:5.9892 :-0.1 :ok  4
2.9946:-9.3224:-0.1803:-4.96  e-2:16.58 e-2:  5.986:-0.094:5.9892 :-0.1 :ok  4
2.9946:-9.3224:-0.1803:-4.96  e-2:14.25 e-2:  5.991:-0.098:5.9892 :-0.1 :ok  4
2.9946:-9.3224:-0.1803:-3.76  e-2:15.43 e-2:  5.987:-0.099:5.9892 :-0.1 :ok  4
2.9946:-9.3224:-0.1803:-6.1   e-2:15.43 e-2:  5.990:-0.093:5.9892 :-0.1 :ok  4
2.9946:-9.2724:-0.1803:-4.955 e-2:15.35 e-2:  5.989:-0.048:5.9892 :-0.05:ok  4
2.9946:-9.2724:-0.1803:-4.955 e-2:16.55 e-2:  5.986:-0.046:5.9892 :-0.05:ok  4
2.9946:-9.2724:-0.1803:-4.955 e-2:14.15 e-2:  5.991:-0.049:5.9892 :-0.05:ok  4
2.9946:-9.2724:-0.1803:-3.8   e-2:15.35 e-2:  5.987:-0.050:5.9892 :-0.05:ok  4
2.9946:-9.2724:-0.1803:-6.15  e-2:15.35 e-2:  5.990:-0.045:5.9892 :-0.05:ok  4
2.9946:-9.2224:-0.1803:-4.96  e-2:15.27 e-2:  5.989: 0.001:5.9892 :     :ok  4
2.9946:-9.2224:-0.1803:-4.96  e-2:16.4  e-2:  5.986: 0.002:5.9892 :     :ok  4
2.9946:-9.2224:-0.1803:-4.96  e-2:14.1  e-2:  5.991:-0.001:5.9892 :     :ok  4
2.9946:-9.2224:-0.1803:-3.70  e-2:15.27 e-2:  5.987:-0.002:5.9892 :     :ok  4
2.9946:-9.2224:-0.1803:-6.1   e-2:15.27 e-2:  5.990: 0.003:5.9892 :     :ok  4
2.9946:-9.1724:-0.1803:-4.96  e-2:15.19 e-2:  5.989: 0.049:5.9892 : 0.05:ok  4
2.9946:-9.1724:-0.1803:-4.96  e-2:16.35 e-2:  5.986: 0.050:5.9892 : 0.05:ok  4
2.9946:-9.1724:-0.1803:-4.96  e-2:14.05 e-2:  5.991: 0.047:5.9892 : 0.05:ok  4
2.9946:-9.1724:-0.1803:-3.85  e-2:15.19 e-2:  5.987: 0.046:5.9892 : 0.05:ok  4
2.9946:-9.1724:-0.1803:-6.1   e-2:15.19 e-2:  5.991: 0.051:5.9892 : 0.05:ok  4
2.9946:-9.1224:-0.1803:-4.96  e-2:15.11 e-2:  5.989: 0.097:5.9892 : 0.1 :ok  4
2.9946:-9.1224:-0.1803:-4.96  e-2:16.25 e-2:  5.987: 0.098:5.9892 : 0.1 :ok  4
2.9946:-9.1224:-0.1803:-4.96  e-2:13.9  e-2:  5.992: 0.096:5.9892 : 0.1 :ok  4
2.9946:-9.1224:-0.1803:-3.85  e-2:15.1  e-2:  5.988: 0.095:5.9892 : 0.1 :ok  4
2.9946:-9.1224:-0.1803:-6.1   e-2:15.1  e-2:  5.991: 0.099:5.9892 : 0.1 :ok  4
```

25 rays SPOTZ1b.RAY

X0	Y0	Z0	U0	V0	Xfinal	Yfinal	Xgoal	Ygoal	note
3.0946	-9.2224	-0.1803	-5.12 e-2	15.27 e-2	-0.092	-0.011	-0.1		ok 2
3.0946	-9.2224	-0.1803	-5.12 e-2	14.1 e-2	-0.095	-0.006	-0.1		ok 2
3.0946	-9.2224	-0.1803	-5.12 e-2	16.37 e-2	-0.089	-0.015	-0.1		ok 2
3.0946	-9.2224	-0.1803	-3.9 e-2	15.28 e-2	-0.089	-0.008	-0.1		ok 2
3.0946	-9.2224	-0.1803	-6.3 e-2	15.28 e-2	-0.095	-0.013	-0.1		ok 2
3.0446	-9.2224	-0.1803	-5.035 e-2	15.27 e-2	-0.043	-0.010	-0.05		ok 2
3.0446	-9.2224	-0.1803	-5.035 e-2	16.50 e-2	-0.040	-0.015	-0.05		ok 2
3.0446	-9.2224	-0.1803	-5.035 e-2	14.0 e-2	-0.046	-0.006	-0.05		ok 2
3.0446	-9.2224	-0.1803	-3.85 e-2	15.26 e-2	-0.040	-0.007	-0.05		ok 2
3.0446	-9.2224	-0.1803	-6.25 e-2	15.26 e-2	-0.046	-0.013	-0.05		ok 2
2.9946	-9.2224	-0.1803	-4.96 e-2	15.27 e-2	0.006	-0.010			ok 2
2.9946	-9.2224	-0.1803	-4.96 e-2	16.45 e-2	0.009	-0.015			ok 2
2.9946	-9.2224	-0.1803	-4.96 e-2	14.05 e-2	0.003	-0.006			ok 2
2.9946	-9.2224	-0.1803	-3.8 e-2	15.28 e-2	0.009	-0.008			ok 2
2.9946	-9.2224	-0.1803	-6.2 e-2	15.28 e-2	0.003	-0.013			ok 2
2.9446	-9.2224	-0.1803	-4.88 e-2	15.27 e-2	0.055	-0.010	0.05		ok 2
2.9446	-9.2224	-0.1803	-4.87 e-2	16.4 e-2	0.058	-0.014	0.05		ok 2
2.9446	-9.2224	-0.1803	-4.87 e-2	14.0 e-2	0.053	-0.005	0.05		ok 2
2.9446	-9.2224	-0.1803	-3.65 e-2	15.28 e-2	0.059	-0.007	0.05		ok 2
2.9446	-9.2224	-0.1803	-6.1 e-2	15.28 e-2	0.052	-0.013	0.05		ok 2
2.8946	-9.2224	-0.1803	-4.79 e-2	15.28 e-2	0.105	-0.010	0.1		ok 2
2.8946	-9.2224	-0.1803	-4.79 e-2	16.5 e-2	0.107	-0.014	0.1		ok 2
2.8946	-9.2224	-0.1803	-4.79 e-2	14.0 e-2	0.102	-0.005	0.1		ok 2
2.8946	-9.2224	-0.1803	-3.55 e-2	15.28 e-2	0.108	-0.007	0.1		ok 2
2.8946	-9.2224	-0.1803	-6.1 e-2	15.28 e-2	0.101	-0.013	0.1		ok 2

25 rays SPOTZb.RAY

X0	Y0	Z0	U0	V0	Xfinal	Yfinal	Xgoal	Ygoal	note
3.0946	-9.2224	-0.1803	-5.12 e-2	15.27 e-2	6.087	0.001	6.0892		ok 4
3.0946	-9.2224	-0.1803	-5.12 e-2	14.1 e-2	6.090	-0.001	6.0892		ok 4
3.0946	-9.2224	-0.1803	-5.12 e-2	16.37 e-2	6.085	0.002	6.0892		ok 4
3.0946	-9.2224	-0.1803	-3.9 e-2	15.28 e-2	6.086	-0.002	6.0892		ok 4
3.0946	-9.2224	-0.1803	-6.3 e-2	15.28 e-2	6.089	0.004	6.0892		ok 4
3.0446	-9.2224	-0.1803	-5.035 e-2	15.27 e-2	6.038	0.001	6.0392		ok 4
3.0446	-9.2224	-0.1803	-5.035 e-2	16.50 e-2	6.035	0.002	6.0392		ok 4
3.0446	-9.2224	-0.1803	-5.035 e-2	14.0 e-2	6.041	-0.001	6.0392		ok 4
3.0446	-9.2224	-0.1803	-3.85 e-2	15.26 e-2	6.037	-0.002	6.0392		ok 4
3.0446	-9.2224	-0.1803	-6.25 e-2	15.26 e-2	6.040	0.004	6.0392		ok 4
2.9946	-9.2224	-0.1803	-4.96 e-2	15.27 e-2	5.989	0.001	5.9392		ok 4
2.9946	-9.2224	-0.1803	-4.96 e-2	16.45 e-2	5.986	0.002	5.9892		ok 4
2.9946	-9.2224	-0.1803	-4.96 e-2	14.05 e-2	5.992	-0.001	5.9892		ok 4
2.9946	-9.2224	-0.1803	-3.8 e-2	15.28 e-2	5.987	-0.002	5.9892		ok 4
2.9946	-9.2224	-0.1803	-6.2 e-2	15.28 e-2	5.990	0.003	5.9892		ok 4
2.9446	-9.2224	-0.1803	-4.88 e-2	15.27 e-2	5.939	0.000	5.9392		ok 4
2.9446	-9.2224	-0.1803	-4.87 e-2	16.4 e-2	5.937	0.002	5.9392		ok 4
2.9446	-9.2224	-0.1803	-4.87 e-2	14.0 e-2	5.942	-0.001	5.9392		ok 4
2.9446	-9.2224	-0.1803	-3.65 e-2	15.28 e-2	5.938	-0.002	5.9392		ok 4
2.9446	-9.2224	-0.1803	-6.1 e-2	15.28 e-2	5.941	0.003	5.9392		ok 4
2.8946	-9.2224	-0.1803	-4.79 e-2	15.28 e-2	5.890	0.000	5.8892		ok 4
2.8946	-9.2224	-0.1803	-4.79 e-2	16.5 e-2	5.887	0.002	5.8892		ok 4
2.8946	-9.2224	-0.1803	-4.79 e-2	14.0 e-2	5.893	-0.002	5.8892		ok 4
2.8946	-9.2224	-0.1803	-3.55 e-2	15.28 e-2	5.888	-0.002	5.8892		ok 4
2.8946	-9.2224	-0.1803	-6.1 e-2	15.28 e-2	5.892	0.003	5.8892		ok 4

APPENDIX G

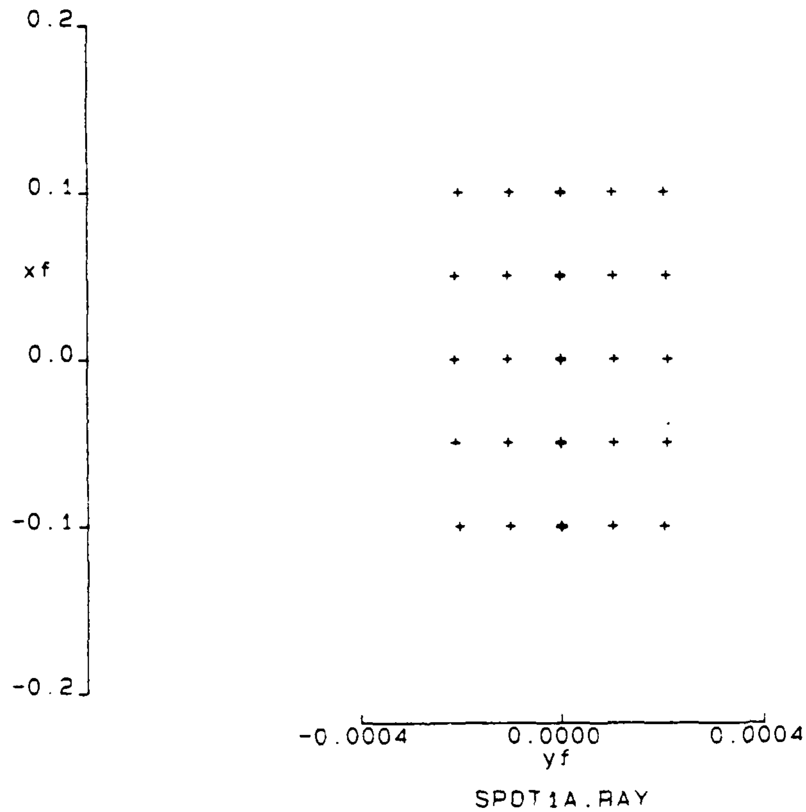

Figure G-1 Simulated Line Spread Function for P45 R_1 Mirror 1

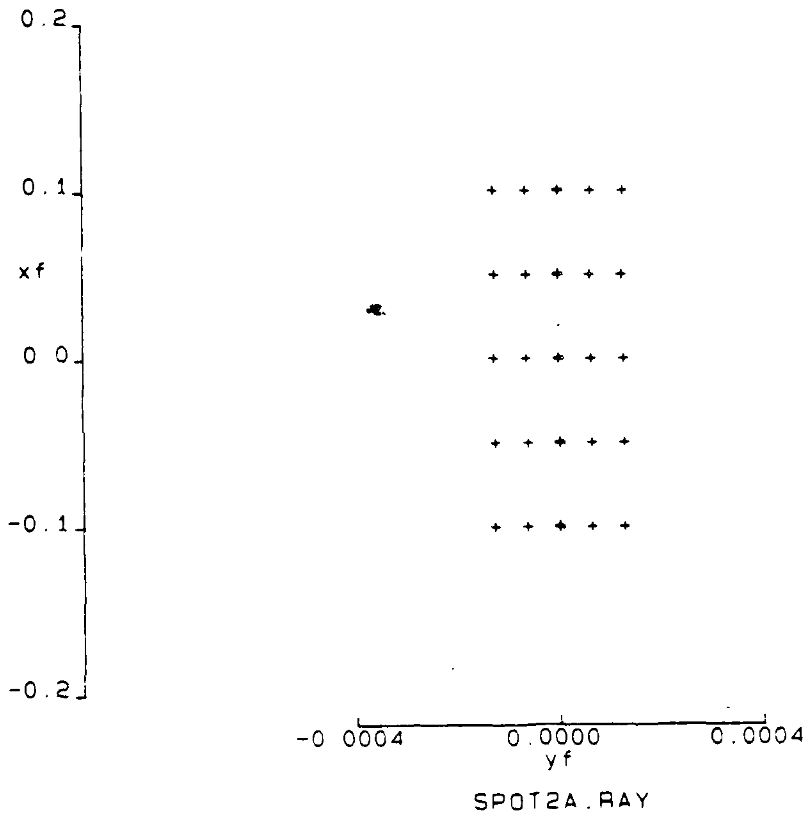

Figure G-2 Simulated Line Spread Function for P45 R_2 Mirror 2

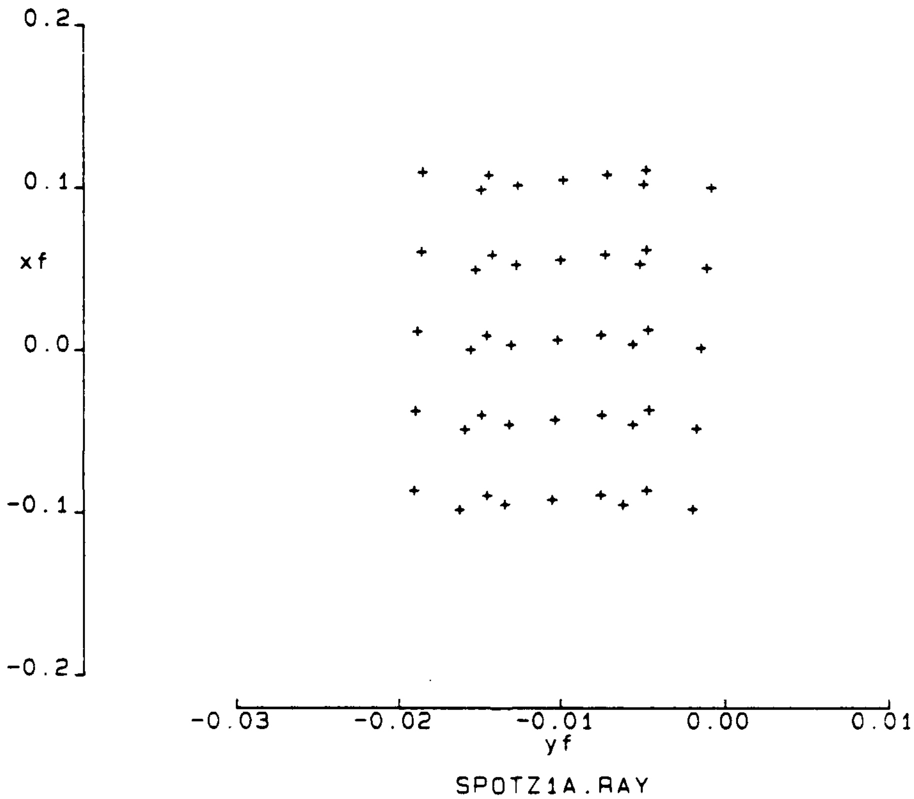

Figure G-3 Simulated Line Spread Function for P45 Mask 1 Vertical Slit

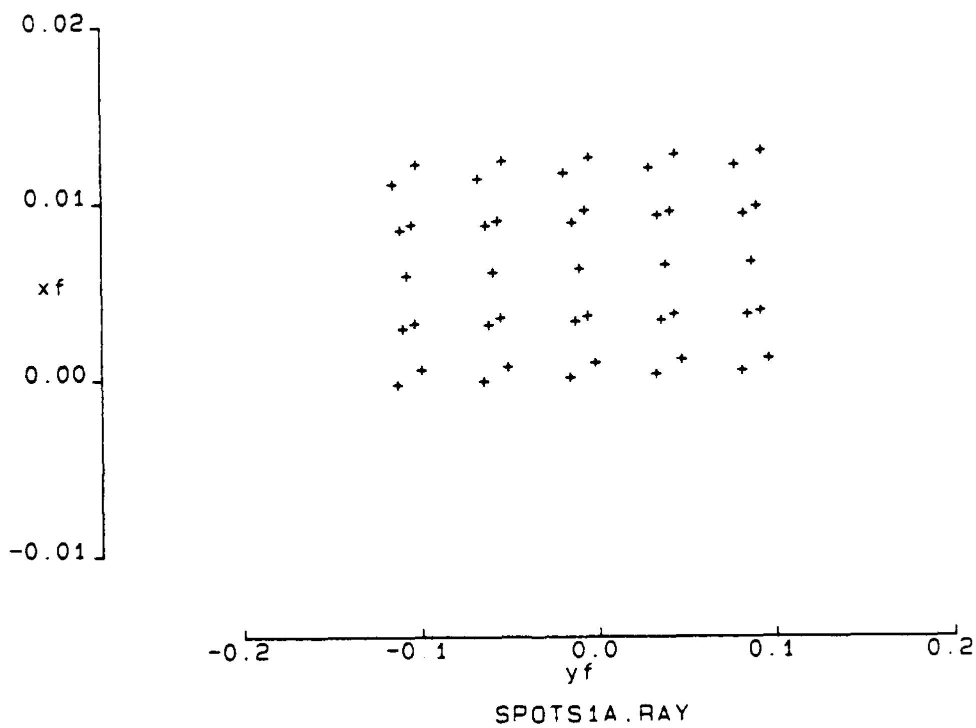

Figure G-4 Simulated Line Spread Function for P45 Mask 1 Horizontal Slit

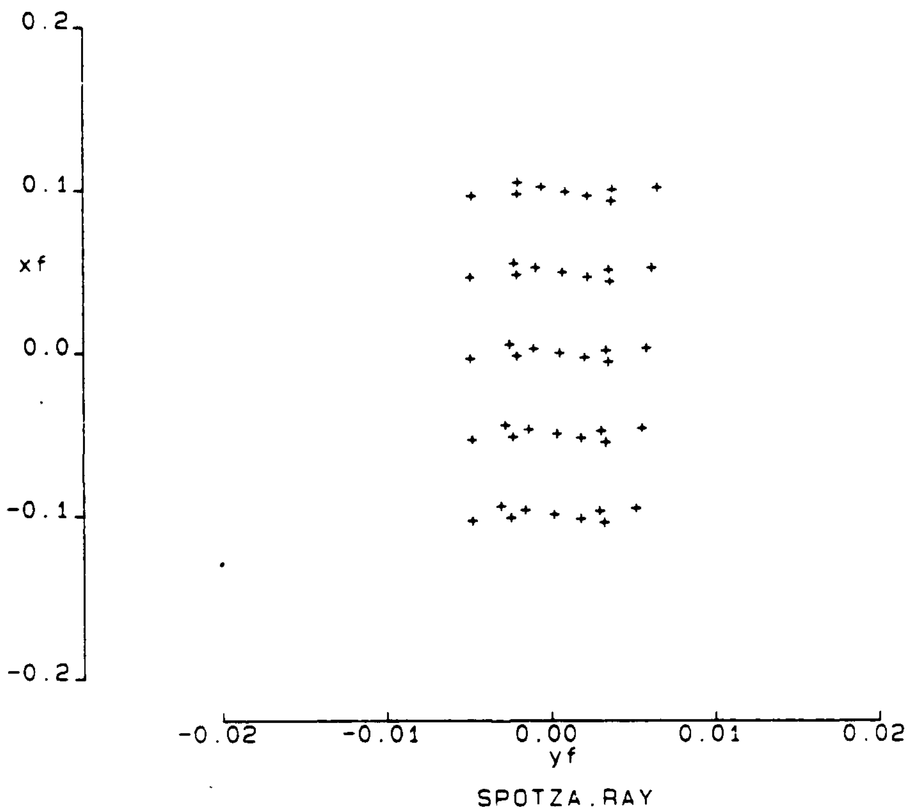

Figure G-5 Simulated Line Spread Function for P45 Mask 2 Vertical Slit

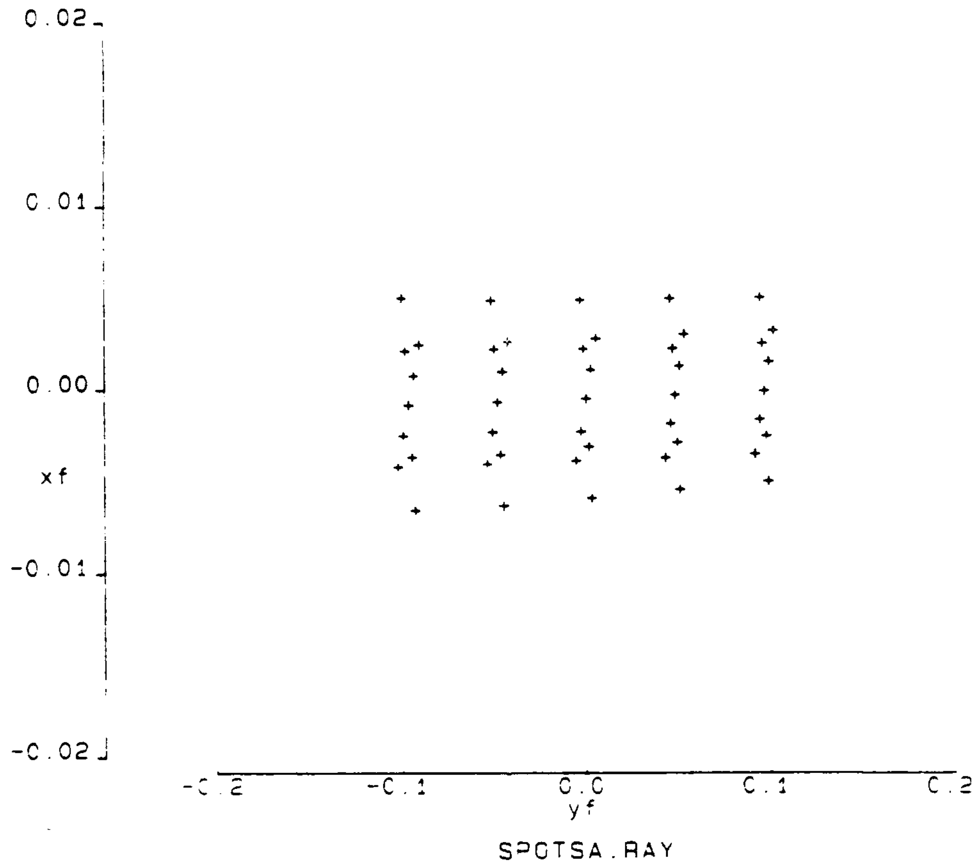

Figure G-6 Simulated Line Spread Function for P45 Mask 2 Horizontal Slit

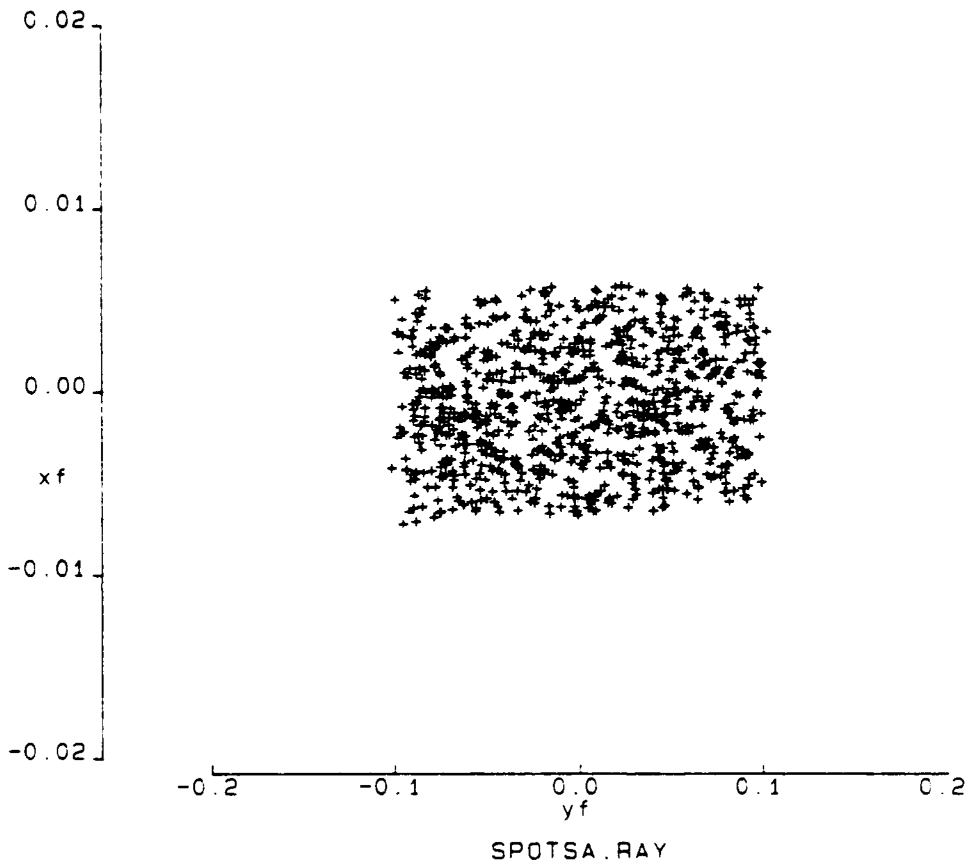

Figure G7 Simulated Line Spread Function for P45 Mask 2 Horizontal Slit

1100 Uniformly, Randomly Distributed Rays

LIST OF REFERENCES

1. Davis, D.S., "An Efficient and Versatile Method for Multiplexed Imaging," paper submitted for publishing.

2. McKenzie, R.H., **A Demonstration of the Use of Walsh Functions For Multiplexed Imaging**, Master's Thesis, Naval Postgraduate School, Monterey, California, December 1990.

3. Musselman, B.J., **A Study of the Diffraction Behavior and Resolution Criteria for Pattern Recognition for a Proposed Multiplexed Imaging Technique**, Master's Thesis, Naval Postgraduate School, Monterey, California, September 1991.

4. Sargent, J.P., **A Design, Fabrication and Test of a Precision Positioning Servo Drive for a Multiplexed Imaging System**, Master's Thesis, Naval Postgraduate School, Monterey, California, September 1991.

5. Parriott, G.R., **Development and Testing of a Prototype Electro-Optical Phase Encoding Position Transducer**, Master's Thesis, Naval Postgraduate School, Monterey, California, December 1991.

6. Beauchamp, K.G., **Applications of a Walsh and Related Functions, with an Introduction to Sequency Theory**, Academic Press, 1984.

7. Decker, J.A., in **Spectrometric Techniques I**, G.A. Vanasse editor, Academic Press, 1977.

8. Harmuth, H.F., **Sequency Theory Foundations and Applications**, Academic Press, 1977.

9. Nussbaum, A. and R.A. Phillips, **Contemporary Optics for Scientists and Engineers**, Prentice, 1976.

10. Möller, K.D., **Optics**, University Science Books, 1988.

11. Hecht, E., **Optics**, 2d ed., Addison-Wesley, 1987.

12. Smith, W.J., **Modern Optical Engineering, The Design of Optical Systems**, 2d ed., McGraw-Hill, 1990.

13. Kirkham, A.R., in **Amateur Telescope Making**, A.G. Ingalls editor, Scientific American, INC., 1974.

14. Reynolds, G.O., J.B. DeVelis, G.B. Parrents, Jr. and B.J. Thompson, **The New Physical Optics Notebook, Tutorials in Fourier Optics**, SPIE Optical Engineering Press, 1989.

INITIAL DISTRIBUTION LIST

1.	Defense Technical Information Center Cameron Station Alexandria, VA 22304-6145	2
2.	Library, Code 52 Naval Postgraduate School Monterey, CA 93943-5002	2
3.	Professor K.E. Woehler, Code PH/Wh Chairman, Department of Physics Naval Postgraduate School Monterey, CA 93943-5000	1
4.	Assoc. Professor D.S. Davis, Code PH/Dv Department of Physics Naval Postgraduate School Monterey, CA 93943-5000	3
5.	Assoc. Professor D.D. Cleary, Code PH/Cl Department of Physics Naval Postgraduate School Monterey, CA 93943-5000	1
6.	Department of Physics Library Naval Postgraduate School Monterey, CA 93943-5000	2
7.	LT Blake D. Huguenin, USN 738 Knollview BLVD Ormond Beach, FL 32174	3